Energy Systems Research

Volume 4 • Number 1 • 2021

Published by
Melentiev Energy Systems Institute
Siberian Branch of Russian Academy of Sciences

Available online: esrj.ru

ISSN 2618-9992

Energy Systems Research

Volume 4 • Number 1 • 2021
International scientific peer-reviewed journal
Available online: http://esrj.ru

About the journal

Energy Systems Research is an international peer-reviewed journal addressing all the aspects of energy systems, including their sustainable development and effective use, smart and reliable operation, control and management, integration and interaction in a complex physical, technical, economic and social environment.

Energy systems research methodology is based on a systems approach considering energy objects as systems with complicated structure and external ties, and includes the methods and technologies of systems analysis.

Within this broad multi-disciplinary scope, topics of particular interest include strategic energy systems development at the international, regional, national and local levels; energy supply reliability and security; energy markets, regulations and policy; technological innovations with their impacts and future-oriented transformations of energy systems.

The journal welcomes papers on advances in heat and electric power industries, energy efficiency and energy saving, renewable energy and clean fossil fuel generation, and other energy technologies.

Energy Systems Research is also concerned with energy systems challenges related to the applications of information and communication technologies, including intelligent control and cyber security, modern approaches of systems analysis, modeling, forecasting, numerical computations and optimization.

The journal is published by Melentiev Energy Systems Institute of Siberian Branch of Russian Academy of Sciences. The journal's ISSN is 2618-9992. There are 4 issues per year (special issues are available). All articles are available online on English as Open access articles.

Topics

- Energy production, conversion, transport and distribution systems
- Integrated energy systems
- Energy technologies
- International, regional, local energy systems
- Energy system protection, control and management
- Smart energy systems, smart grids
- Energy systems reliability and energy security
- Electricity, heating, cooling, gas and oil systems
- Energy system development and operation
- Demand-side management
- Energy economics and policy
- Renewable energy and clean fossil fuel based systems
- Distributed energy systems
- Sustainable energy transitions
- System problems of power and thermal engineering
- Artificial intelligence in energy systems
- Information and communication technologies in energy systems
- Energy systems analysis and modelling
- Computational methods and optimization in energy systems

Publishing board

Executive secretary:	Dmitry Zolotarev
Copyeditor:	Marina Ozerova
Math proofreading editor	Evgenia Markova

Contacts

Scientific secretary:	Alexey Mikheev, Dr. of Eng.
E-mail:	info@esrj.ru
Tel:	+7 (3952) 950980 (English, Russian)
Fax:	+7 (3952) 426796
Address:	130, Lermontov str., Irkutsk, 664033, Russia

Contents

Dependence of the Possible and Allowable Projection Error on the Projection Time Frame

Yu.D. Kononov, D.Yu. Kononov*

Melentiev Energy Systems Institute of Siberian Branch of Russian Academy of Sciences, Irkutsk, Russia

***Abstract* — This study addresses the issues of assessing and factoring in the effect of uncertainty growth on the possible performance of projections and their allowable errors. Relying on projects of nuclear power plants and combined cycle power plants as a case study, we assess the dependence of their economic performance indicators on possible changes in the conditions of their future operation in a given year. To assess the effect of the range and nature of input data uncertainty on the projections of the development of regional energy supply systems, we proposed a methodological toolkit that combines optimization with the Monte Carlo simulation. Its application to one of the options for commissioning new power plants in European Russia enabled us to estimate the possible response of the average and marginal cost of electricity in this aggregated region to the broadening of the uncertainty range of the gas price. We note that the assessment and comparison of the possible error of projected indicators with the requirements for their accuracy in making priority investment and other decisions facilitate the justification of the acceptable complexity of employed models and projection methods.**

***Index Terms*: projections, electric power industry, uncertainty, reliability.**

* Corresponding author.
E-mail: kononov@isem.irk.ru

http://dx.doi.org/10.38028/esr.2021.01.0001
Received March 06, 2021. Revised March 19, 2021.
Accepted March 30, 2021. Available online May 26, 2021.

I. Introduction

As the projection time frame extends into the future, this increases the uncertainty of future conditions of the energy industry development and compromises the performance of long-term projections, i.e., Their reliability, accuracy, and value.

Published projections of energy development in the USA and Europe to 2030-2035 compellingly demonstrate the nonlinear nature of growth of the uncertainty range as the projection time frame extends. For example, in the U.S. Energy projections [1], the uncertainty range for primary energy consumption volumes for all cases covered by the projections grows from the low 5-10% for the 5-year time frame to the high 13-23% and 22-38% for the projections for 15 and 25 years, respectively.

In “The energy strategy of Russia to 2030” (es-2030), as approved in 2009 (es-2030), the difference between the total energy consumption under the worst- and best-case scenarios amounts to 7% for the first 5 years and subsequently grows to 22% and 31% for the projections for 15 and 20 years into the future, respectively.

A key performance indicator of the projections is their reliability, which can be characterized by an uncertainty range, i.e., The percentage difference between the highest and lowest values of a projected variable, as well as the coefficient of variation and dispersion (spread) of the values of projected variables set against their mean values or reference case values. The width of the range within which the projected system parameters can fluctuate determines the accuracy of the projection.

Statistical methods of estimating the projection error are well-known and widely used in practice (e.g., [2, 3]). However, they are suitable mainly for past projections or those of the dynamics of individual indicators based on their trends. When projecting the development of such

Table 1. Deviation of the electricity cost from its value in the deterministic case of the projection when the uncertainty range increases for the gas price, %

Federal district	Cost	Uncertainty range		
		15%	30%	50%
Central	Average	2.4	3.7	4.8
	Marginal	3.9	7.5	13.1
Northwestern	Average	2.5	4.1	5.1
	Marginal	3.8	7.5	12.6
Southern	Average	3.1	5.9	9.1
	Marginal	3.3	7.8	13.0
Ural	Average	0.9	1.5	2.5
	Marginal	3.5	7.1	12.1
The aggregated region as a whole	Average	1.1	3.1	4.6
	Marginal	3.5	7.4	12.4

Note. Calculations for one of the development options of regional energy supply systems in european russia in 2030-2035.

complex systems as the energy sector of a country or its regions, it becomes important to assess not only the likely and unavoidable error but also the allowable error of the projection. As of now, there are no generally accepted and universally applicable methods that would facilitate such an assessment.

In what follows, relying on the example of a projection of the development of power supply systems, we consider possible approaches to assessing the acceptable requirements for the quality of projections.

II. Estimating the unavoidable error

The inevitable error of projections of the dynamics of certain indicators depends to a greater extent on the error of the input data used in the calculations. It is possible to capture this dependence in the form of a regression equation with sufficient confidence only for a specific and very simple system. For example, the dependence of the average cost of electricity generation by existing power plants in the region on the range of uncertainty of the cost of gas lends itself to such a description. However, a gross error proves inevitable when assessing the projection error of the dynamics of this indicator while taking into account the effect of gas prices on the mix of new capacity additions under changing conditions.

Optimization models (e.g., [4, 5]) are deemed suitable for incorporating this effect, for assessing the sensitivity of projections of the development of complex systems such as the energy sector to possible changes in individual input data. The minimum cash cost of meeting a given demand for energy carriers serves as the criterion of optimality in such models. Based on their change when varying different indicators, we can judge possible and allowable error in the projections of these indicators and their significance.

In the case that necessitates taking into account the effect of the uncertainty of several interrelated input data variables on the reliability of the projection of the development of the energy sector or the systems of its individual industries, the stochastic models [6] combining the optimization with the well-known Monte Carlo method [7] can be instrumental. Such a model is used, for example, in projections of generation costs [8], electricity prices [9], and energy markets [10].

The Monte Carlo method combined with optimization is used in the miss-el model [11]. It was used to assess the effect of a range of uncertainty of gas prices and other indicators on the electricity cost in European Russia including the Urals. The calculations were performed given interval-valued input data and the normal distribution of their probable values within the specified ranges. In this case, only the gas price uncertainty range was varied. The calculation results were compared against the deterministic case.

The broadening of this range leads to an increase in the average gas price and causes a change in the mix of new power plant capacity additions, which affected the cost of electricity generation. Marginal cost, i.e., The discounted cost of electricity generation at the most expensive power plants of those to be commissioned, grows particularly significantly and nonlinearly. As the table shows, with a 50 percent increase in gas price uncertainty, the average price in the European part of the country could increase by 4-5 percent, and the marginal one — by more than 12 percent (under the assumed projection conditions). At the same time, there is a noticeable difference in the response of individual federal districts to the uncertainty in gas prices.

Additional calculations with the MISS-EL model were performed assuming the uniform probability distribution of the gas price within the same ranges as under its normal distribution. The calculation results did not affect the conclusion claiming a noticeable and growing unavoidable projection error as the uncertainty range of the key input data increases.

III. The allowable projection error

The allowable projection error depends on the aims of the projection and its importance for making strategic decisions by investors, the state, and society. Its numerical value is primarily determined by the probable damage (economic, environmental, or social) due to the projection error.

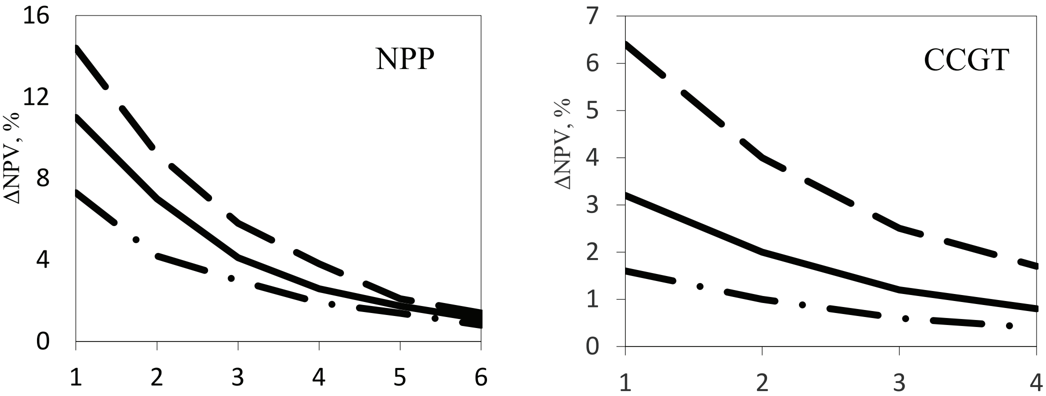

Five-year period, in which the demand for electricity decreases (an NPP project) or the gas price increases (a CCGT project)

Fig. 1. Effect of changes (error) in previously projected conditions on the decrease in the economic performance of power plant projects. In one of the five-year periods. Note. We considered a range of change in electricity demand by 10-20% and that in gas prices by 25-100% (the lower and upper boundaries in the figure, respectively).

For the investor (company), the damage is usually measured by a decrease in expected profits. The damage for the state can be characterized by a possible decline in budget revenues, living standards of the population, and economic growth rates. In this case, one has to set an allowable change in the value of the employed optimality criterion by relying on expert judgment. When projecting the development of the energy sector under the considered scenarios, such a criterion is, as a rule, the minimum cost of meeting a given demand for energy carriers.

It is difficult to judge the error of the system development projection with no estimate of the allowable error of the expected dynamics of the key projected indicators. Such indicators in the energy sector projections are energy demand and prices, the development of regional energy supply systems and new technologies, and the extent to which energy security requirements are met.

As the time frame in question increases, the requirements for reliability and accuracy of projections decrease, which is due to an exponential rise in the uncertainty of conditions, a decrease in the importance of the projection results for making priority decisions, an increase in the opportunities (time margin) to prevent the anticipated threats.

When making investment decisions in the energy sector, one of the primary objectives is to assess the efficiency and risks of large-scale capacity addition projects in the electric power industry or the fuel industry. The investor values the revenues of a more distant future less than those of an immediate one, which is reflected in the discounting of indicators that measure the financial performance of projects: net present value (npv), internal rate of return, payback period, and others.

By varying the values of key input data variables for any of the periods within the projection time frame and by tracing the effect of such variations on the project value, we can get an idea of an acceptable decrease in the projection accuracy as these periods gradually extend further into the future.

This approach was applied in the analysis of the sensitivity of the performance of nuclear power plant project to a possible variation in electricity demand (electricity production) over time and sensitivity of the performance of combined cycle power plant project to a change in gas prices.

The calculation results shown in the figure indicate a marked nonlinear decrease in this sensitivity as the time of these changes gets more remote from the present.

Given the assumed input data, fluctuations in electricity demand as low as those within the range of 15-20% have a noticeable impact on the net present value only in the first 15 years of the projection period under consideration. Consequently, the requirements for the accuracy of projecting the utilized capacity of the nuclear power plant at the end of its service life also get less stringent. The required reliability of gas price projections for valuation of the ccgt project in the third five-year period is two times lower than in the first one. The increase in the discount rate (in the calculations it was taken to be equal to 10%) further reduces the requirements for the accuracy of long-term projections of the indicators that affect the valuation of projects.

IV. Conclusion

The estimation and comparison of the likely error for the projected variables against the requirements of their accuracy (reliability), when making investment and other decisions, facilitate a more well-grounded choice of the acceptable level of complexity of employed economic and mathematical models. Should an elaboration of these models, when compared against the currently employed models, lead to a change in the solution (i.e., The projection) by a magnitude less than the allowable error, the appropriateness of such innovation is anything but obvious.

The methods to assess the quality and value of the input data, the requirements set for such data, and the reliability of energy projections for various time frames need further development. To this end, one should consider the specific features of problems to be solved within a given projection.

The study was carried out under a state assignment project (no. FWEU-2021-0003 reg. No. AAAA-A21-121012090014-5) of the program for basic research of the russian federation for 2021-2030.

References

[1] Annual Energy Outlook [Electronic publication] / U.S. Energy Information Administration. Available at: http://www.eia.gov/forecasts/aeo/ (1999-2014)

[2] L.N. Slutskin. An MBA course on forecasting in business. Moscow: Alpina Business Books, 2006, 277 p. (in Russian)

[3] A. Dovydenko, R. Fildes. “Measuring forecasting accuracy: The case of judgmental adjustments to SKU – level demand forecasts,” International Journal of Forecasting, no. 29, pp. 510–522, 2013.

[4] A.V. Lagerev. “A dynamic territorial and production model for the development of scenarios of mutually aligned development of Russia's energy industry as concerns its federal subjects,” Izvestija RAN, Energetika, no. 4, pp. 26–32, 2004. (in Russian)

[5] S.Messner, M. Strubegger. User’s Guide for MESSAGE III/WR-95-69. IIASA, Laxenburg, Austria, 1995.

[6] Kurt Marti. Stochastic Optimization Methods. Springer, 2005, 317 p.

[7] S.M. Ermakov. Monte Carlo methods and related problems. Moscow: Nauka, 1975, 472 p. (in Russian)

[8] J. Valenzuela, M. Muzumdar. “Monte Carlo Computation of Power Generation Production Cost Under Operating Constraints,” IEEE Transactions on Power Systems, vol. 16, no. 4, Nov. 2001.

[9] A. Poullikkas. “An adaptive long-term electricity price forecasting modeling using Monte Carlo simulation,” Journal of Power Technologies, vol. 98, no. 3, pp. 207–273, 2018.

[10] M. Amelin, L. Soder. “On Monte Carlo Simulation of Electricity Markets with Uncertainties in Precipitation and Loud Forecasts,” in IEEE Porto Power Tech Proceedings, vol. 1, Porto, 2001.

[11] Yu.D. Kononov, V.N. Tyrtyshnyi, D.Yu. Kononov. “The application of stochastic modeling in choosing regional energy supply options while addressing investment risks,” Informatsionnye i matematicheskie tekhnologii v nauke i upravlenii (Information and Mathematical Technologies in Science and Management), no. 2(10), pp. 80–87, 2018. (in Russian)

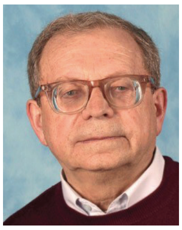

Yuri Kononov — Doctor of Economics, Professor, Honored Worker of science of the Russian Federation, chief researcher of Melentiev Energy Systems Institute of Siberian Branch of the Russian Academy of Sciences, Russia, Irkutsk. His research interests are modeling and research of interaction between energy and economy; methods to enhance the validity of long-term forecasts of energy development.

Dmitry Kononov — Ph. D., Senior researcher of Melentiev Energy Systems Institute of Siberian Branch of the Russian Academy of Sciences, Russia, Irkutsk. His research interests are consideration of the impact of the uncertainty factors on the methods for the evaluation of strategic threats to power industry development.

Development of Low Carbon Cities: Assessment of Carbon Dioxide Emissions from Energy Facilities in Irkutsk City

E.P. Maysyuk*

Melentiev Energy Systems Institute of Siberian Branch of Russian Academy of Sciences, Irkutsk, Russia

Abstract — **Decrease in greenhouse gas emissions is a current trend in solving the climate change problems. The concept of low-carbon cities is extensively discussed nowadays. It aims to reduce greenhouse gas emissions through integrated mechanisms and measures, which comply with socio-economic development and city management. Since a considerable part of the population lives in cities, the utmost goal of the study is to analyze the situation with emissions of the main greenhouse gas, i.e., carbon dioxide, in the urban environment. The major sources of carbon dioxide emissions are stationary energy facilities of different capacities burning fuel. The paper considers the city of Irkutsk as an example of the populated area included in the study on low carbon cities under the auspices of the Social and Economic Commission for Asia and the Pacific of the UN - UNESCAP. The first stage of the studies involved assessing the current carbon dioxide emissions from energy facilities of the city through the calculation of carbon dioxide emissions from boiler houses and the city cogeneration plant for 1990. The findings revealed the potential of reducing carbon dioxide emissions from energy facilities in Irkutsk. The paper suggests the basic directions and measures to mitigate greenhouse gas emissions from the urban energy facilities.**

Index Terms: **Climate change, International agreements, greenhouse gas emissions, the city of Irkutsk, boiler houses, the Novo-Irkutsk cogeneration plant.**

* Corresponding author.
E-mail: maysyuk@isem.irk.ru

http://dx.doi.org/10.38028/esr.2021.01.0002
Received March 01, 2021. Revised March 09, 2021.
Accepted March 15, 2021. Available online May 26, 2021.

I. Introduction

At present, the world community raises an issue on the role of cities as the major sources of greenhouse gas emissions increasingly more often. In 2011, the UN Economic Commission published the report “Climatically neutral cities” [1], which analyzed the role of cities and their effect on climate change. The bulk of the population resides in cities concentrating on business activity, social and intellectual life. Therefore, the urban environment possesses the greatest resources to decrease energy intensity and energy consumption and thus mitigate greenhouse gas emissions. The concept of low carbon cities suggests not only a direct cutdown in emissions but also the design of mechanisms and complex measures that are integrated within the city and aimed at making coordinated decisions on the reduction of carbon dioxide emissions.

The idea of low carbon cities was supported by the Social and Economic Commission for Asia and the Pacific of the UN (UNESCAP). The Commission is developing some programs on environmental cooperation in Northeast Asia. The platform on the low carbon cities in Northeast Asia - NEALCCP (Northeast Asia Low Carbon City Platform) operates under the auspices of UNESCAP. The platform aims to involve different stakeholders in climate protection and the development of low carbon cities, i.e., cities with a low level of carbon dioxide emissions. The twenty-third panel of UNESCAP in October 2019 supported the proposal put forward by Mongolia and the Russian Federation to expand the activities and incorporate the Mongolian (Chingis, Tsetserleg) and the Russian (Ulan-Ude and Irkutsk) cities in the study on the development of low carbon cities.

The development of comprehensive measures on the mitigation of carbon dioxide emissions in the cities requires, first of all, an analysis of the current general state of the settlement (population, economy, climate, transport, and energy infrastructure), and also the ecological state.

This study considers the energy sector as one of the chief sectors of the economy in Irkutsk. The paper presents an assessment of carbon dioxide emissions caused by the operation of energy facilities.

II. Literature review

The world community has been discussing the issues of greenhouse gas emissions for long. The first reliable information on changes in climate and possible causes of its fluctuations appeared as far back as the 19th century [2], and the relation between these changes and the higher carbon dioxide concentration is validated by numerous studies [3-5].

However, the debates concerning the effect of greenhouse gases on climate both locally and globally are still going on. Of special concern is the human contribution to the accelerated warming in the last decades. The opinions of scientists on this issue vary. Some of them discuss the theories of natural cyclical changes caused by the release of space and solar plasma [6, 7], while others lay the stress on the anthropogenic effects due to human activity and increase in carbon dioxide emissions as a result of growing business activity [8, 9].

Recent decades have seen new records of the climatic changes, the mean temperatures rise, and the distribution of atmospheric precipitation changes. The area of glaciers, ice sheets, and arctic seawater ices shrinks faster than it was forecasted. The most significant climate change consequences both observed and forecasted were revealed in all European regions. Accordingly, the climate change consequences for seas are related to the rise in water temperature and acidity. In the coastal zones, the sea level rose, the shorelines eroded, the storms became more frequent and severe [10]. It is expected that in the future, there will be more intensive and numerous climate changes. Even if the greenhouse gas emissions were completely stopped now, the climate would continue to change for many decades because of earlier releases and inertia of the climatic system [10].

At present, the planet climate conservation issue is the focus of attention of practically all world's countries. The UN Framework Convention on Climate Change (UN FCCC) reflected the interest of the international community in decreasing greenhouse gas emissions in 1992. The goal of the Convention was to stabilize the greenhouse gas concentrations in the atmosphere at a level, which would prevent dangerous man-induced impact on the climatic system [11]. This Convention was signed by 197 countries, including those of the former USSR and all industrially developed countries. Later, in 1997, the Framework Convention was supplemented by the Kyoto Protocol that fostered the development of the provisions of the UN FCCC, calling for the developed countries to limit and cut down greenhouse gas emissions under the agreed national commitments. The Protocol was adopted since the Convention of 1992 contained only the calls to these countries to pursue a policy and take measures to prevent climate change. The Kyoto Protocol establishes specific emission reduction commitments for industrially developed countries, including the European countries. Generally, these commitments correspond to approximately a five-percent decrease in emissions against the 2012 levels [12]. With the complex process of the Kyoto Protocol ratification and the need to solve the problems of climate change, in 2015, the world community once again adopted the worldwide document, the so-called Paris Climate Agreement [13]. It formulates the issues of greenhouse gas emission mitigation somewhat differently. The Agreement suggested limiting global warming, providing temperature change by no more than 2°C by 2050, and preferably 1.5°C by 2040 with further zero (zeroing) growth of the global temperature on the planet. Essentially, it declared a transition to carbon-free technologies.

It is worth noting that many world's countries are affiliated with this process. The Paris Agreement was signed by 196 countries of the world, including Russia, China, Mongolia, Japan, European countries, and others. At the beginning of 2021, the USA also signed this Agreement.

The Russian Federation confirmed its commitment to the Paris Agreement (as of 2015) by the Russian Government Decree of September 21, 2019, and became an authorized participant in this international-legal instrument. In 2014, before signing the Agreement, Russia developed an Action Plan to ensure a reduction in greenhouse gas emissions by 2020 to a level of no more than 75% of the 1990 level (approved by the Decree of the Government of the Russian Federation of April 2, 2014, No. 504-r). And every five years, the Russian Federation undertakes to submit a report on Russia's contribution to the reduction of anthropogenic greenhouse gas emissions to the Secretariat of the UN Framework Convention on Climate Change. The Russian Federation adopted the Orders and Decrees (2014, 2015) on the inventory of greenhouse gas emissions, developed the guidelines for assessing emissions for various types of economic activities. In 2020, the Ministry of Economic Development of Russia prepared a draft long-term strategy for the development of the Russian Federation with a low level of greenhouse gas emissions until 2050 (March 2020).

The Asia-Pacific region countries also seek to transition to carbon-free technologies in their energy development [14]. The primary technologies aimed at achieving a climate-neutral world (zeroing emissions by 2050) include the use of renewable energy sources instead of coal for energy purposes; the involvement of electric transport (electric vehicles) with additional preferences in its operation; promotion of studies on the development of hydrogen technologies; bans on deforestation, and others.

The main focus is, of course, on the transformation of the energy sector, i.e., a change in the fuel and energy balance structure; energy conservation; an introduction of innovative technologies and intelligent systems for energy consumption and production; use of renewable energy resources, including hydro resources; industrial energy disposal, and others.

Table 1. The values of potentials of global warming caused by greenhouse gases.

Greenhouse gas	Chemical formula	Potential of global warming, t CO_2-equiv./t	Production process
Carbon dioxide	CO_2	1	Stationary fuel combustion, flaring, fugitive emissions, oil refining. Production: coke, concrete, lime, glass, ceramic wares, ammonia, ferroalloys, primary aluminum. Petrochemistry, ferrous industry, air, railway transport, and other industrial processes.
Methane	CH_4	25	Flaring, fugitive emissions
Nitrogen oxide	N_2O	298	Production of nitric acid, caprolactam, glyoxal, and glyoxalic acid.
Fluoroform	CHF_3	14 800	Production of fluorine-containing compounds.
Perfluoromethane	CF_4	7 390	Production of primary aluminum.
Perfluoroethane	C_2F_6	12 200	Production of primary aluminum.
Sulfur hexafluoride	SF_6	22 800	Production of fluorine-containing compounds

Since it is rather difficult to stop using fossil fuel in the near future, the world community has proposed developing commercially viable clean coal technologies with 100% of CO_2 capture as soon as possible. Carbon capture and storage technology allows capturing waste carbon dioxide from flue gases of power plants based on the methods of absorption, adsorption, membrane gas separation, and others [15]. Experts claim that technically the capture and storage of large amounts of CO_2 will not pose a big problem. Moreover, the widespread use of these technologies can significantly contribute to the achievement of the ambitious climate targets set by the Paris Agreement.

In 2019, the world had 17 carbon disposal projects aimed at capturing up to 31.5 million tons of CO_2 per year, with 3.7 million tons stored in geological structures [16].

At the initiative of the Global Energy Association for the development of international research and projects in the field of energy and with the direct participation of the world expert community representatives, breakthrough energy technologies have been developed to minimize or avoid carbon dioxide emissions [17].

The technologies for mitigation of greenhouse gas emissions also include new technologies for energy production and conversion, which involve creating closed thermodynamic cycles with zero emissions [18]. Specific features and advantages of such technologies are oxygen fuel combustion accompanied by the production of water vapor and carbon dioxide with the condensation of the latter, its capture, and transportation to the storage site.

The efficient use of resources and the creation of a low carbon society are the focus of the world's discussions on the transition to the "green" economy, which is reflected in the mid-and long-term plans of Europe's development [19]. The Action Plan for the transition to the low carbon economy suggests that the emissions of the European community must be decreased by 80% by 2050 against the 1990 level based on the internal mitigations.

Thus, to date, a global opinion has been formed, which is supported and authorized by the relevant documents aimed at reducing greenhouse gas emissions and using carbon-free or low carbon technologies for the vital activities of the planet's population.

III. The Methodology of Investigation

Since June 2015, the Order of the Ministry of Natural Resources of the Russian Federation No. 300 has been in effect in Russia, which approves methodological guidelines and guidance for quantifying the greenhouse gas emissions by organizations engaged in various economic activities [20]. These guidelines are based on the Action Plan to decrease greenhouse gas emissions by 2020, which was approved by Order No. 504-r of the Government of the Russian Federation dated April 2, 2014. The main goal of the Plan is to ensure that by 2020 Russia's greenhouse gas emissions do not exceed 75% of the 1990 emissions [21].

The methodological guidelines establish a procedure for quantifying greenhouse gas emissions for their monitoring, reporting, and verifying. Since 2017, all enterprises with emissions of more than 50 thousand tons of CO_2-equiv. per year must report on greenhouse gas emissions.

The developed Greenhouse Gas Inventory Methods are based on the international recommendations, are approved by the Ministry of Natural Resources of the Russian Federation, and include all categories of sources and sinks of greenhouse gases.

In general, seven gaseous compounds, which cause the so-called greenhouse effect, i.e., upset the planet's heat exchange, are classified as greenhouse gases (Table 1). The data on the global warming potential for the selected greenhouse gases were developed following Decision 24 / SR.19 of the Conference of the Parties engaged in the UN Framework Convention on Climate Change, ratified by Federal Law No. 34 of 04.11.1994 "On Ratification of the UN Framework Convention on Climate Change" [22, 23]. The gases indicated in the Table have different warming potential: carbon dioxide has the lowest potential, and sulfur hexafluoride (released during the production of fluorine-containing compounds) has the highest potential.

Among different production processes, energy facilities and especially fossil fuel combustion cause the greatest emissions of greenhouse gases and primarily CO_2.

The greenhouse gas emissions are determined quantitatively by different methods designed for corresponding categories of their sources:

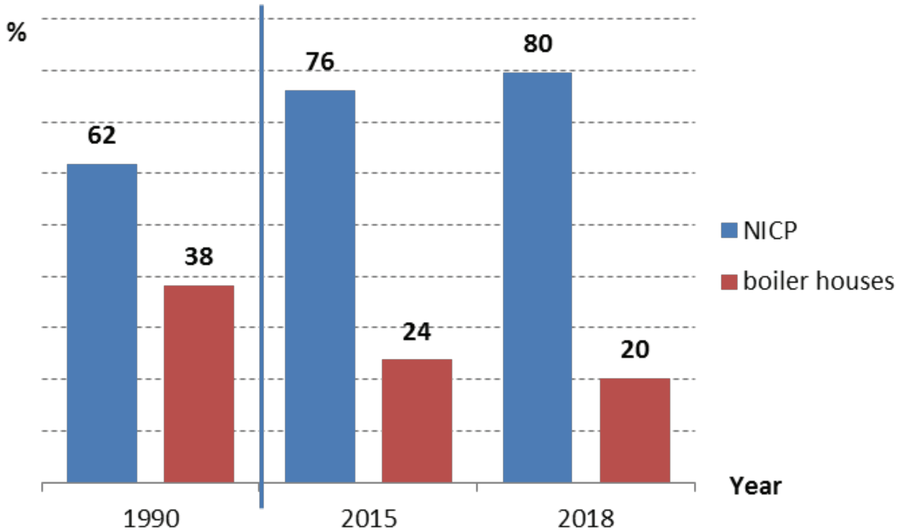

Fig. 1. Dynamics of fuel consumption structure by energy facilities in the city of Irkutsk.

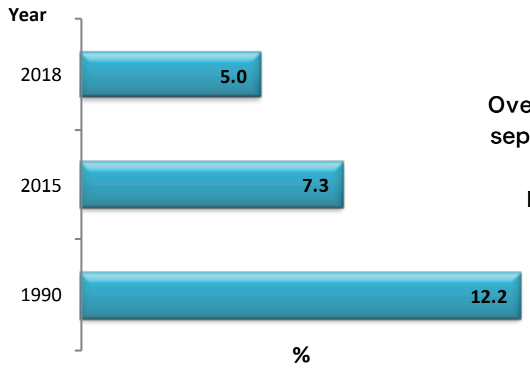

	1990	2015	2018
Overall, energy facilities		1615,7	1658,4
sep.: fuel oil	205,2	117,5	82,6
coal	1473,9	1498,2	1575,9
proportion of fuel oil	12,2	7,3	5,0

Fig. 2. Dynamics and share of fuel oil in fuel consumption structure for energy facilities in the city of Irkutsk.

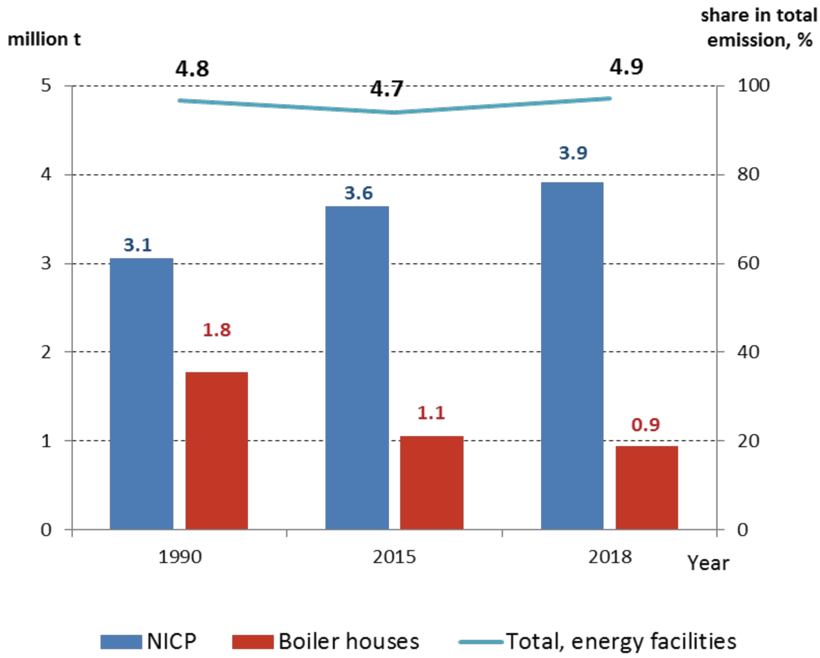

Fig. 3. Dynamics of emissions and assessment of the contribution of energy facilities to the total CO_2 emission in Irkutsk city in 1990, 2015 and 2018.

Table 2. Dynamics of fuel consumption by type in irkutsk, thousand tce.

Energy facilities	Fuel			Year	
			1990	2015	2018
NICP	fuel oil		17.9	2.4	2.1
	brown coal		1 019.5	1 228.5	1 319.6
		total	*1 037.4*	*1 230.9*	*1 321.7*
Boiler houses	fuel oil		187.3	115.1	80.4
	coal	brown	454.4	253.6	246.4
		hard		16.1	9.9
		total	*641.7*	*384.8*	*336.7*
Total			1 679.1	1 615.7	1 658.4

- the calculation method based on the periodic measurements of emissions;
- the method of the continuous monitoring of greenhouse gas emissions;
- the calculation method based on material balance;
- the calculation method based on the data on the enterprise performance and the emission factors.

The calculation methods relying on periodic measurements and continuous monitoring of greenhouse gas emissions employ the results of instrumental measurements at the enterprises for a period (year) at issue. These results are given in the protocols of measurements, technical specifications, reports of inventory checks of emission sources, data on in-process control of emissions and production of waste, and others. The rate of data logging and the methods of their averaging are chosen by the organization individually so as to provide their objectivity for the considered period.

Calculation based on the material balance assumes the use of data from the accounting documents on the consumption of raw materials, fuel, and materials; production of products (for example, technical reports, balances, statistical reporting forms, and others); quality certificates, and other sources of information. The calculation takes into account changes in the reserves of resources at the enterprise [20].

The input data for the greenhouse gas emission calculation by the method based on the data on enterprise performance and emission factors are the actual data, which characterize the enterprise activity for the sample period (for example, fuel consumption by type, consumption of carbon-containing materials), greenhouse gas emission factors, calculated factors of carbon content in fuel, and component composition for gaseous fuel.

This study relies on the methodological guidelines [20] for the category of stationary fuel combustion to estimate the greenhouse gas emissions from energy enterprises generating electric and thermal energy. At the same time, only carbon dioxide (CO_2) emissions are classified as greenhouse gas emissions subject to mandatory accounting (in this category of emission sources).

IV. Results

The primary energy facilities for electricity and heat supply to the population and industrial enterprises of Irkutsk are boiler houses of different capacities, the Irkutsk HPP, and one large thermal power plant, i.e., the Novo-Irkutsk cogeneration plant (NICP). The installed capacity of the Irkutsk HPP is 662.4 MW, NICP – 708 MW, which characterizes Irkutsk as the city with a high share of renewable energy sources. The electric power generated at the Irkutsk HPP covers the city's demands and ensures the functioning of large enterprises in the nearest populated areas: the Irkutsk aluminum smelter (Shelekhov town) and Irkutsk aircraft plant, which is currently increasing its production capacities. On the whole, the industry share in energy consumption of the city reaches 66%. The rest of the electric power covers population needs. The main consumers of thermal energy produced by the NICP and municipal and departmental boiler houses are the population and social infrastructure.

In 2018 there were 89 boiler houses in the city, of which 57 used coal, 17 used liquid fuel (primarily fuel oil), and 15 were electric boiler houses. One boiler house burns fuelwood, i.e., sawdust. The city has no renewable energy sources for large-scale thermal energy production. Electric boiler houses and a boiler house running on fuelwood are not considered in assessing the CO2 emissions from boiler houses, and only coal and fuel oil-fired boiler plants will be analyzed further.

To calculate the CO2 emissions from energy facilities (boiler houses on fossil fuel and the NICP) in Irkutsk, fuel consumption was analyzed for 1990, 2015, and 2018.

A. Fuel consumption by energy facilities in the city of Irkutsk

The consumption of fuel in 2015 and 2018, given its types, was determined using the data of heat supply schemes of Irkutsk for different years of their updating [24, 25], the State report on the protection of Lake Baikal [26], and the data of technical specifications of heat sources of the municipality of Irkutsk [27]. Brown coal is the primary fuel for thermal energy facilities of the city, Table 2.

Table 3. Calculated co2 emission from energy facilities in irkutsk city, thousand tons/year.

Energy facility	Year		
	1990	2015	2018
NICP	3 058.4	3 641.7	3 910.9
Boiler houses	1 770.2	1 056.6	939.3
Total	4 828.5	4 698.4	4 850.1

The data on the amount of fuel burnt by the Irkutsk boiler plants and the NICP in 1990 are taken from the 1995 and 1999 official letters of the JSC “Irkutskenergo”.

At present, the NICP burns primarily brown coal imported from the Kansk-Achinsk basin. Boiler houses use coal from local deposits of the Irkutsk region: brown coals and, in small amounts, hard coal.

For the considered period, the total fuel consumption (coal and fuel oil) by all energy facilities of the city is estimated at 1.6-1.7 million tce per year.

The major fuel consumer among the energy facilities is the NICP, with its share in the fuel consumption structure ranging from 62 to 80% in different years, Figure 1.

As seen from Figure 1, the share of boiler houses in the total fuel consumption declined almost twice (from 38% in 1990 to 20% in 2018) with a significant increase in the share of NICP.

In the total fuel consumption structure, the fuel oil share gradually decreases from 12.2% in 1990 to 5% in 2018, i.e., by 2.5 times, Figure 2.

B. Assessment of carbon dioxide emissions from energy facilities in the city of Irkutsk

The calculations of carbon dioxide emissions from energy facilities with stationary fuel combustion are based on Order No. 300 of June 15, 2015 [28]. It is worth noting that greenhouse gases emitted by this category of sources includes only CO_2 emissions due to the combustion of all liquid and hard fuel types used at boiler units to produce heat and/or electricity. Methane (CH4) and nitrogen oxide (N2O) emissions, which are potentially likely during stationary fuel combustion, are not considered.

The calculation results for carbon dioxide emissions from energy facilities of Irkutsk city are presented in Table 3.

The calculations show that the amount of CO2 from the city's energy facilities in different periods is 4.7 (2015) to 4.9 million tons (2018). The emissions of 2018 exceed those of the so-called reference year of 1990 by 21.6 thousand tons. Whereas according to the plans of the Russian Government, the emissions in 2020 must be equal to 75% of the 1990 level, i.e., no more than 3.6 million tons for Irkutsk city.

The thermal power plant (Novo-Irkutsk cogeneration plant) is the main contributor to CO_2 emissions, with its share in the total carbon dioxide emissions increased from 63% to 80% in 2018, compared to 1990 (Fig. 3). Correspondingly, the contribution of boiler houses to the total CO2 emissions from energy facilities in Irkutsk city reduced from 37% in 1990 to 19% in 2018.

A decrease in coal consumption by boiler houses and the replacement of some of them with one large-scale energy source, i.e., the Novo-Irkutsk cogeneration plant, led to an increase in the plant fuel consumption. In turn, carbon dioxide emission from the NICP increased by 26% against the 1990 level.

The lowest-carbon energy facilities are electric boiler houses. However, their number has not changed over the period under review (15 electric boiler houses in 2018 [25]). Moreover, future measures to improve heat supply to consumers in Irkutsk city do not include any plans for increasing the number of electric boiler houses and sources using renewable energy.

Although the regional energy companies make their efforts to implement the program to close economically and environmentally ineffective small-capacity boiler houses and connect heat consumers to the main source in the city, i.e., the NICP, the issue of reducing carbon dioxide emissions is unlikely to be resolved. In this regard, measures are necessary to reduce (save) fuel consumption at all energy facilities of the city, including the NICP.

V. Conclusion

The study provides a comparative analysis of the estimated carbon dioxide emissions from energy facilities in Irkutsk in 1990 and 2018. It is a starting stage in creating a city with a low carbon status, i.e., a city with low carbon dioxide emissions. Currently, emissions from energy facilities being the primary sources of CO_2 in the city, are estimated at 4.9 million tons per year. These emissions have already exceeded the level of 1990 by 26 thousand tons. The set goals (75% of the 1990 level) can be achieved by reducing carbon dioxide emissions by at least 1.3 million tons.

With the existing energy infrastructure, Irkutsk has the potential to reduce carbon dioxide emissions. It can be implemented by cutting down fuel consumption through the adoption of innovative combustion technologies, the use of available coal-grading technology, and the increase in the number of electric boiler houses.

Modernization of the Irkutsk hydropower plant through the replacement of hydraulic units with expired service life by new ones will contribute to the energy efficiency enhancement in the near future, which will increase the plant's capacity by 20%. Thus, it will be possible to additionally generate up to 200 million kWh of electricity per year, using the same amount of water as before the reconstruction.

The low carbon development of the city will largely depend on the development plans of Irkutsk city in the future. The question of whether Irkutsk will be a low carbon city is complicated as it requires answers to many sub-questions related to the development of a healthy urban environment. It is necessary to organize constant and continuous metering of energy consumption, to establish an energy conservation service, which will enable both individual enterprises and the entire city to significantly save energy resources.

Conversion of the city's energy facilities to gas can be one of the essential and realistically achievable measures. The use of natural gas as a fuel in the boiler houses and the cogeneration plant of the city will reduce carbon dioxide emissions more than twice against the 2018 level. Moreover, there is the Kovykta gas condensate field prepared for large-scale production in the Irkutsk region. Coordinated actions of the city and regional authorities will make it possible to convert consumers to gas not only in the cities and towns of the Irkutsk region but also in the neighboring regions.

Special attention should be paid to the transport segment, both public and personal means of transportation. Given that the city has the lowest electricity tariff in Russia, this fact should become the main stimulus for the development of electric transport.

With such a tariff policy pursued, it is also possible to carry out a gradual transition of private households to electric heating instead of the stove and often coal heating.

Wind generators and solar panels are represented by single instances (in the private sector) in Irkutsk city. The prospects for the development of renewable energy sources are limited, first of all, by the low cost of electricity. The successful use of renewable energy sources in the city in general seems unlikely without a policy focused on their support at the municipal, regional and federal levels.

Thus, to reduce carbon dioxide emissions in Irkutsk city, it is necessary to formulate a comprehensive program of carbon-free development, which should reflect not only the stages of a gradual transition to low carbon technologies but also a list of dedicated measures for specific types of economic activity. This issue must be addressed comprehensively in both the city energy sector and the entire infrastructure, from urban development to enterprises related to life support and fulfillment of various needs of citizens.

Acknowledgments

The research was carried out under the State Assignment Project of the Fundamental Research Program of Russian Federation 2021-2030 (FWEU-2021-0004 № AAAA-A21-121012090010-7).

References

[1] *Climatically neutral cities.* UN Economic Commission for Europe, Geneva, Switzerland, 2011, 116 pp. (in Russian).

[2] S. Arrhenius, "On the influence of carbonic acid in the air upon the temperature of the Earth," *The Astronomical Society of the Pacific*, Vol 9, No 54, pp 14-24, 1897. Available at: https://doi.org/10.1086/121158. (accessed 05.02.2021)

[3] J.T. Houghton, Y. Ding, D.J. Griggs, et al., "Climate change 2001: the scientific basis", *The Press Syndicate of the University of Cambridge*, 2001.

[4] Intergovernmental Panel of Climate Change, "Climate change 2014: mitigation of climate change", *Cambridge University Press*, Vol. 3, 2005.

[5] K.Ya. Kondratiev, V.F. Krapivin, "Modeling the global carbon cycle," Moscow, Russia, FIZMATLIT, 2004, 336 p. (in Russian).

[6] L.S. Kartunova, "Climate changes, causes and effects," *Science, education and culture*, No 1 (25), Moscow, Russia, 2018. Available at: https://cyberleninka.ru/article/n/izmeneniya-klimata-prichiny-i-posledstviya/viewer (accessed 05.02.2021) (in Russian).

[7] N.V. Petrov, "The clue to understanding the mechanism of global climate change of the planet and its long-term forecast," *Academy of Trinitarianism*, El No 77-6567, publ.26667, Moscow, Russia, 2020. Available at: http://www.trinitas.ru/rus/doc/0016/001h/00164494.htm (accessed 15.02.2021) (in Russian).

[8] L.V. Bondarenko, O.V. Maslova, A.V. Belkina, K.V. Sukhareva, "Global climate change and its effects," *Bulletin of the Plekhanov Russian University of Economics*, no (2), p. 84-93, 2018. Available at: https://doi.org/10.21686/2413-2829-2018-2-84-93 (accessed 02.15.2021) (in Russian).

[9] Yu.G. Peshcherov, G.I. Peshcherov, "Focused anthropogenic influence on climate as a threat to vital activity of human society," *Bulletin of Eurasian Science*, No 2, 2018. https://esj.today/PDF/89NZVN218.pdf (Free access) Available at: https://cyberleninka.ru/article/n/tselenapravlennoe-antropogennoe-vliyanie-na-klimat-kak-ugroza-zhiznedeyatelnosti-chelovecheskogo-obschestva/viewer (accessed 02.05.2021) (in Russian).

[10] *The environment of Europe. State and prospects 2015.* Synthesis report, European Environment Agency, EEA, Copenhagen, 2015, 199 p. (in Russian).

[11] *UN Framework Convention on Climate Change, as of May 9, 1992,* UN Site, 2021. Available at: https://www.un.org/ru/contact-us/index.html. (accessed 05.02.2021) (in Russian)

[12] *What is the Kyoto Protocol?* United Nations Framework Convention on Climate Change, UN Site, 2021. Available at: https://unfccc.int/ru/kyoto_protocol (accessed 26.02.2021) (in Russian).

[13] *The Paris Agreement, 2015*, UN Site. Available at: https://unfccc.int/process-and-meetings/the-paris-agreement/the-paris-agreement (accessed 26.02.2021) (in Russian).

[14] *Materials of the North-Asian International Conference "NICE' for Economic Development",* Niigata, Japan, 3-rd Stage "Japan-Russia Energy and Environment Dialogue – the Paris Agreement and Energy Security in Northeast Asia," 2021, Available at: https://www.erina.or.jp/en/activities/seminars/nice/2021nice/3rd-stage/ (accessed 26.02.2021)

[15] M. Bui, C.S. Adjiman, A. Bardow, E.J. Anthony, A.

Boston, S. Brown, P.S. Fennell, S. Fuss, A. Galindo, L.A. Hackett, "Carbon capture and storage (CCS): the way forward," JP, 2018.

[16] B. Metz, O. Davidson, H. C. de Coninck, M. Loos, and L.A. Meyer (eds.), "IPCC special report on Carbon Dioxide Capture and Storage," *Cambridge University Press*, Prepared by working group III of the Intergovernmental Panel on Climate Change, Cambridge, United Kingdom and New York, NY, USA, 2005.

[17] *Ten breakthrough ideas in the energy sector for the next ten years,* Association "Global energy," 2020, 106 p. (in Russian).

[18] V.O. Kindra, A.N. Rogalev, N.D. Rogalev, "The oxyfuel technologies of electricity generation with zero emissions of harmful substances into the atmosphere," *Proc. of the International Scientific Conference of Young Scientists and Experts "Ecology of energy-2017"*, Moscow, Russia, Publishing House of MEI, 2017, pp.110-113.

[19] *Net Zero: The UK's contribution to stopping global warming*, The Committee on Climate Change, 2019.

[20] *Methodological guidelines and guidance of quantitative determination of volumes of greenhouse gas emissions by the organizations undertaking economic and other activities in the Russian Federation. Approved by the Order of the Ministry of Natural Resources of Russia of 30.06.2015.* Moscow, Russia, 2015. Available at: http://sro150.ru/metodiki/371-metodika-rascheta-vybrosov-parnikovykh-gazov (accessed 26.02.2021) (in Russian).

[21] *Regulation of the RF Government No. 504-r of 02.04.2014 (ed. 17.06.2016) "On approval of the action plan to ensure the reduction of greenhouse gas emission volumes by 2020".* Moscow, Russia, 2016. Available at: https://legalacts.ru/doc/rasporjazhenie-pravitelstva-rf-ot-02042014-n-504-r/ (accessed 26.02.2021) (in Russian).

[22] *The Federal Law No. 34-FZ of 04.11.1994 "On ratification of the UN Framework on Climate Change."* Moscow, Russia, 1994. Available at: https://legalacts.ru/doc/federalnyi-zakon-ot-04111994-n-34-fz-o/ (accessed 26.02.2021) (in Russian).

[23] *Framework Convention on Climate Change*, The official site of the United Nations Organization. Available at: http://unfccc.int/ (accessed 26.02.2021) (in Russian).

[24] *The heat supply scheme of the city of Irkutsk up to 2031 (updating for 2018).* Irkutsk, Russia, 2019. Available at: https://admirk.ru/Pages/search.aspx?k=схема%20теплоснабжения%20г.%20иркутск%20до%202031%20г (accessed 15.09. 2020) (in Russian).

[25] *The heat supply scheme of the city of Irkutsk up to 2033 (updating for 2020).* Irkutsk, Russia, 2020. Available at: https://admirk.ru/Pages/generalniy-plan-goroda.aspx (accessed 15.09. 2020) (in Russian).

[26] The State report "On the state of Lake Baikal and measures on its protection in 2017," Irkutsk, ANO "CC Expert," Russia, 2018, 340 p. (in Russian).

[27] The Passport of the housing and communal services of MF of Irkutsk as of 1.01.2015, Irkutsk: RGD "Analytic operating-dispatching department of the housing and communal services of the Irkutsk region," Russia, 2015. (in Russian).

[28] *The Order No. 300 of the Ministry of Natural Resources of Russia of 30.6.2015 "On approval of methodological guidelines and guidance of quantitative determination of volumes of greenhouse gas emissions by the organizations undertaking economic and other activities in the Russian Federation."* Moscow, Russia, 2015. Available at: https://www.rosteplo.ru/Npb_files/npb_shablon.php?id=1740 (accessed 20.07.2020) (in Russian).

Elena Maysyuk Ph.D. in economics (2002), Senior Researcher of the Laboratory of Energy Supply to Off-grid Consumers, Melentiev Energy Systems Institute SB RAS, Irkutsk.
She graduated from the Energy faculty of the Irkutsk Polytechnic Institute with a major in Heat power plants (1989).
Her research area includes environmental issues of energy systems development in East Siberia and the Far East.
She authored and co-authored more than 85 publications, including chapters and sections in 20 collective monographs.

An Optimization Algorithm to Determine Apparent Power of Active Filter

L.I. Kovernikova[1, 2*], Bui Ngoc Hung[2, 3], O.N. Vojtov[1], L.V. Semenova[1], Ha Thi Chuc[3], Pham Duc Tien[4]

[1] Melentiev Energy Systems Institute of Siberian Branch of Russian Academy of Sciences, Irkutsk, Russia
[2] Irkutsk National Research Technical University, Irkutsk, Russia
[3] Ha Noi University of Mining and Geology, Ha Noi, Viet Nam
[4] Wong Bi - TKV - Vinasovin Coal Company, Ha Noi, Viet Nam

***Abstract* — The coal grading plants in Viet Nam extensively apply induction motors. Induction motors consume active and reactive power from the power supply systems. The reactive power flowing through the electrical network creates active power losses. The reactive power received from power utilities reduces the load power factor at the node where coal sorting plants are connected to the supply network. Frequency-controlled induction motors introduce distortions into the electrical network because they are electrical equipment with a nonlinear current-voltage characteristic. Non-sinusoidal current and voltage cause additional losses of active power in the electrical network and electrical equipment, thereby shortening its service life, reducing the reliability of operation, and causing economic damage. Active filters can solve these problems. The paper proposes an optimization algorithm for determining the apparent power of the active filter, which provides the load power factor and power quality indices corresponding to the regulatory documents. The algorithm is used to calculate the apparent power of the active filter for the coal grading plant owned by the Vietnamese company "Cua Ong-Vinacomin."**

***Index Terms*—Active filter, algorithm, harmonic, load power factor, power quality index.**

* Corresponding author.
E-mail: kovernikova@isem.irk.ru

http://dx.doi.org/10.38028/esr.2021.01.0003
Received March 05, 2021. Revised March 07, 2021.
Accepted March 13, 2021. Available online May 26, 2021.

I. Introduction

Coal mining is one of the most important economic industries of Viet Nam. Mines and quarries have coal grading plants. Induction motors, primarily with frequency control, drive the manufacturing equipment of the plants. They are nonlinear loads for the power supply system and distort power quality. The harmonic factors of voltage exceed the established standards [1]. Voltages and currents contain both harmonics and interharmonics [2]. The load power factors are lower than the value established by the normative documents [3].

In [4-7], the authors determine the active filter power to reduce the voltage and current harmonics in the electrical network. The power of the active filter is not only determined by the power of the harmonics. The use of the active filter is not confined only by the need to reduce harmonic values. Many consumers have additional economic losses because their electrical equipment receives reactive power from the supply network. In this context, the load power factor at the node connecting the power supply system of consumers to the supply network is lower than the standard value established for consumers. In [8-11], the authors use the active filter to compensate for reactive power and reduce harmonics. The authors of these papers do not consider active power losses due to reactive power transmission through the electrical network. Consumers have to pay for these losses and thus face additional economic damage. In [12-15], the authors determine the power of active filter to compensate for reactive power and reduce the values of harmonics, thereby providing the minimum losses of active power during the transmission of reactive power and the flow of harmonic currents in the electrical network of the power supply system.

The paper is concerned with an analysis of the power supply system of the coal grading plant, and results of the power quality tests. It formulates an optimization

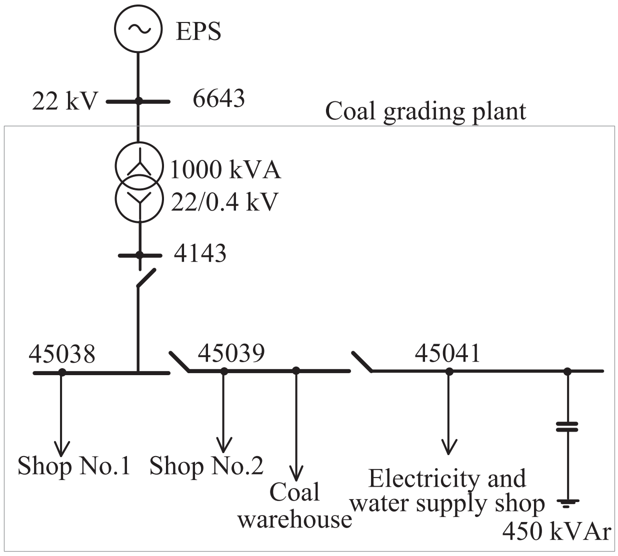

Fig. 1. Power supply system of the coal grading plant.

problem, describes an algorithm to determine the apparent power of the active filter, and presents specially designed software and results of the active filter apparent power calculation for the coal grading plant of the company "Cua Ong-Vinacomin."

II. Characteristic of the power supply system and loads of the coal grading plant

Fig.1 presents a scheme of the power supply system of the coal grading plant.

Electrical power from the 22 kV substation buses of the power supply utility (node 6643) is supplied to the 0.4 kV network of the power supply system of the coal grading plant (node 4143) by the 1000 kVA step-down transformer that belongs to the plant. The distance between nodes 4143 and 45038 is 60 meters. The total length of the 0.4 kV electrical network exceeds 12 km. The plant has two coal grading shops (shop No.1, shop No. 2), a shop of electricity and water supply, and a coal warehouse. Coal is mined in the quarry and transported to the warehouse of the coal grading plant. In the warehouse, the excavator unloads coal on the conveyor. The conveyor delivers coal to the shops for grading it by size. Fifty-eight induction motors with a capacity of 4 to 185 kW put the technological equipment of the shops into operation.

The following indices and norms for their values were established in [1] to assess voltage and current values in the 0.4 kV network:

- the voltage deviation $|\delta U| \leq 5.0\%$;
- the total harmonic distortion $K_U \leq 6.5\%$;
- the h-th harmonic factor of voltage $K_{U(h)} \leq 3\%$;
- the h-th harmonic factor of current $K_{I(h)} \leq 12\%$.

In [2], the load power factor (cos φ) at the connection node of the plant to the supply network should meet the condition cos φ ≥0.85. If this condition is not fulfilled, the company, owner of the plant, pays penalties to the power supply utility. The value of cos φ can be low because of large reactive power consumption by the electrical motors of the plant, active power losses when transmitted over the electrical network, and losses caused by harmonics and interharmonics. Power quality indices and the value of cos φ at node 4143 were tested.

Table 1. Measured δU, K_U, %.

Parameter	Phase A	Phase B	Phase C
δU_{max}	4.1	4.5	4.6
δU_{min}	-1.3	-1.7	-1.4
$\lvert\delta U_{norm}\rvert$		≤ 5.0	
K_{Umax}	**16.8**	**15.3**	**17.1**
K_{Unorm}		≤ 6.5	

Table 2. Measured $K_{U(h)}$, $K_{I(h)}$, %.

Parameter	Harmonic						
	3	5	7	11	13	17	23
$K_{U(h)maxA}$	2.5	**12.7**	**12.8**	**4.6**	2.1	**3.3**	**3.1**
$K_{U(h)maxB}$	**3.9**	**12.3**	**11.8**	**4.6**	**3.1**	2.7	2.8
$K_{U(h)maxC}$	2.0	**12.3**	**12.8**	**3.6**	2.8	**3.4**	**3.4**
$K_{U(h)norm}$				≤ 3.0			
$K_{I(h)maxA}$	7.1	6.8	6.7	3.9	1.9	2.3	2.7
$K_{I(n)maxB}$	3.9	4.2	1.7	0.8	1.1	0.5	0.4
$K_{I(h)maxC}$	3.6	4.9	3.3	1.2	1.7	1.5	1.2
$K_{I(h)norm}$				≤ 12.0			

Table 3. Measured $K_{U(M)}$, %, $I_{(M)}$, A.

Parameter	Interharmonic						
	1.5	3.5	5.5	7.5	17.5	19.5	21.5
$K_{U(m)maxA}$	3.9	1.0	1.7	1.8	1.2	1.5	2.3
$K_{U(m)maxB}$	3.3	0.8	1.9	1.9	1.0	1.3	2.3
$K_{U(m)maxC}$	3.8	0.9	0.9	1.2	1.7	1.7	1.7
$I_{(m)maxA}$	16.6	6.0	5.1	4.3	7.5	8.5	9.6
$I_{(m)maxB}$	17.2	4.8	5.0	2.7	1.9	2.7	3.2
$I_{(m)maxC}$	18.0	7.3	6.4	5.3	9.2	9.7	7.5

Table 4. Measured cos φ, p.u.

Parameter	Phase A	Phase B	Phase C
cos φ_{max}	0.98	0.92	0.99
cos φ_{min}	0.89	**0.72**	0.89
cos φ_{norm}		≥0.85	

III. Results of the electrical energy tests

The tests included 24-hour measurements of the voltage and current quality indices and cos φ by the device PQ-Box150 [16] with a time interval of measurements equal to 1 second.

Table 1 presents the measured values of δU, which meet the requirements [1]. The Table also shows the measured values of K_U and their normative values from [1]. The measured values of K_U exceed the norm more than twice. They are shown in bold type.

Table 2 presents the measured and normative values of $K_{U(h)}$ and $K_{I(h)}$ for the harmonics that exceed the norms

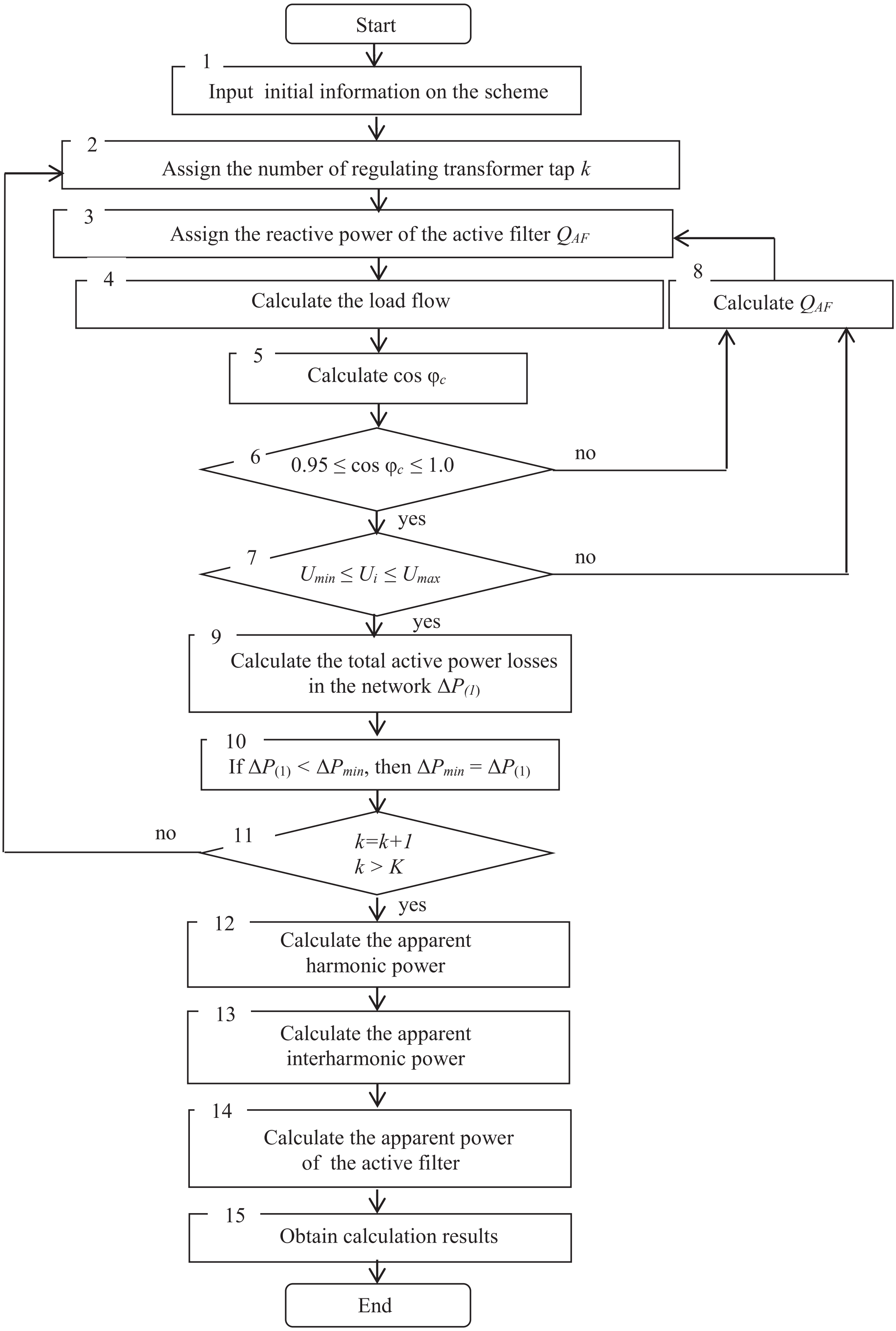

Fig. 2. Block-diagram of the algorithm to determine the power of the active filter.

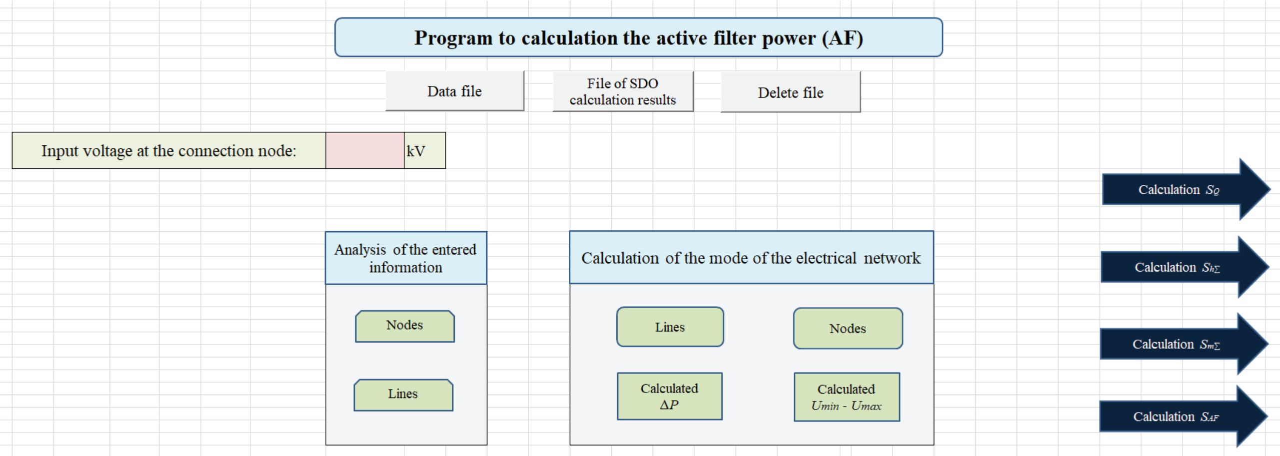

Fig. 3. Sheet 1 of the program.

most frequently [1]. The measured values of $K_{I(h)}$ are not higher than the normative value.

The measured values of $K_{U(m)}$ for some interharmonics and the values of currents $I_{(m)max}$ of these interharmonics (m – the number of the interharmonic) are given in Table 3. The normative values for them are not determined.

The measured values of cos φ and its normative value determined in [3] are shown in Table 4. At phase B, the value of cos φ is lower than the norm.

The problems caused by harmonics, interharmonics, and cos φ can be resolved using a shunt active filter connected to the network in parallel to the nonlinear load [7-15, 17-20].

IV. Optimization problem to determine the power of the active filter

The power of the active filter is determined by the reactive power to be generated to compensate for the reactive power of load and apparent power required to get rid of harmonics and interharmonics of the current at the point of the filter connection to the network. This can be achieved by solving an optimization problem with the objective function assumed to be the minimum active power losses in the power system network after installation of the active filter, i.e.,

$$\sum_{h=1}^{H} \Delta P_{(h)} + \sum_{m=1}^{M} \Delta P_{(m+\frac{1}{2})} = \min \,, \qquad (1)$$

where H is the highest number of the harmonic, $(M - 1/2)$ is the highest number of interharmonic. In this case, the following constraints are to be met

$$0.95 \le \cos\varphi \le 1.0, \qquad (2)$$

$$U_{min} \le U_i \le U_{max}, \qquad (3)$$

$$K_{U(h)min} \le K_{U(h)f} \le K_{U(h)max}, \qquad (4)$$

$$K_{Umin} \le K_{Uf} \le K_{Umax}, \qquad (5)$$

$$K_{I(h)min} \le K_{I(h)f} \le K_{I(h)max}, \qquad (6)$$

where i is the network node number; U_i is the voltage of the fundamental frequency; U_{min}, U_{max} are the normative minimum and maximum voltages of the fundamental frequency; cos φ is the load power factor at the node connecting the plant to the supply network; $K_{U(h)f}$ is the h-th harmonic factor of voltage after installation of the active filter; $K_{U(h)min}$, $K_{U(h)max}$ are the normative maximum and minimum of the h-th harmonic factor of voltages; K_{Uf} is the total harmonic distortion after installation of the active filter; K_{Umin}, K_{Umax} are the normative maximum and minimum of the total harmonic distortion; $K_{I(h)f}$ is the h-th harmonic factor of current after installation of the active filter; $K_{I(h)min}$, $K_{I(h)max}$ are the normative maximum and minimum of the h-th harmonic factor of current. Constraint (2) was established by the company "Cua Ong-Vinacomin".

The optimization problem consists of three subproblems:

1. calculation of the apparent power of the active filter to provide the normative cos φ;
2. calculation of the apparent power of the active filter to eliminate current harmonics;

Table 5. Q_{AF} and $\Delta P_{(1)\Sigma}$ calculated by the algorithm.

U_{4143}, kV	Q_{AF}, kVAr	$\Delta P_{(1)\Sigma}$, kW
0.38	350	297
0.39	480	290
0.40	330	192
0.41	450	134
0.42	580	110

Table 6. U_{min}, U_{max}, and cos φ_{4143} calculated by the algorithm.

U_{4143}, kV	cos ϕ_{4143}, p.u.	U_{min}, kV	U_{max}, kV
0.38	0.98	0.38	0.39
0.39	0.97	0.38	0.39
0.40	1.00	0.38	0.39
0.41	0.99	0.38	0.41
0.42	1.00	0.38	0.41

Table 7. Active, reactive, and apparent powers of harmonics.

Parameter	Phase A	Phase B	Phase C
P_h, kW	8.9	6.9	7.2
Q_h, kVAr	11.0	7.3	14.4
S_h, kVA	14.1	10.1	16.1

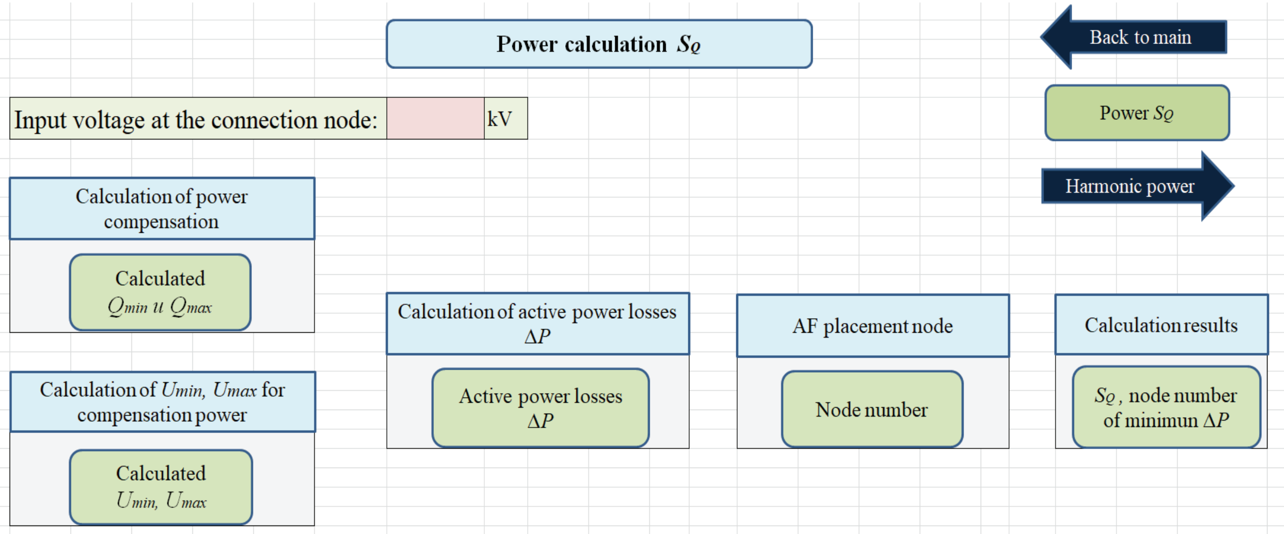

Fig. 4. Sheet 2 of the program.

3. calculation of the apparent power of the active harmonic filter to eliminate current interharmonics.

The first subproblem is formulated as follows: minimize the total active power losses in the network at the fundamental frequency, i.e.

$$\Delta P_{(1)} = \min. \tag{7}$$

In this case, constraints (2) and (3) should be fulfilled. If a node for active filter installation is not assigned, all nodes of the network must be considered as candidates for installation. The algorithm must consider transformer capabilities of voltage control on the lower side with the connected load. The suggested algorithm was developed based on the software "SDO" to calculate the fundamental frequency load flow [21-22]. The block diagram of the algorithm is presented in Fig. 2.

Block 1. Input initial information on the electrical network scheme.

Block 2. Assign the number of transformer tap k, $k = \overline{1,K}$, K is the quantity of taps.

Block 3. Assign the reactive power value of the active filter at the first step $Q_{AF} = 0$.

Block 4. Calculate the load flow.

Block 5. Calculate cos φ at the connection node of the power supply system of the plant to the supply network based on the results of calculation using the expression $\cos\varphi_c = P_{ij}/\sqrt{P_{ij}^2 + Q_{ij}^2}$, where "*c*" is an abbreviation of "calculated," P_{ij} and Q_{ij} are the active and reactive powers, *i, j* are the network node numbers.

Block 6. Test fulfillment of constraint (2). If it is fulfilled, go to Block 7, otherwise, go to Block 8

Block 7. Test fulfillment of constraint (3) at all network nodes. If it is fulfilled, go to Block 9, otherwise, go to Block 8.

Block 8. Calculate the reactive power of the active filter. The reactive power is calculated as

$$Q_{AF} = P_{ij}\,(\text{tg}\,\varphi_c - \text{tg}\,\varphi_d),$$

where "*d*" is an abbreviation of "desired." The value of tg φ_c is determined based on cos φ_c. The value of tg φ_d is calculated using constraint (2). Since the feasible value of cos φ is within the interval

$$\cos\varphi_{min} \le \cos\varphi \le \cos\varphi_{max},$$

the value of the reactive power of the active filter is also within the interval

$$Q_{min} \le Q_{AF} \le Q_{max}.$$

The required phase angle φ_d should be calculated using cos φ_{min} and cos $\varphi_{\max}$. The highest and lowest values of Q_{AF} are calculated by the expressions

$$Q_{min} = P_{ij}\,(\text{tg}\,\varphi_c - \text{tg}\,\varphi_{min}),$$
$$Q_{max} = P_{ij}\,(\text{tg}\,\varphi_c - \text{tg}\,\varphi_{max}).$$

Block 9. Calculate the total active power losses in the network based on the load flow calculation.

Block 10. Compare the active power losses of the preceding calculation step with the losses of the current step to determine minimum losses, namely, if

$$\Delta P_{(1)} < \Delta P_{min}, \text{ then } \Delta P_{min} = \Delta P_{(1)}.$$

Block 11. Change the number of the transformer tap $k = k + 1$. If $k > K$, then go to Block 12, if the condition is not fulfilled, go to Block 2.

Block 12. Minimize the active power losses caused by harmonics in the network, i.e., $\sum_{h=2}^{H} \Delta P_{(h)} = \min$.

In this case, constraints (4)–(6) should be met by eliminating the harmonics of current with the help of the active filter at the node of filter connection. The apparent harmonic power is calculated as $S_{h\text{ó}} = \sqrt{P_h^2 + Q_h^2}$ [23], where

$$P_h = \sum_{h=2}^{H} U_h I_h \cos\varphi_h\,,$$

$$Q_h = \sum_{h=2}^{H} U_h I_h \sin\varphi_h$$

were calculated by the measured voltages U_h, currents I_h and phase angle φ_h.

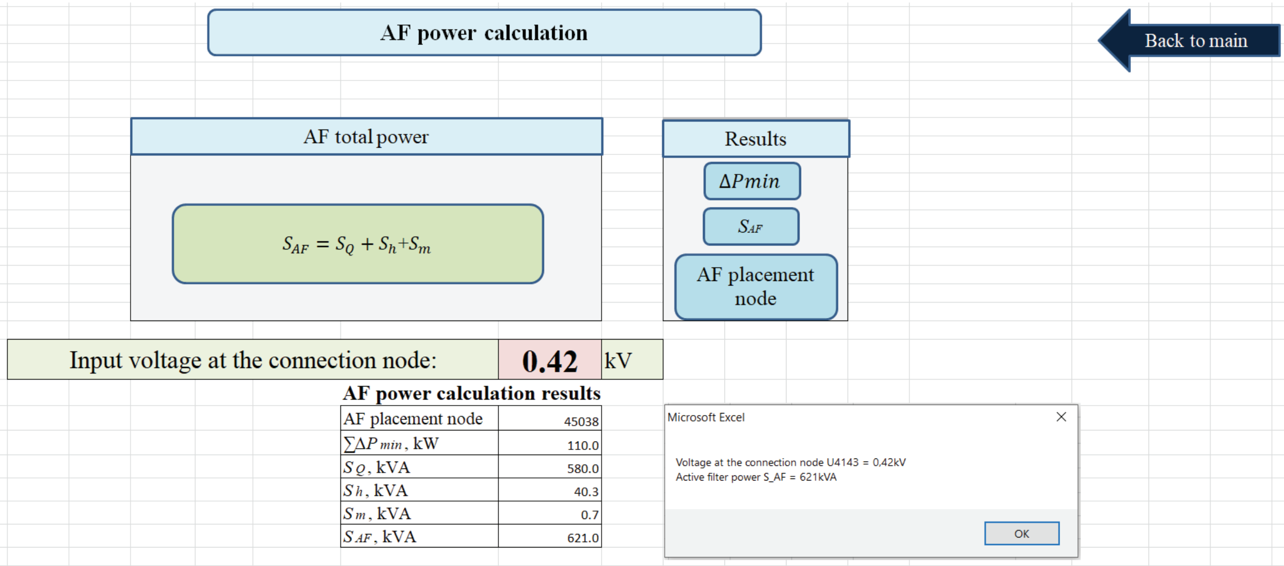

Fig. 5. Sheet 5 of the program.

Block 13. Minimize the active power losses caused by the interharmonics in the network, i.e.,

$$\sum_{m=1}^{M} \Delta P_{(m+\frac{1}{2})} = \min .$$

For this purpose, the interharmonics of current should be eliminated by the active filter at the node of filter connection. The apparent power of interharmonics is calculated as $S_{m\Sigma} = \sum_{m=1}^{M} U_{m+1/2} I_{m+1/2}$ by the measured voltages U_m and currents I_m.

Block 14. Calculate the apparent power of the active filter as a sum of three powers:

$$S_{AF} = S_{QAF} + S_{h\Sigma} + S_{m\Sigma}.$$

Block 15. Obtain calculation results.

V. The computer program to calculate the active filter power

The computer program [24] was developed based on the algorithm built to determine the active filter power presented in Fig. 2. It is written in MS Excel and the programming environment Visual Basic for Windows applications. The program is designed to determine the apparent active filter power to compensate for the reactive load power for improving the power factor, and eliminating harmonics and interharmonics. The program makes it possible to determine a network node for placing an active filter.

The computer program component of the mentioned software "The stationary feasible optimal condition" (the software "SDO") is applied to calculate the value of power to be generated by the active filter for compensation for the reactive load power and to determine the network node for installation of the active filter [20-21]. This software is intended for the calculation of the steady-state conditions in electrical networks. It implements algorithms for calculation of feasible and optimal conditions in terms of the active and reactive power losses in the electrical networks with different voltage levels, including the steady-state unbalanced conditions of low-voltage distribution networks.

The program for calculation of active load power filter consists of five MS Excel sheets: sheet 1 is "Primary", sheet 2 is "Power Q_{AF}", sheet 3 is "Harmonics power S_h", sheet 4 is "Interharmonics power S_m", sheet 5 is "Power S_{AF}". Figure 3 presents the first sheet as an example. The fundamental frequency load flow and the comparative evaluation of cos φ and U_k values, which were measured and calculated using the software "SDO" at the node connecting the power supply system of the plant to the supply network, were calculated using the commands of the first sheet. Comparison of the calculated parameters with the results of measurements and their close values confirms that modeling of the electrical network for calculation of the reactive power value was correct.

The reactive power value consumed by the load generated by the active filter is calculated in sheet 2 (Fig. 4). The electrical network node for the installation of the active filter is identified through calculation. If the node is determined correctly, the active power losses in the network elements will be minimal.

Table 8. Apparent powers of interharmonics.

S_m,VA	Interharmonic					
	1.5	3.5	5.5	17.5	19.5	11.5
Phase A	16.6	6.0	5.1	7.5	8.5	5.1
Phase B	17.2	4.8	5.0	1.9	2.7	3.7
Phase C	18.0	7.3	6.4	9.2	9.7	5.0
$S_{m\Sigma A,B,C}$	51.8	18.1	16.5	18.6	20.9	13.8
S_m,VA	Interharmonic					
	13.5	21.5	23.5	25.5	27.5	29.5
Phase A	5.1	9.6	13.1	12.5	7.0	7.5
Phase B	2.2	3.2	3.0	2.7	1.9	1.4
Phase C	5.2	7.5	5.7	6.5	3.8	3.6
$S_{m\Sigma A,B,C}$	12.5	20.3	21.8	21.7	12.7	12.5

The apparent power values of harmonics and interharmonics to be eliminated by the active filter are calculated in sheets 3 and 4. The powers are calculated by the results of measurements of harmonic load flow parameters and power quality indices at the electrical network node chosen for the active filter installation.

The apparent power of the active filter is calculated in sheet 5 of the program. Sheet 5 with the Table of the calculation results is presented in Fig. 5. The Table indicates the number of the network node for installation of the active filter, the value of the minimum active power losses, the reactive power of the fundamental frequency, the harmonic power, the interharmonic power, and the apparent power of the active filter.

VI. Determination of the apparent power of the active filter harmonics for the coal grading plant of the company "Cua Ong-Vinacomin"

The management company of the coal grading plant has chosen node 45038 for the installation of an active filter in the power supply system (Fig. 1). The transformer supplying electrical power to the power supply system of the plant has five taps. They make it possible to have the voltages of 0.38 kV, 0.39 kV, 0.4 kV, 0.41 kV, and 0.42 kV at node 4143. The calculation results show that if the voltage at node 4143 changes from 0.38 kV to 0.42 kV, at 57 network nodes of 0.4 kV the voltages range from 0.36 kV to 0.39 kV. Hence, the requirements of [3] are not fulfilled. In this case, the load power factor at node 4143 takes the values from 0.88 to 0.99, which meets partially the company requirements. Thus, the generation of reactive power can increase the voltage at the system nodes and the load power factor at node 4143.

The computer program for calculating the active filter power following the proposed algorithm was applied to calculate the reactive power value of the active filter. The intermediate calculation results are presented in Tables 5 and 6.

The lowest active power losses in the network equal to 110 kW are observed with the tap of the 0.42 kV transformer and the reactive power of the active filter of 580 kVAr. All the voltage conditions at the network nodes and node 4143 are met.

Harmonic powers were calculated based on measured parameters and are shown in Table 7. The active filter must have no less than 16 kVA at each phase to eliminate harmonic currents. The total apparent power of harmonics in three phases is 40.3 kVA.

Table 8 presents the values of phase apparent power of some interharmonics and the total apparent powers of three phases, which were calculated by measured parameters. The total apparent power of interharmonics of three phases is 0.7 kVA, which is less than 1% of the harmonic power.

Figure 5 demonstrates the calculation results presented in the fifth sheet of the computer program. The Figure shows that at node 45038 of the active filter connection, the active power losses in the electrical network of the coal grading plant will be minimal and equal to 110 kW with the transformer tap of 0.42 kV and the apparent power of the active filter of 621.1 kVA.

VII. Conclusion

The measurements have shown that the load current contains harmonics and interharmonics, the indices $K_{U(n)}$ and K_U exceed the normative values, and cos φ is lower than the norm.

Reduction in total harmonic distortion and increase in load power factor can be achieved with an active filter installed. The power of the active filter was determined using the developed optimization algorithm and measurements of load flow parameters.

The active filter power was determined for the coal grading plant of the company "Cua Ong-Vinacomin."

Acknowledgment

The research was carried out under State Assignment Project (No. FWEU-2021-0001) of the Fundamental Research Program of Russian Federation 2021-2030.

References

[1] Circular No.39/2015/TT-BCT *of the Ministry of Industry and Trade of Viet Nam for the distribution of Electrical Energy*

[2] *Electromagnetic compatibility of technical equipment. A general guide on harmonics and interharmonics measuring instruments and measurement for power supply systems and equipment connected thereto*, GOST 30804.4.7-2013 (IEC 61000-4-7:2009), ISC Standard, 2013.

[3] *National Technical Regulation on Electric Power,* Viet Nam, 2015.

[4] B. Singh, K. Al-Haddad, A. Chandra, "A review of active filters for power quality improvement," *IEEE Transactions on Industrial Electronics*, vol. 46, no. 5, pp. 960-971, 1999.

[5] Gong Maozhong, Liu Hankui, Gu Jianjun, Xu Dianguo, "Active power filter based on novel current reference calculation," in *Proc. IEEE ICIT'02*, Thailand, 2003, DOI: 10.1109/ICIT.2002.1189916.

[6] C. H. da Silva, V. F. da Silva, L. E. B. da Silva, "Evaluation of Power-Ratings for Active Series Filters under Unbalanced Conditions for a Three Phase - Four Wire System," in *Proc. IEEE 36th PESC*, Brazil, 2006, DOI: 10.1109/PESC.2005.1581638.

[7] Shekh Saddam Husen, Patel Pinkal J., "A literature review and industrial survey on active power filter," *International journal of engineering development and research*, vol. 2, no. 1, pp. 118-125, 2014.

[8] M.El-Habrouk, M.K. Darwish, P. Mehta, "Active power filter: A review," *IEEE Proceedings in Electric Power Applications*, vol. 147, no. 5, pp. 403-413, 2000.

[9] Salvador Orts; Francisco J. Gimeno-Sales; Antonio Abellan; Salvador Segui-Chilet; Miguel Alcaniz, Rafael Masot, "Achieving maximum efficiency in three-phase systems with a shunt active power compensator based on IEEE Std. 1459, " *IEEE Transactions on Power Delivery* vol. 23, no. 2, pp. 812-822, 2008, DOI: 10.1109/TPWRD.2007.915910.

[10] Abbas Mariani, Luigi Piegari, Saeed Saeedallah Mortazavi, Mohammad-Sadegh Ghazizadeh, "Active Power Filter Commitment for Harmonic Compensation in Microgrids," *in Proc. IECON 2019 - 45th Annual Conference of the IEEE IES*, Portugal, 2019, DOI: 10.1109/IECON.2019.8927668.

[11] A. Kouzou, B. S. Khaldi, S. Saadi, M. O. Mahmoudi, M.S. Boucherit, "Apparent power ratio of the Shunt Active Power Filter," *in Proc. 13th International EPE-PEMC*, Poland, DOI: 10.1109/EPEPEMC.2008.4635557.

[12] Gary W Chang, "A New Method for Determining Reference Compensating Currents of Three-Phase Shunt Active Power Filters," *IEEE Power Engineering Review*, vol. 22, issue 4, pp. 68-70, April 2002, DOI: 10.1109/MPER.2002.4312116.

[13] Faegheh Irannezhad, Seyed Hossein Hosseinian, Mehrdad Abedi, Behrooz Vahidis, "Using the Instantaneous Power Theory in order to control the current in the parallel active filter to compensate reactive power and reduction of harmonics," *in Proc. PEDES 2012*, India, DOI: 10.1109/PEDES.2012.6484390.

[14] Jun Yang, Yue Wang, Zhaoan Wang, "A DSP controlled hybrid power filter used to compensate the harmonics and reactive power caused by electrical traction loads," *IEEE Cat. No.03CH37491*, Canada, 2004, DOI: 10.1109/PES.2003.1267397.

[15] Izzeldin Idris Abdalla, K. S. Rama Rao, N. Perumal, "Three-phase four-leg shunt active power filter to compensate harmonics and reactive power," *in Proc. ISCI*, Malaysia, 2011, DOI: 10.1109/ISCI.2011.5958965.

[16] *Operating Manual Network Analyzer PQ-Box 150 Power-Quality Evaluation Software*, A. Eberle GmbH, and Co. KG, 2017, [Online]. Available: https://www.a-eberle.de/sites/default/files/media/BA_PQBox150_EN_ 201803.pdf (Accessed on Jan. 6, 2021).

[17] M. Maciazek, D Grabowski, and M. Pasko, "Active power filters - optimization of sizing and placement," *Bulletin of the polish academy of sciences "Technical sciences,"* vol. 61, no. 4, pp. 847-853, 2013.

[18] Vahid Chakeri, M. T. Hagh, "Optimal Allocation of the Distributed Active Filters Based on Total Loss Reduction," *Int. Journal of Smart Electrical Engineering*, vol. 6, no. 4, pp. 171-175, 2017.

[19] Sarita Samal, Prakash Kumar Hota, Prasanta Kumar Barik, "Harmonics Mitigation by using Shunt Active Power Filter under Different Load Condition," *in Proc. SCOPES*, India, 2016, DOI: 10.1109/SCOPES.2016.7955598.

[20] G. M. Mustafa, S. I. Gusev S.I. "Active filter-compensating devices of shunt and series type in electrical networks," *Energetik*, 2019, no. 8, pp. 3-10.

[21] O. N. Voitov, E. V. Popova, L. V. Semenova, "Algorithms for load flow calculation in electric networks in terms of the temperature of overhead line conductors and their implementation," *Elektrichestvo*, 2013, no. 3, pp.19-26.

[22] Certificate of conformity no. ROSS RU.SP20.N00008 "*Software SDO-7 for analysis, optimization of steady states and evaluation of electric power losses in electric networks*" – Certificate scheme GOST R Gosstandart Rossii. Expiration date: from 31.01.2009 to 31.01.2012.

[23] A. E. Emanuel, "*Three-Phase Nonsinusoidal and Unbalanced Conditions"* in *Power definitions and the physical mechanism of power flow,* Worcester Polytechnic Institute, USA, IEEE PRESS, John Wiley and Sons, Ltd., Publication, 2010, pp. 185-203.

[24] Certificate of state registration of a computer program No. 2021613837 "Program for calculating the active filter power," Federal Service for Intellectual Property. Expiration date: from 15.01.2021 to 15.01.2035.

Lidia Kovernikova is a Senior Researcher of Melentiev Energy Systems Institute of the Russian Academy of Sciences, Irkutsk, Russia. She graduated from Novosibirsk Electrotechnical Institute in 1976. L.I. Kovernikova received her Ph.D. degree in engineering from the Siberian Energy Institute in 1995. Her research interests include modeling non-sinusoidal conditions of electrical power systems, analyzing the power quality in electrical networks, and developing technical means to improve the power quality.

Bui Ngoc Hung is a graduate student of Irkutsk National Research Technical University, Irkutsk, Russia. He graduated from Ha Noi University of Mining and Geology in 2006. Bui Ngoc Hung completed his Ph.D. in electrical engineering at Ha Noi University of Mines and Geology. His research interests include power quality in electrical networks and developing technical means to improve the power quality.

Oleg Voitov is a Senior Researcher of Melentiev Energy Systems Institute of the Russian Academy of Sciences, Irkutsk, Russia. He graduated from Moscow Power Engineering Institute in 1971. O.N. Voitov received his Ph.D. degree in engineering from the Siberian Energy Institute in 1993. His research interests include modeling the steady-state conditions of electric power systems in a single-line representation and phase coordinates, the development of algorithms for analyzing and optimizing instantaneous and short-term operating conditions in the context of discrete parameter changes.

Lyudmila Semenova is the Lead Engineer of Melentiev Energy Systems Institute of the Russian Academy of Sciences, Irkutsk, Russia. L. V. Semenova graduated from Irkutsk Polytechnic Institute in 1974. Her research interests include the development and implementation of methods and models for studying the functioning of power systems.

Pham Duc Tien is a power engineer at the Wong Bi - TKV - Vinasovin Coal Company in Viet Nam. He teaches at the College of Construction of the Ministry of Construction. He graduated from Ha Noi University of Mining and Geology in 2006. Pham Duc Tien completed his master's degree in electrical engineering at Ha Noi University of Mining and Geology. His research interests include power quality, development of technical methods to improve it, safety and operation of high voltage power supply.

Ha Thi Chuc is a lecturer at the University of Mining and Geology, Ha Noi, Viet Nam. She graduated from Ha Noi University of Transport and Communication in 2008. Ha Thi Chuc completed her Ph.D. in Electrical and Electronic Engineering at the Ha Noi University of Transport and Communication. Her research interests include power quality, developing technical means to improve the power.

Component Contribution to the Total Reliability of the WAMS Network

M. I. Uspensky*

Institute for Social, Economic and Energy Problems of the North, Federal Research Center of the Komi Science Center of the Ural Branch of the Russian Academy of Sciences, Syktyvkar, Russia.

***Abstract* — Nowadays, the control of power systems relies on wide-area monitoring and control system (WAMS), which continuously measures and registers state vector values and is synchronized by signals from the uniform time system. A significant part of this system is the local information network, whose reliability largely determines the proper functioning of WAMS. One can assess the said reliability by dividing it into components. These are hardware or technical reliability associated with failure (destruction) of transmission channel elements or the integrity of communication lines, traffic reliability determined by time loss or data distortion without failure of a transmission channel element, software reliability related to errors in the development of exchange execution programs, and resilience against an external deliberate impact on the transmitted information. This paper addresses the assessment of the first three reliability components of the information network, shows its total value, and estimates the contribution of each component. The last component (resistance to an external deliberate action) is described in a huge number of works, which is why it is not considered in this paper.**

***Index Terms*: Wide-area monitoring and control system, local infor-mation network, hardware and software reliability and availability, traffic availability.**

I. Introduction

The need for a correct estimation of power system state has led to the creation of a hierarchical system for monitoring transient conditions, i.e., a wide-area monitoring and control system (WAMS). It is based on the technology for measuring phasors (phase vectors) to collect vector information with the aid of phasor measurement units (PMUs) using the signals from the global navigation systems that provide simultaneous measurement of phasors [1]. WAMS includes measuring transformers (PMUs), phasor data concentrators (PDCs), and equipment of the local information network (LIN). It allows us to control power system behavior by continuously observing system events. The WAMS reliability is determined by the reliability of every monitoring system component.

The network failure is determined by the loss of terminal communication, which implies not only the absence of such communication but also the distortion of the transmitted information. Then the network reliability includes four components. These are 1) hardware or technical reliability associated with a failure of transmission channel components or destruction of the integrity of communication lines, 2) traffic reliability determined by the time loss or distortion of data without a failure of the transmission channel component, 3) software reliability related to errors in the development of exchange execution programs, and 4) resistance to external actions targeted on the transmitted information.

The paper presents an approach to assessing three first components. An algorithm and implementation of this approach are considered on the example of a 10-node power system. Some features of the information network model are noted.

II. Hardware reliability of WAMS network

The hardware of WAMS network comprises network connections, electronics of PMUs and PDCs. Since the operation of PDC central processor and communication interface during duplication is similar to the operation of these components in PMU, we will use the reliability assessment of these blocks in [2] obtained from the system of Markov equations of state probabilities, given different lengths of the main and redundant communication channels. Then the availability of communication link of a network consisting of a duplicated information source (PMU, PDC, or, if necessary, an intermediate amplifier) and communication channel lines can be defined as

$$A_{ch} = A_{PDC} \cdot A_{com}, \quad (1)$$

where

$$A_{PDC} = \frac{\mu_{PDC}^2}{\left(\mu_{PDC} + \lambda_{PDC}\right)^2}, \quad (2)$$

* Corresponding author.
E-mail: uspensky@energy.komisc.ru

http://dx.doi.org/10.38028/esr.2021.01.0004
Received April 13, 2021. Revised April 17, 2021.
Accepted April 25, 2021. Available online May 26, 2021.

Table 1. C37.118-2011 frame structure.

Field	Size
Sync byte (SYNC)	2 bytes
Byte number of frame (FRAMESIZE)	2 bytes
PMU Identifier (IDCODE)	2 bytes
Seconds of counting (SOC)	4 bytes
Second fraction/quality flag (FRACSEC)	4 bytes
Status flag (STAT)	2 bytes
Vectors (PHASORS)	$8 \cdot n$ bytes (floating point)
Frequency (FREQ)	4 bytes (floating point)
Frequency change rate (DFREQ)	4 bytes (floating point)
Analog data (ANALOG)	$8 \cdot m$ bytes (floating point)
Digital data (DIGITAL)	$2 \cdot l$ bytes (discrete values)
Cyclic Redundancy Check (CHK)	2 bytes

l is the number of discrete information sources; *m* is the number of analog information sources; *n* is synchronized vectors (magnitude and phase).

Table 2. Required channel bandwidth, Kbit/s.

Samples per second	Number of PMUs			
	2	10	40	100
25	50	249	997	2392
50	100	499	1994	4984
100	200	997	3988	9969

since PDCs are of the same type, and

$$A_{com} = \frac{\mu_{ml} \cdot \mu_{bl}}{(\mu_{ml} + \lambda_{ml})(\mu_{rl} + \lambda_{rl})}. \quad (3)$$

Here A_{PDC} is the availability of the redundant information source; λ_{PDC} and μ_{PDC} are failure and recovery rates of the source, respectively. The physical availability of each element of the information carriers (twisted pair, optical fiber, high-frequency channel) is characterized by length l_i, specific failure rate λ_{ml} for the main line and λ_{rl} for the redundant line, and the average recovery time r_{ml} for the main and r_{rl} for the redundant line *i* per unit length. Since reliability indices of communication lines λ_l and r_l approximately linearly depend on their length, and $\mu_l = 1/r_l$, it is easy to evaluate the working state probability of an information carrier element (*i*-th line availability) as

$$A_{ln,i} = \frac{\mu_{ln,i}}{\mu_{ln,i} + \lambda_{ln,i}} = \frac{1/(r_{ln,i} \cdot l_i)}{1/(r_{ln,i} \cdot l_i) + \lambda_{ln,i} \cdot l_i} = \frac{1}{1 + \lambda_{ln,i} \cdot r_{ln,i} \cdot l_i^2}. \quad (4)$$

It is worth noting that $r_{ln,i}$ includes two components: the distance-dependent failure search variable, and the recovery-related constant. Since the second component has small values, we neglect it. Consequently, the availability of the communication line is inversely proportional to its squared length. In contrast to duplication in electronics, where the backup device usually repeats the basic one, the storage media are most often duplicated by the elements of various reliability indices. This is because under normal conditions, communication is provided via the shortest line in the communication network, and in the case of redundancy, the information goes through the line remaining in the communication network, which can be significantly longer than the main one. Moreover, the approach to solving such a problem is the same as in the case of duplicating electronic units (2) but considers different values of λ_j and μ_j for the *j*-th communication line (3).

III. Traffic reliability

The traffic reliability lies in timely information transmission, without loss and distortion associated with the exchange channel loading. Traffic-related losses are associated with an unacceptable delay or loss of some information due to the information channel overload but are not associated with the failure of channel device elements, which is taken into account in hardware reliability. Therefore, the traffic reliability is determined by the choice of channel capacity, given a delay in the transmitted information.

The information frame from the generation unit or power line, formed by each PMU, combines 9 vector measurements (3 currents and 3 voltages (magnitude and phase), 3 active and reactive power components); 2 analog values (generator current and voltage); the state of PMU, and the state of switching components. The transmission packet also includes the frequency and speed of its change, the time stamp, and the binding for interaction with the information network in the standard C.37.118-2011. The data frame structure is given in Table 1. The amount of information from one PMU takes $b_{in} = 8 \cdot 9 + 2 \cdot 8 + 2 + 2 = 92$ (bytes). The amount of information per frame of one node (the first six points in Table 1) is $b_{fr} = 6 + 8 + 8 + 2 = 24$ (bytes). Depending on the number of PMUs (information sources of measurement), and transmitted measurements per second, the packet volume often varies from 100 to 400 bytes. The approximate channel bandwidth in Kbit/s, depending on the number of source devices and sampling rate, given a margin of 10 percent, is indicated in Table 2 [3]. In this case, 1 Kbit = 1024 bit.

Information delay is associated with both the type of the exchange channel and the time of unloading its receiving buffer. Packet delivery to a receiver requires time T_d, which, in the general case, is determined by the signal propagation time T_{sp}, the time of packet transmission over the communication line T_{pt} and the packet waiting time T_{wp} in the queue in the communication unit

$$T_d = T_{sp} + T_{pt} + T_{wp}. \quad (5)$$

The signal propagation time, T_{sp} in most communication systems is determined by the propagation time of the electric or optical signal (electromagnetic field). The pulse

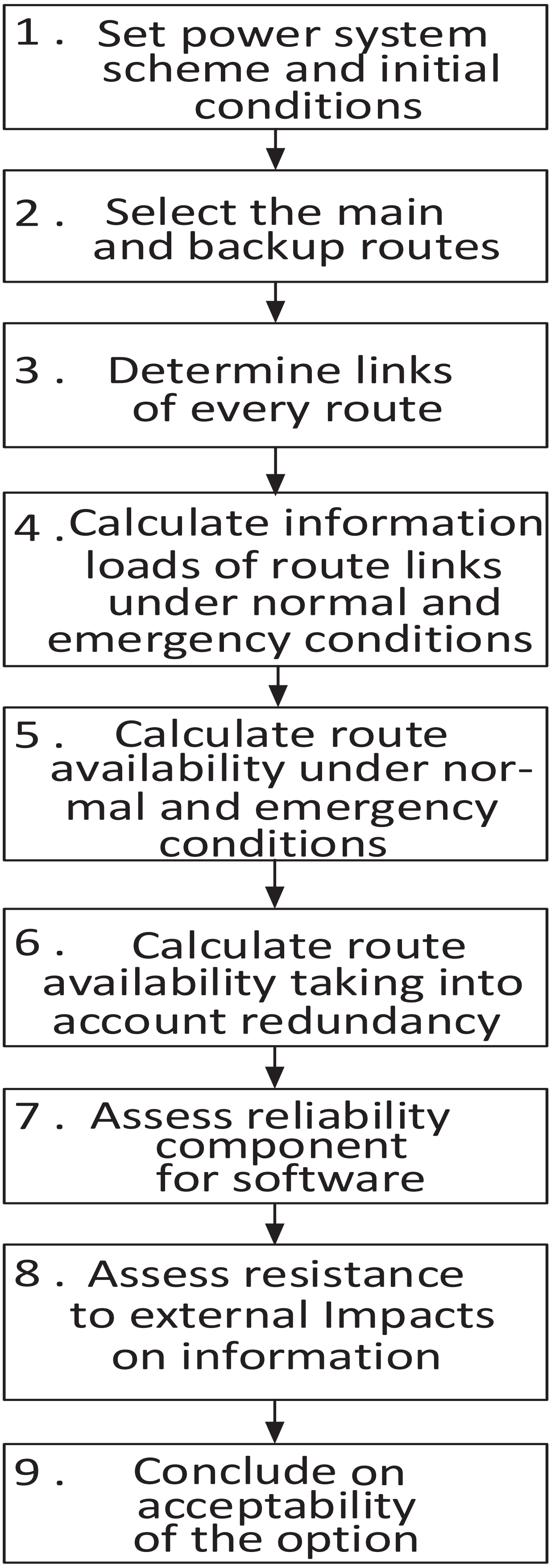

Fig. 1. Algorithm to research the information network reliability.

delay in the optical fiber is (3.5–5)·l (ns) [4] and in the copper wire 5·l (μs) [5], where l is the channel length in km.

The packet transmission time, T_{pt}, depends on the rate of data transfer via the communication line ν_{tr} (Kbit/s) and the packet volume or length L_p (Kbit)

$$T_{pt} = L_p/\nu_{tr}. \tag{6}$$

The propagation speed depends only on the channel material. Therefore, the propagation time along the channel is constant. Transmission time depends only on the packet length.

The main idea behind the design of a data transmission network is to ensure the balance between traffic (the flow of requests λ, in our case, the measurement frequency), the number of network resources (bandwidth) and the service quality (service flow μ, parameter of request processing). Solving this problem involves considering two levels of the open system interaction model (OSI): network and channel.

Network level. Traffic routes over the network are considered at the network level. To this end, it is convenient to describe the communication network as a graph model [6] (in this case, non-oriented), in which the network nodes (routers) correspond to the graph vertices and the communication lines correspond to the graph arcs. The transmission time to the receiving node is the time spent by the packet in the network line. This time is random to a certain extent.

The intensity of load on the arcs of the network graph ρ_{ij} is determined by the ratio of the intensity of request flow from the information source node i to the intensity of the service flow from the destination node j (λ_i/μ_j) and depends on the number of devices and the amount of information from each device. In our case, the request flow intensity is determined by the frequency of parameter measurements at the nodes of the power system $\lambda = f_{msr} = 1/T_{msr}$, service flow intensity is determined by the reciprocals of the packet delivery time $\mu = 1/T_d = 1/(L_p/\nu_{tr}+T_{pc})$, and since this time is shorter than the request period, $T_{wp} = 0$. On the other hand, the receiver electronics creates an additional delay, T_{re}, of about 5 μs on average. Then

$$\rho_{ij} = \frac{L_p / \nu_{tr} + T_{sp} + T_{re}}{T_{msr.}}. \tag{7}$$

Channel level. This level requires the evaluation of the necessary bandwidth of communication lines between network nodes. In the general case, an approximate formula can be used to estimate the probability of losses [7]

$$q_{ij} = \frac{1-\rho_{ij}}{1-\rho_{ij}^{N_j+1}}\rho_{ij}^{N_j}, \tag{8}$$

where N_j is the number of sections in the receiver storage j; ρ_{ij} is the load intensity of line ij.

The absence of loss is determined as

$$p_{ij} = 1 - q_{ij}. \tag{9}$$

Such an assessment corresponds to one information line connecting two nodes. Taking into account the sequence of switching the communication lines of two nodes passing through the intermediate nodes, the overall assessment of the information loss probability is determined as

$$Q_\Sigma = 1 - \prod_{ij} p_{ij} = 1 - \prod_{ij} \left(1 - q_{ij}\right). \qquad (10)$$

IV. Failure of the software

The failure of the software (SW) is associated with its inconsistency with the objectives set. There are many definitions of software reliability. The most acceptable definition seems to be as follows *Software reliability is the probability that the program will work without failures for a certain time, given the degree of their influence on the output results* [8].

The frequency of statistical data errors reduced to 100 percent is given in Table 3 with a detailed description of "Incomplete or erroneous task."

The software is not subject to wear and tear and its reliability is determined only by the development errors. Thus, over time, this index should increase if the correction of detected errors does not introduce new errors.

Table 3. Frequency of some types of errors [9].

Cause of error	**Frequency, %**
Deviation from the task	12
Neglect of programming rules	10
Incorrect data sampling	10
Erroneous logic or sequence of operations	12
Erroneous arithmetic operations	9
Lack of time to resolve	4
Incorrect interrupt handling	4
Invalid constants or source data	3
Inaccurate recording	8
Incomplete or erroneous task	28
	⇓
Errors in numeric values	12
Insufficient accuracy requirements	4
Erroneous characters or signs	2
Registration errors	15
Incorrect hardware description	2
Incomplete or inaccurate development basics	52
Ambiguity of requirements	13

Table 4. Routes for the main and redundant information exchange channels.

Source node	Main channel	Redundant channel
1	1-7-4	1-9-8-6-4
2	2-7-4	2-9-7-4
3	3-4	3-5-4
5	5-4	5-6-4
6	6-4	6-5-4
7	7-4	7-6-4
8	8-6-4	8-9-7-4
9	9-7-4	9-8-6-4
10	10-2-7-4	-

For critical applications, which should include the WAMS software, by the time the system is delivered to the client, it may contain from 4 to 15 errors per 100 000 lines of program code [10]. For clarity, we note that the number of code lines of WINDOWS XP is above 45 million, NASA has 40 million code lines, and Linux 4.11 kernel has more than 18 million code lines [11].

When evaluating the WAMS program of 10 million lines of code, the number of errors at the beginning of program operation is E = (V/100 000)·4 = 400 (errors). Then, using the formula for the mean time between the software failures, we get

$$\lambda_{SW} = \beta \frac{E}{V} = 0.01 \frac{400}{10^7} = 4 \cdot 10^{-7}$$

or

$$t_{SW} = \frac{1}{\lambda_{SW} \cdot 8760} = \frac{10^7}{4 \cdot 8760} \approx 285\ ,$$

where E is the number of errors per program accepted for operation, V is the program volume in lines of code, β is the program complexity coefficient, usually in the range of 0.001 to 0.01, λ_{SW} is the failure rate and t_{SW} is the mean time between the software failures (years), 8760 is the number of hours per year. With a value of one error per 1 000 code lines, accepted for applied software after testing with the same number of code lines, E = 10 000 errors:

$$\lambda_{SW} = \beta \frac{E}{V} = 0.01 \frac{10\,000}{10^7} = 10^{-5}$$

or

$$t_{SW} = \frac{1}{\lambda_{SW} \cdot 8760} = \frac{10^5}{8760} \approx 11.4$$

or about one failure in 12 years.

V. Procedure for assessing the LIN reliability

Since the reliability of the local information network (LIN) is investigated for a given scheme, the research algorithm is as follows (Fig. 1).

1. Set a scheme of information exchange in the form of links between nodes, the length of links, and the type of links (wired, fiber-optic, high-frequency, etc.). Set also the initial conditions. These are the failure and recovery rates of information sources (PMUs) λ_{is} and μ_{is}, respectively; specific failure rates of the main and redundant lines (λ_{ml} and λ_{rl}); the average recovery time of the main and redundant lines (r_{ml} and r_{rl}) per unit of length; propagation delay T_{sp}; delay in electronic devices T_{re}; transmission rate v_{tr}; transmission frequency or measurement period T_{msr}, and the number of information sources at each node. A link means a connection between the adjacent nodes in the network.
2. Select the main and backup routes for the information exchange between the sources and the dispatching point. The main route is usually determined by the shortest path from the information source to the dispatching point, the backup one depends on the failed communication link.

3. Determine a route by its set of links.
4. Calculate information loads of links of every route under normal and emergency conditions in terms of link failure.
5. Based on the prepared information, calculate the hardware availability and traffic reliability of the routes under normal and emergency conditions.
6. Calculate the availability of routes taking into account redundancy.
7. Estimate the software component, in terms of software development reliability.
8. Assess the resistance to external impact on the information. Mentioning this point, we do not dwell in detail on such an assessment but refer the reader to the literary sources, for example, [12, 13].
9. Make a conclusion on the acceptability of the option under study and, if necessary, its weak points.

Table 5. Availability of links of fiber-optic information exchange channel.

Link	l, km	λ_{con}, fail./yr.	r_{con}, hr./recov.	A_{link}	Link	l, km	λ_{con}, fail./yr.	r_{con}, hr./recov.	A_{link}
1-7	150.0	2.628	31.32	0.990433883	4-6	30.0	0.5256	6.264	0.999364399
1-9	75.0	1.314	15.66	0.997397114	4-7	50.0	0.876	10.44	0.99869736
2-7	150.0	2.628	31.32	0.990433883	5-6	50.0	0.876	10.44	0.99869736
2-9	75.0	1.314	15.66	0.997397114	6-7	47.0	0.82344	9.8136	0.998818611
2-10	70.0	1.2264	14.616	0.997698469	6-8	145.0	2.5404	30.276	0.991038641
3-4	70.0	1.2264	14.616	0.997698469	7-9	130.0	2.2776	27.144	0.99273384
3-5	50.0	0.876	10.44	0.99869736	8-9	40.0	0.7008	8.352	0.99907246
4-5	40.0	0.7008	8.352	0.99907246					

Table 6. Availability of the fiber-optic information exchange channel.

Node	$A_{main\ channel}$	$A_{redundant\ channel}$	$A_{channel\ with\ redundancy}$	Node	$A_{main\ channel}$	$A_{redundant\ channel}$	$A_{channel\ with\ redundancy}$
1	0.989400945	0.987684744	0.99986947	7	0.990433883	0.998443352	0.999985109
2	0.989400945	0.989374459	0.999887379	8	0.990666305	0.991036328	0.999916336
3	0.997698469	0.998030512	0.999995467	9	0.991698503	0.99000482	0.999917025
5	0.99907246	0.998322147	0.999998444	10	0.987380523	0	0.987380523
6	0.999364399	0.998030512	0.999998748				

Table 7. Availability of links of the power line information exchange channel.

Link	l, km	λ_{con}, fail./yr.	r_{con}, hr./recov.	A_{link}	Link	l, km	λ_{con}, fail./yr.	r_{con}, hr./recov.	A_{link}
1-7	150.0	2.94	28.5	0.990268019	4-6	30.0	0.588	5.7	0.999357643
1-9	75.0	1.47	14.25	0.997355058	4-7	50.0	0.98	9.5	0.998678619
2-7	150.0	2.94	28.5	0.990268019	5-6	50.0	0.98	9.5	0.998678619
2-9	75.0	1.47	14.25	0.997355058	6-7	47.0	0.9212	8.93	0.998802048
2-10	70.0	1.372	13.3	0.997661811	6-8	145.0	2.842	27.55	0.990883459
3-4	70.0	1.372	13.3	0.997661811	7-9	130.0	2.548	24.7	0.992608673
3-5	50.0	0.98	9.5	0.998678619	8-9	40.0	0.784	7.6	0.999060456
4-5	40.0	0.784	7.6	0.999060456					

Table 8. Availability of the power line information exchange channel.

Node	$A_{main\ channel}$	$A_{redundant\ channel}$	$A_{channel\ with\ redundancy}$	Node	$A_{main\ channel}$	$A_{redundant\ channel}$	$A_{channel\ with\ redundancy}$
1	0.98921669	0.987469907	0.999864884	7	0.99026802	0.998420046	0.999984624
2	0.98921669	0.989189439	0.999883426	8	0.99050449	0.990880875	0.999913409
3	0.99766181	0.997999793	0.999995323	9	0.99155486	0.989831215	0.999914123
5	0.99906046	0.998296664	0.9999984	10	0.98716037	0	0.98716037
6	0.99935764	0.997999793	0.999998715				

Table 9. Resulting λΣ and μΣ values of communication channels.

Source - node	Fiber-optic channels		Power line channels	
	λ_Σ	μ_Σ	λ_Σ	μ_Σ
1	0.09589628	734.572164	0.109127394	807.5486398
2	0.083695895	743.08248	0.095243883	816.9324165
3	0.006031754	1330.67373	0.006854215	1465.551612
5	0.002472612	1588.79738	0.00280486	1752.642178
6	0.00203475	1625.44545	0.002306221	1794.935514
7	0.016936974	1137.37422	0.019264457	1252.864972
8	0.062884682	751.569245	0.071559069	826.33357
9	0.062221822	749.824533	0.070804518	824.418488
10	0.077536602	642.210362	0.088232547	706.0262268

Table 10. Input data on the information network.

Link	l, km	b_{in}	b_{fr}	$\sum b_{in}^{nr}$	$\sum b_{fr}^{nr}$	$\sum b_{in}^{em}$	$\sum b_{fr}^{em}$
1-7	150	2	1	2	1	5	3
2-9	75	2	1	3	2	5	3
10-2	70	1	1	1	1	1	1
3-4	70	6	2	6	2	6	2
3-5	50	0	0	0	0	6	2
9-7	130	1	1	4	3	6	4
9-8	40	0	0	0	0	6	4
8-6	145	1	1	1	1	7	5
7-4	50	1	1	7	5	7	5
6-5	50	1	1	0	0	7	3
6-4	30	6	2	7	3	13	7
5-4	40	1	1	1	1	8	4
7-6	50	6	2	0	0	7	5
2-7	150	0	0	0	0	5	3
1-9	75	0	0	0	0	5	3

Table 11. Loads ρ_{ij} and probabilities q_{ij} of information loss of an individual link.

Link	ρ_{ij}^{nr}	q_{ij}^{nr}	ρ_{ij}^{em}	q_{ij}^{em}
1-7	0.01593	1.008E-09	0.04065	1.0643E-07
2-9	0.02477	9.099E-09	0.04064	1.0638E-07
10-2	0.00890	5.545E-11	0.00890	5.5455E-11
3-4	0.04583	1.929E-07	0.04580	1.9296E-07
3-5	–	–	0.04583	1.9289E-07
9-7	0.03363	4.154E-08	0.04949	2.8233E-07
9-8	–	–	0,04949	2.8221E-07
8-6	0.00891	5.557E-11	0.05835	6.3671E-07
7-4	0.05834	6.364E-07	0.05834	6.3645E-07
6-5	–	–	0.05468	4.6204E-07
6-4	0.05468	4.619E-07	0.10412	1.0961E-05
5-4	0.00890	5.541E-11	0.06353	9.6904E-07
7-6	–	–	0.05834	6.3644E-07
2-7	–	–	0.04065	1.0649E-07
1-9	–	–	0.04064	1.0638E-07

VI. Power system model with WAMS

Let us consider the described approach on the example of a 10-node system considered in [14], Fig. 2. Without dwelling on the optimal composition of PMUs, we will assign PMU to each node of the network and select sites for PDCs at nodes 4 and 9. We determine the main and redundant channels of information exchange from the PMU of each node (Table 4 and Fig. 3). Fig. 4a indicates such links without redundancy, and Fig. 4b presents them with redundancy. For fiber-optic communication lines, the specific indices according to Table 12.4 from [15] and data from [16, 17] are $\lambda_l = 0.01752$ failure/(km/yr.); $r_l = 0.2088$ hr./(km/recovery). Reliability indices of electronic devices with their duplication are $\lambda_{PMU} = 1.539 \cdot 10^{-3}$ failure/yr., $\mu_{PMU} = 5.922$ recovery/yr., $A_{PMU} = 0.999740$ [2], $\lambda_{PDC} = 2.673 \cdot 10^{-6}$ failure/yr. and $\mu_{PDC} = 740$ recovery/yr., $A_{PDC} = 0.999999996$ [15].

VII. Technical availability of local information network

Table 5 presents the determined link availabilities of the information exchange channel, each including an information source (PMU or PDC) and the actual fiber-optic connection, given that $\mu_{con} = 8760/r_{con}$ recovery/yr. Then the availability of individual information channel is determined as the product of availabilities of sequential links, which corresponds to a channel without redundancy, and the availability of the i-th channel with redundancy is calculated as

$$A_{ch,i} = 1 - (1 - A_{m\_ch,i}) \cdot (1 - A_{r\_ch,i}), \qquad (11)$$

where $A_{m\_ch,i}$ is the i-th main channel connection availability, and $A_{r\_ch,i}$ is the i-th redundant channel connection availability. The channel availabilities are given in Table 6 according to the connections (Table 4) and to the availabilities of the links (Table 5).

Let the line from the source to the dispatching node be a "channel" consisting of links between neighboring nodes. Table 6 shows that with a single set of links of communication channel, its availability varies in the range of one to three nines after the decimal point. The availability of communication with redundancy is maintained at the level of three nines after the decimal point, even if a source is located sufficiently far from the dispatching node, such as nodes 1 and 2. The availability of channel 10 is the value of the main channel availability since this channel has no redundancy, i.e., redundant communication lines.

Table 12. Probabilities of the route information loss.

Route	$Q^{nr}_{\Sigma u}$	Route	$Q^{em}_{\Sigma u}$
1-7-4	6.37E-07	1-9-8-6-4	1.199E-05
2-9-7-4	6.87E-07	2-7-4	7.429E-07
3-4	1.93E-07	3-5-4	1.162E-06
5-4	5.54E-11	5-6-4	1.142E-05
6-4	4.62E-07	6-5-4	1.431E-06
7-4	6.36E-07	7-6-4	1.16E-05
8-6-4	4.62E-07	8-9-7-4	1.201E-06
9-7-4	6.78E-07	9-8-6-4	1.188E-05
10-2-7-4	6.37E-07	–	–

Table 13. Influence of load intensity ρ and the number of sections N on the probability of information loss q and error-free operation p for link 7-4.

#	ρ	N	p	q	#	ρ	N	p	q
1		0	0	1	5		7	0.9998469	0.0001531
2		1	0.99009901	0.00990099	6	0.3	10	0.999995867	4.13344E-06
3		3	0.99999901	9.9E-07	7		100	1	0
4	0.01	5	1	9.9E-11	1		0	0	1
5		7	1	9.88098E-15	2		1	0.666666667	0.333333333
6		10	1	0	3		3	0.933333333	0.066666667
7		100	1	0	4	0.5	5	0.984126984	0.015873016
1		0	0	1	5		7	0.996078431	0.003921569
2		1	0.944874979	0.055125021	6		10	0.99951148	0.00048852
3		3	0.999813008	0.000186992	7		100	1	0
4	0.058341	5	0.999999364	6.36452E-07	1		0	0	1
5		7	0.999999998	2.16628E-09	2		1	0.588235294	0.411764706
6		10	1	4.30211E-13	3		3	0.864587446	0.135412554
7		100	1	0	4	0.7	5	0.942856074	0.057143926
1		0	0.000000000	1.000000000	5		7	0.973782312	0.026217688
2		1	0.909090909	0.090909090	6		10	0.991354799	0.008645201
3		3	0.999099909	0.000900090	7		100	1	1.11022E-16
4	0.1	5	0.999990999	0.000009000	1		0	0	1
5		7	0.999999909	0.000000090	2		1	0.500000025	0.499999975
6		10	0.999999999	9.000007E-11	3		3	0.750000038	0.249999962
7		100	1.000000000	0.000000000	4	0.9999999	5	0.833333375	0.166666625
1		0	0	1	5		7	0.875000044	0.124999956
2	0.3	1	0.769230769	0.230769231	6		10	0.909090955	0.090909045
3		3	0.98094566	0.01905434	7		100	0.990099059	0.009900941
4		5	0.998297759	0.001702241					

The specific indices for communication lines using a high-frequency signal on power lines (Table 12.3 [4]) are λ_l = 0.0196 failure/(km/yr.); r_l = 0.19 hr./(km/recovery). The rest of the data are the same. The availabilities of channel link and information exchange channels are given in Tables 7 and Table 8, respectively.

A comparison of Tables 5, 6 and 7, and 8 shows that the difference in availability between fiber-optic and high-frequency transmission is negligible. Table 8 shows that for optical fiber only the main channel determines the availability of node 10.

Based on the sequential connection of links of the main or redundant information channel and parallel operation of these channels on the server, we determine the failure rate λ_Σ and the recovery rate μ_Σ for fiber-optic information exchange channels. Then, $\lambda_{i,\Sigma} = \sum_j \lambda_{i,j}$, where i is the main or redundant information channel, j is the link of this channel. Further, we determine $\mu_{i,\Sigma} = \dfrac{\lambda_{i,\Sigma} \cdot A_{ch,i}}{1 - A_{ch,i}}$ from the relation $A = \dfrac{\mu}{\mu + \lambda}$ and find $\mu_\Sigma = \sum_i \mu_{i,\Sigma}$, and $\lambda_\Sigma = \dfrac{\mu_\Sigma \left(1 - A_{ch,i}\right)}{A_{ch,i}}$. The resulting λ_Σ and μ_Σ for fiber-optic and power lines are summarized in Table 9.

With a complex network of information connections, we can find a redundant connection from the server node to the node with failed connection, excluding the latter one. To do this, we use the depth-first and breadth-first search algorithm as proposed in [17]. It allows finding a backup path with failed connections, if one exists, or warning about its absence. When searching, the column "Redundant channel" is built in Table 4, and then the hardware reliability is evaluated for the found path. These backup routes are stored in Table 1 in the order of

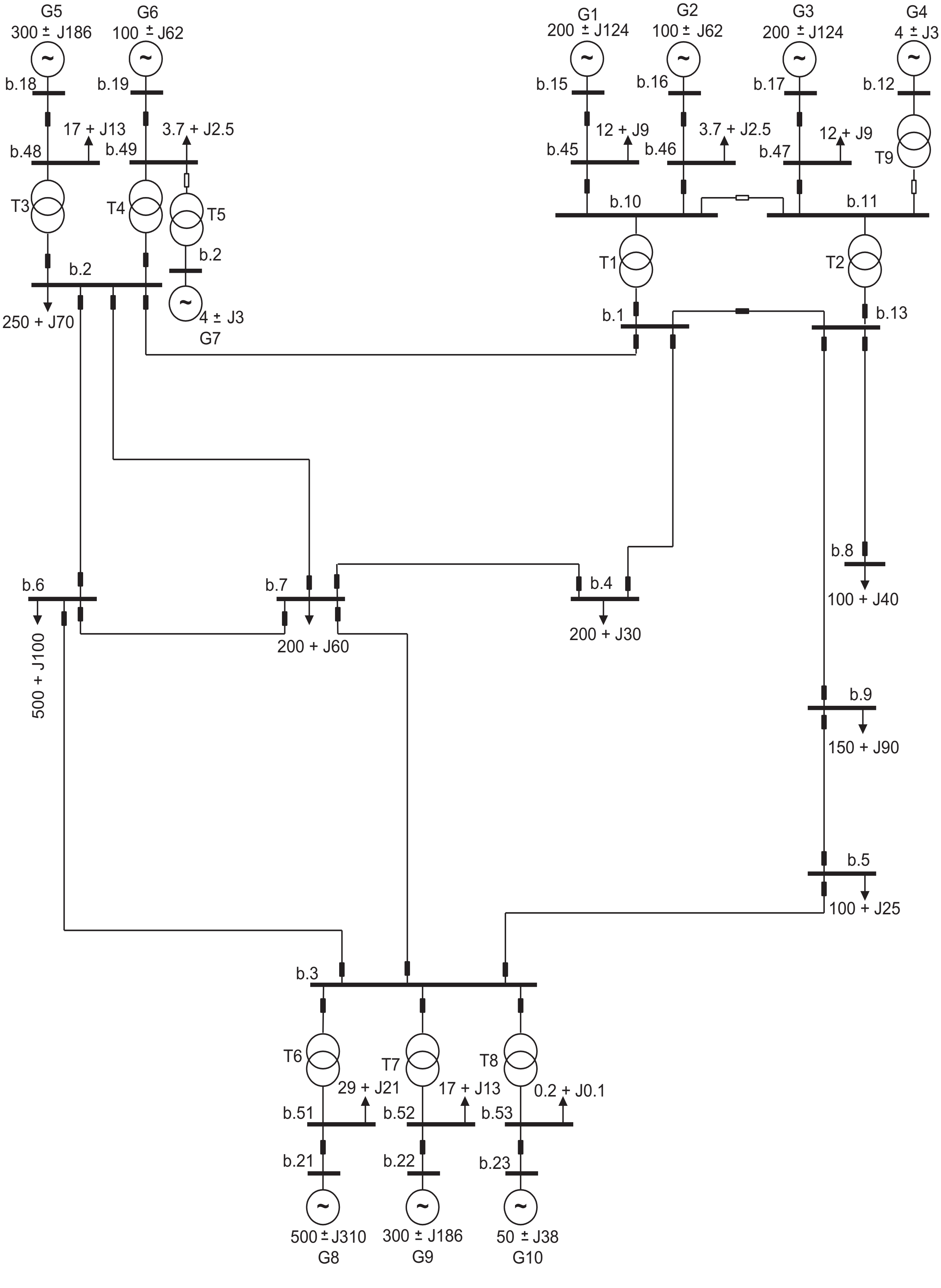

Fig. 2. Model diagram of the test power system. The black switch is on, the white one is off.

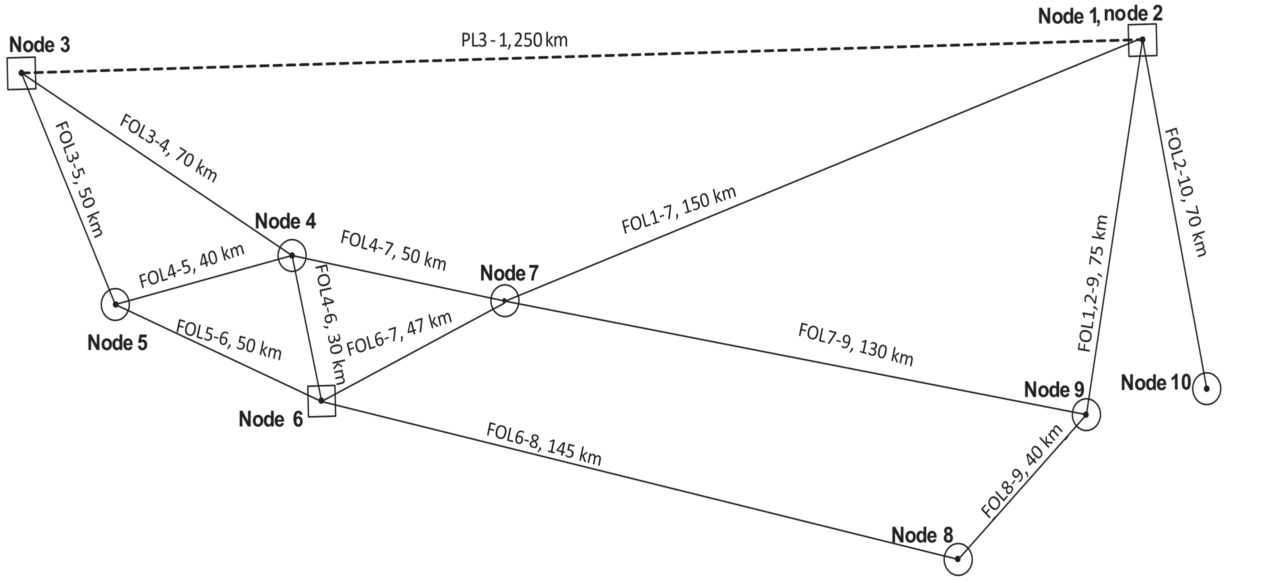

Fig. 3. The geographical location of the test power system (scale: 1cm = 20 km). Rectangle nodes contain generation. Circular nodes have only load.

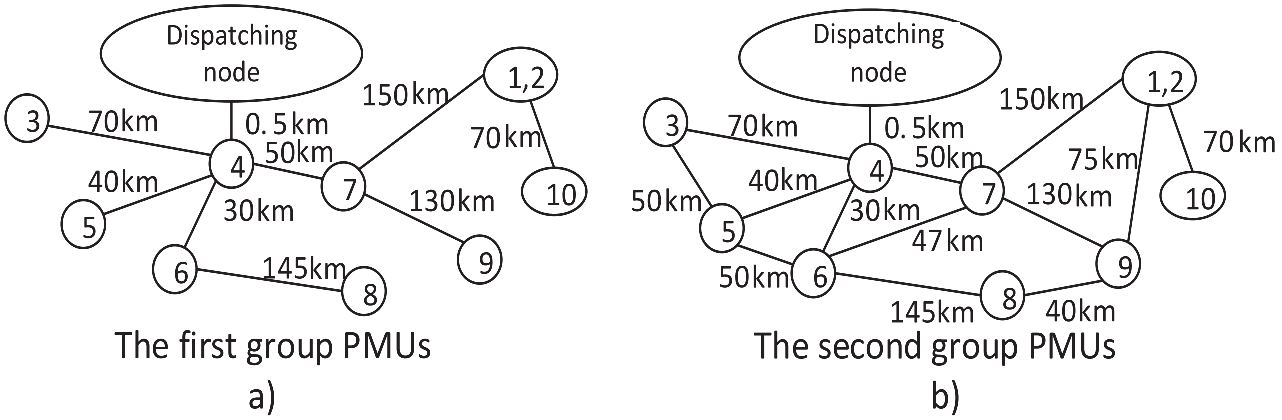

Fig. 4. Communication channels: a) without redundancy, b) with redundancy.

Table 14. An example of the difference between the values of two schemes by contribution of reliability components.

R_1	R_2	R_3	R_4	Q_a	Q_b	$\frac{Q_b - Q_a}{Q_a}100\%$
0.9	0.9	0.9	0.9	0.0199	0.0361	44.87534626
0.9	0.8	0.8	0.9	0.0396	0.0784	49.48979592
0.8	0.9	0.8	0.9	0.0396	0.0684	42.10526316
0.8	0.8	0.8	0.8	0.0784	0.1296	39.50617284

Table 15. The difference in the reliability component contributions for two equivalent circuits.

A_{main}	$A_{redundant}$	P_{nr}	P_{em}	$Q_{paral.}$	$Q_{sequen.}$	$\frac{Q_{sequen.} - Q_{paral.}}{Q_{paral.}}100\%$
0.989400945	0.987684744	0.999999363	0.99998801	0.00013053	0.000130663	0.102001899
0.989400945	0.989374459	0.999999313	0.9999992571	0.000112621	0.000112636	0.013328578
0.997698469	0.998030512	0.999999807	0.999998838	4.53284E-06	4.53589E-06	0.067205108
0.99907246	0.998322147	0.9999999999	0.99998569	1.55628E-06	1.56953E-06	0.844266885
0.999364399	0.998030512	0.999999538	0.999998569	1.25181E-06	1.25363E-06	0.144945673
0.990433883	0.998443352	0.999999364	0.9999884	1.48911E-05	1.50029E-05	0.745022642
0.990666305	0.991036328	0.999999538	0.999998799	8.36642E-05	8.36794E-05	0.018178718
0.991698503	0.99000482	0.999999322	0.99998812	8.2975E-05	8.30793E-05	0.125610524
0.987380523	0	0.999999363	0	0.012620106	0.012620106	0

Table 16. Data for calculating the contribution of components.

Source node	$A_{\text{channel with redundancy}}$	$Q^{em}_{\Sigma M,i}$	$\frac{1}{t_{SW} \cdot n}$
1	0.99986947	1.199E-05	1/285/10 = 3.5087719E-04
2	0.999887379	7.429E-07	
3	0.999995467	1.162E-06	
5	0.999998444	1.142E-05	
6	0.999998748	1.431E-06	
7	0.990433883	1.16E-05	
8	0.990666305	1.201E-06	
9	0.991698503	1.188E-05	
10	0.987380523	6.37E-07	

Table 17. Calculation results of the contribution by component.

Source -node	$Con_{A,i}$, 100%	$Con_{Q,i}$, 100%	$Con_{SW,i}$, 100%	$Con_{\Sigma,i}$, 100%	$A_{\Sigma,i}$
1	73.49342727	6.750832704	19.75574003	0.01776077	0.999822399
2	75.86377335	0.500432399	23.63579425	0.01484516	0.999851552
3	11.11500184	2.849246004	86.03575216	0.00407827	0.999959217
5	3.237369106	23.76012545	73.00250545	0.00480637	0.999951937
6	3.31473698	3.788649056	92.89661396	0.00377707	0.999962229
7	24.18205538	18.83767661	56.98026802	0.00615787	0.999938422
8	69.74748092	1.001227823	29.25129126	0.01199527	0.99988005
9	63.85505894	9.14248991	27.00245115	0.01299427	0.999870062
10	99.71770723	0.005033503	0.277259265	1.26552017	0.987345249

decreasing availability. A similar operation is performed in the process of network building. In actuality, a redundant channel with operational connections and the highest availability is used, if necessary.

VIII. Traffic reliability

Let us consider the WAMS information channels for the power system, Fig. 2. The scheme of information connections with the distance scale is shown above in Fig. 3. Let us define the network conditions and characteristics. All data connections are made using fiber optics with a propagation delay T_{sp} = 5 ns. Electronic delay is T_{re} = 5 μs. The transmission speed is v_{tr} = 1 Mbit/s = 1048576 bit/s [17]. Measurement transmission frequency is 10 Hz or T_{msr} = 0.1 s. Control center is located at node 4 of the power system (Fig. 4), information routes of each information transmission channel under normal and emergency conditions are shown in Table 4, and its last column shows the connection of the source node to node 4 via bypass routes in the case of failure of the main route component. Note that failure of link 10-2 results in a complete loss of communication with node 10. The initial data for the calculations are summarized in Table 10. Here, b_{in} and b_{fr} in the third and fourth columns are the values of bytes associated directly with the corresponding link of the line; Σb^{nr} and Σb^{em} are byte groups, including intermediate communication packets under both normal and emergency conditions caused by a failure of one of the links. N is determined by the maximum frame under normal operating conditions and equals 5.

The simulation results are shown in Tables 11 and 12, which indicate that the probability of information loss in the case of the calculated loads is very low. Let us consider the relationship between the information loss probability q and the load intensity ρ using the example of connection 7-4 with the rest of the same conditions. Using the same example, consider the effect of the number of storage sections N, Table 13.

It is clear that for N = 0, the probability of losing information is 1 since there is simply nowhere to receive it. With an increase in N, the value of q drops rather steeply, turning almost to zero already at N = 10. It is also obvious that the greater the load intensity ρ the greater the probability of information loss q. The rise is quick, which requires an increase in the number N of receiver storage sections.

IX. The component contribution to the total reliability of local information network

In the above sections, we determined the components of the WAMS information network reliability. In this section, we seek to determine the total reliability and the contribution of each component to this value. Initially, the question arose, what should be the contribution model of the component reliability should have? Let $R_{i,1}$ be hardware reliability of the main i-th route, $R_{i,2}$ be hardware reliability of the backup i-th route, $R_{i,3}$ be the traffic reliability of the main i-th route, $R_{i,4}$ be the traffic reliability of the backup i-th route. The contribution model can have one of the following schemes (Fig. 5). In scheme (a), the hardware and the traffic component are combined first, and then the main and backup routes are combined. In scheme (b), firstly, the hardware components of the main and backup routes are combined, then the traffic components of the same routes are combined, after which the obtained equivalents are connected sequentially. Equivalent values are determined as

$$R_a = 1 - (1 - R_1R_3)(1 - R_2R_4), \quad (12)$$

$$R_b = [1 - (1 - R_1)(1 - R_3)]\,[1 - (1 - R_2)(1 - R_4)], \quad (13)$$

With a large difference in the values of R_i, the relative difference between the equivalent values $Q_i = 1 - R_i$ can reach ten percent. Thus, for example, if the difference between R_i is 0.1, this difference lies between 39 and 49 percent (Table 14).

Let us consider such a relationship (Table 15) between the availability values of the route of fiber-optic information exchange channel (A_{main} and $A_{redundant}$ from Table 6) and the probabilities of the absence of information loss over a route due to the traffic load (Q_{nr} and Q_{em} from Table 12). Table 15 indicates that for the test scheme such a difference lies in the range of 0.01 to 0.85 percent, i.e., less than 1 percent. Therefore, when evaluating the components, any of the considered equivalent circuits can be used.

Further, we will estimate the contribution of reliability components to the local information network operation. It is more convenient to do that based on the component unavailability, i.e.,

$$Con_{A,i} = \frac{1 - A_{channel\ with\ redun.,i}}{Con_{\Sigma,i}} 100\%;$$

$$Con_{Q,i} = \frac{Q^{a}_{\Sigma M,i}}{Con_{\Sigma,i}} 100\%; \quad Con_{SW,i} = \frac{1}{t_{SW} \cdot n \cdot Con_{\Sigma,i}} 100\%;$$

$$Con_{\Sigma,i} = (Con_{A,i} + Con_{Q,i} + Con_{SW,i}) \cdot 100\%, \quad (14)$$

where $Con_{A,i}$ is a share of technical unavailability, $Con_{Q,i}$ is a share of unavailability due to traffic. Here $Q^{a}_{\Sigma M,i}$ is used for an adverse event. $Con_{SW,i}$ is a share of unavailability for software, n is the number of the information source nodes. Here we rely on the assumption that the software is divided equally among the node devices, i.e., in our case n = 10. $Con_{\Sigma,i}$ is the sum of the shares of component unavailabilities. The total availability of a LIN route can be determined as

$$A_{\Sigma,i} = A_{channel\ with\ redun.,i} \cdot (1 - Q^{a}_{\Sigma M,i}) \cdot \left(1 - \frac{1}{t_{SW} \cdot n}\right) \quad (15)$$

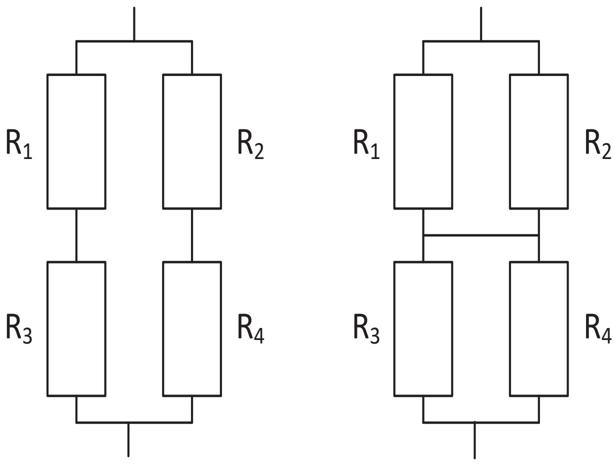

a) *b)*

Fig. 5. Models of the route reliability component contribution to the total reliability.

For the considered scheme, the initial data on the fiber-optic network are summarized in Table 16. The calculation results are shown in Table 17.

Table 17 shows that the farther the source node from the dispatching node, the greater the weight of the hardware reliability component. On the other hand, the closer the source to the dispatching node, the heavier the traffic, which levels the total route availability out.

X. Conclusions

The proper functioning of the WAMS information network is ensured by four components of its reliability. These are hardware or technical reliability associated with the failure of transmission channel elements or destruction of the integrity of information transmission lines; software reliability related to errors in the development of exchange execution programs; traffic reliability determined by the time loss or distortion of data without a failure of the transmission channel elements; and resistance to external deliberate impact on the transmitted information. The influence of the latter component is discussed in many works, for example, [12, 13], which is why it is not considered in the paper.

Convenient algorithmization of the assessment of the components of the local information network reliability simplifies the implementation of computer applications of the assessment.

The reliability of hardware (PMUs, PDCs) of such a network largely depends on the reliability of information carriers (optical fiber, radio waves, and others) and devices that ensure its operation. The paper deals with an approach designed to determine the parameters of such reliability on the example of a 10-node power system. Thus, with the appropriate redundancy, the hardware availability of the network, including information sources (PMUs), exceeds three nines after the decimal point for fiber optics and is slightly less when information exchange occurs over power lines. The ways of increasing the hardware reliability of the information network are considered.

The traffic reliability component is determined by the load intensity of each link and the information receiving capabilities associated with the receiver storage capacity. It is worth noting that there is a strong dependence of the probability of information loss on the number of sections in the receiver storage device, whose increase makes it possible to compensate within some range for the growth of this probability with an increase in the load intensity. The test network traffic availability also exceeded three nines after the decimal point.

In terms of software, the impact of the number of code lines on the value of this parameter is noted and its assessment is shown depending on the number of commands. A significant property of this index is its improvement with an increase in operating time. However, it can be incorrect due to new errors appearing when correction is made under operation. For the example of a WAMS program of 10 million code lines, the mean time between failures should be 285 years.

The study has revealed that despite different results obtained for various equivalent circuits, the error in their calculations for the range of requirements for their values lies within acceptable limits.

The contribution of the considered components to the total reliability has been assessed for the test scheme. The findings have shown that the greater the distance between the source node and the dispatching node, the greater the weight of the hardware reliability component. On the other hand, the closer the source to the dispatch center, the heavier the traffic, which equalizes the total availability of different routes.

References

[1] A. G. Phadke and J. S. Thorp, “Synchronized Phasor Measurements and Their Applications,” New York, NY, USA: Springer, 2008, 260 p.

[2] M. I. Uspensky, “Estimation of the functioning reliability for the device of synchronized vector measurements,” *Relay protection and automation*, no. 3, pp. 39-44, 2017. (In Russian).

[3] *Real-Time Application of Synchrophasors for Improving Reliability*, NERC, Princeton, NJ, USA, 10/18/2010, 77 p. Available at: http://www.naspi.org (accessed 09.02.2020)

[4] V. N. Tsukanov, M. Ya. Yakovlev, “Fiber-optic technology. Practical Guide,” Moscow, M., Russia: Infra-Engineering, 2014, 304 p. (In Russian).

[5] A. E. Davydov, P. I. Smirnov, A. I. Paramonov, “Design of telecommunication systems and networks. Calculation of communication network parameters and traffic analysis,” St. Petersburg, Russia: ITMO University, 2016, 47 p. (In Russian).

[6] M. O. Asanov, V. A. Baransky, V. V. Rasin, “Discrete mathematics: graphs, matroids, algorithms,” Moscow, M., Russia: RHD, 2001, 288 p. (In Russian).

[7] N. B. Zeliger, O. S. Chugreev, G. G. Yanovsky, “Designing networks and transmission systems for discrete messages,” Moscow, M., Russia: Radio and communications, 1984, 177 p. (In Russian)

[8] Yu. M. Morozov, “Reliability of hardware and software systems,” St. Petersburg, Russia: State Polytechnic University, 2011, 136 p. (In Russian)

[9] V. N. Shklyar, “Reliability of control systems,” Tomsk, Russia: Publishing house of Tomsk Polytechnic University, 2009, 126 p. (In Russian)

[10] V. O. Chukanov, V. V. Gurov, E.V. Prokopyeva, “Methods of ensuring software and hardware reliability for computing systems,” Russia, Presentation of the report at the seminar, .1-44 p. Available at: http://www.mcst.ru/files/5357 ec/dd0cd8/50af39/000000/seminar_metody_obespecheniya_apparatno-programmnoy_nadezhnosti_vychislitelnyh_sistem.pdf (In Russian). (accessed 12.03.2019)

[11] S. M. Borovikov, S. S. Dik, N. K. Fomenko, “A method for predicting applied software tools at the early stages of their development,” Reports of the Belarusian State University of Informatics and Radioelectronics. 2019, no.5, pp. 45-51.

[12] Y. Zhang *et al.*, "Cyber-Physical Security Analytics for Transactive Energy Systems," *IEEE Trans. on Smart Grid*, vol. 11, no. 2, pp. 931-941, March 2020.

[13] E. Martel, R. Kariger, P.-A. Graf, “Cyber Resilience in the Electricity Ecosystem: Principles and Guidance for Boards,” Geneva, Switzerland, Centre for Cybersecurity and Electricity Industry Community, January 2019, 29 p. Available at: www3.weforum.org. (accessed 19.03.2020)

[14] M. I. Uspensky, S. O. Smirnov, “The Occurrence Reasons and Countermeasures to Power System Blackouts,” *The International Journal of Energy Engineering*, no. 1, pp.1-8, 2014.

[15] W. Li, “Risk Assessment of Power Systems: Models, Methods, and Applications,” New York, NY, USA: Wiley-IEEE Press, 2005, 325 p.

[16] “Reliability evaluation of the designed FOCL,” Available at: http://www.icete.ru/pegibs-567-1.html. (In Russian). (accessed 23.11.2020)

[17] V. N. Gordienko *et al.*, “Optical telecommunication systems. Textbook for high schools,” Moscow, M., Russia: Hotline – Telecom, 2011, 368 p. (In Russian)

[18] M. I. Uspensky, I. V. Kyzrodev, “Power supply restoration in distributive networks,” *Reliability: Theory & Applications*, vol.2, no. 2, June, pp. 72-84. 2011.

Michael Igorevich Uspensky graduated from Leningrad (St. Petersburg) Polytechnic Institute in 1971. He received his Ph.D. degree in engineering from Leningrad Polytechnic Institute in 1985. At present, he is a leading scientist at the Laboratory of Power Systems. M.I. Uspensky works for the Institute for Social, Economic and Energy Problems of the North at the Komi Science Center of the Ural Branch of the Russian Academy of Sciences in Syktyvkar, Russia.

His research interests include operating control and reliability of power system facilities.

Digital Control of Electric Power Flows in Unbalanced Distribution Networks as Part of The Automated Metering and Control System

T.T.Omorov[1,*,] B.K.Takyrbashev[1,] K.E.Zakiriaev[2,] T.Zh.Koibagarov[1]

[1] National Academy of Sciences of the Kyrgyz Republic, Institute of Mechanical Engineering and Automation, Bishkek
[2] Issyk-Kul State University named after K. Tynystanov, Karakol, Kyrgyz Republic

Abstract — **This paper aims to address the problem of controlling the electricity flows in power distribution networks (PDN) operating under current and voltage unbalance. As is known, the unbalance factor is responsible for significant losses of active power and, therefore, is detrimental to the PDN efficiency and technical and economic performance. The purpose of control is to minimize technical power losses in the distribution network. This is to be achieved by building an information control system (ICS) for balancing a three-phase network as part of the automated metering and control system (AMCS). The latter is currently being widely adopted to automate information processes in PDNs. However, the AMCS does not include technologies for solving the problem in question. We propose an algorithm of the digital controller operation for the ICS. Its primary function is to maintain phase power at a given level in real-time. The algorithm concept is based on the idea of required redistribution of electricity flows between the phases of the distribution network by appropriately switching single-phase loads of consumers (users) to ensure a minimum spread of phase powers relative to their required level. To achieve the goal of control, we construct criterion functions that determine qualitative indices of the ICS operation and develop computational schemes for their minimization. Control actions to be generated by the digital controller and performed on the facility represent a digital code that contains data on the coordinates of three-phase network loads to be switched to another phase.**

Index Terms: **distribution network, unbalanced mode, control of electricity flows, digital controller, control algorithm.**

* Corresponding author.
E-mail: omorovtt@mail.ru

http://dx.doi.org/10.38028/esr.2021.01.0005
Received March 26, 2021. Revised April 03, 2021.
Accepted April 13, 2021. Available online May 26, 2021.

I. Introduction

At present, power distribution networks (PDN) are widely adopting advanced digital technologies in the form of automated metering and control systems (AMCSs) to automate their processes and make them data-driven [1]. These systems are elements of the Smart Grid technology [2]. An analysis of the functional structure of existing (conventional) AMCSs shows that they mainly perform metering and fiscal metering of electricity and belong to the class of information and measurement systems. The latter lack tools designed to solve the problem of balancing three-phase distribution networks. At the same time, most of the 0.4 kV power distribution networks operate under current and voltage unbalance [3-5], which causes nonoptimal operating conditions. Unbalance of PDN results from unbalance of loads and their uneven distribution over phases of a three-phase network. According to the published research data, in networks with distributed load, which have a deviation (unbalance) of phase currents from their average values, technical losses increase significantly [6-8]. The results of experimental studies of power supply systems indicate that technical losses in power lines and transformer substations (TS) supplying them amount to more than 6% of the total electricity supplied to the inputs of distribution networks [9]. At the same time, the quality of electricity deteriorates, and the likelihood of failure of household appliances and industrial installations also increases [8]. Although many methods and devices were proposed [10-13] for balancing distribution networks, their practical use proves difficult. This is due to the technical challenges of creating automated balancing systems on their basis for three-phase distribution networks with a large number of electricity consumers. For the technical implementation of these solutions, at points of load connection to the network phases, it is necessary to create separate local subsystems with individual units as their parts to perform functions of parameter measurement, control, and data processing. However, building such subsystems involves rather elaborate processing algorithms based on measurements of a group of information parameters. For example, the method outlined in [10] requires measurements of the active power of a zero wire of line, voltage and current signals of the zero wire at the points of load connection to the network, while the reactive power control system [13] uses positive sequence, negative sequence, and zero sequence currents of loads. In modern electricity meters [16], which are part of the AMCS, these measurement functions are not available. In this regard, the use of the above technologies as part of modern AMCSs seems to be problematic. In [14, 15], one of the possible approaches proposed to solve the given problem is based on a digital system for automatic control of the network balancing process as part of the data concentrator of the AMCS. As is known, a data concentrator in conventional automated systems collects data from a group of electricity meters installed at the side of network users and performs computing operations related to fiscal metering of electricity. According to this approach, the data concentrator is assigned with an additional function of digital control, which provides the required redistribution of electricity flows between the network phases by switching single-phase loads from a more loaded phase to a less loaded one. At the same time, electricity meters must have dedicated actuating elements, i.e., phase current switches (PCS), as their part. The creation of such PCSs is a feasible task since modern single-phase and three-phase meters [16, 17] have relays with powerful contacts up to 100A, which can be used to switch power consumers from one phase to another [15].

The present study aims to develop this approach for solving problems of control of electricity flows in unbalanced distribution networks.

II. Problem statement

Let us consider a three-phase four-wire distribution network to which a power supply transformer substation (TS) and a group of n electricity meters $\{Em_{vk}\}$ installed at single-phase consumers are connected. Its simplified diagram is shown in Fig. 1, where k, v are index variables denoting, respectively, the numbers of phases A, B, C ($k=\overline{1,3}$) and loads (electrical consumers) of network users ($v=\overline{1,n}$); $\tilde{I}_k$, $\tilde{U}_k$ are sinusoidal instantaneous current and voltage at the input of the k-th phase; Z_{vk} is the load with the coordinate (v, k); $\tilde{I}_{vk}$, $\tilde{U}_{vk}$ are instantaneous current and voltage across the load Z_{vk}; $\tilde{J}$ is instantaneous current in the zero wire; $\dot{P}_k$ is complex power of the k-th phase; $\dot{P}_{vk}$ is complex power consumed by the consumer load with the coordinate (v, k); PCS_{vk} is a switch of phase currents of the meter Em_{vk}.

Next, we make the following assumptions:

1. the three-phase network operates under current and voltage unbalance;
2. the phase current switches (PCS_{vk}) are a part of the electricity meters (Em_{vk});
3. the concentrator at discrete moments of time $t = t_\xi$ ($\xi = 1, 2, ...$) periodically polls the head-end three-phase electricity meter (Em^{TS}) and groups of consumers' meters connected to phases A, B, C, and writes to the database AMCS values of the following quantities:

- active p_{vk} and reactive q_{vk} power consumed by loads of network users with coordinates (v, k);
- active p_k and reactive q_k powers consumed by the corresponding phases at the input of the three-phase network.

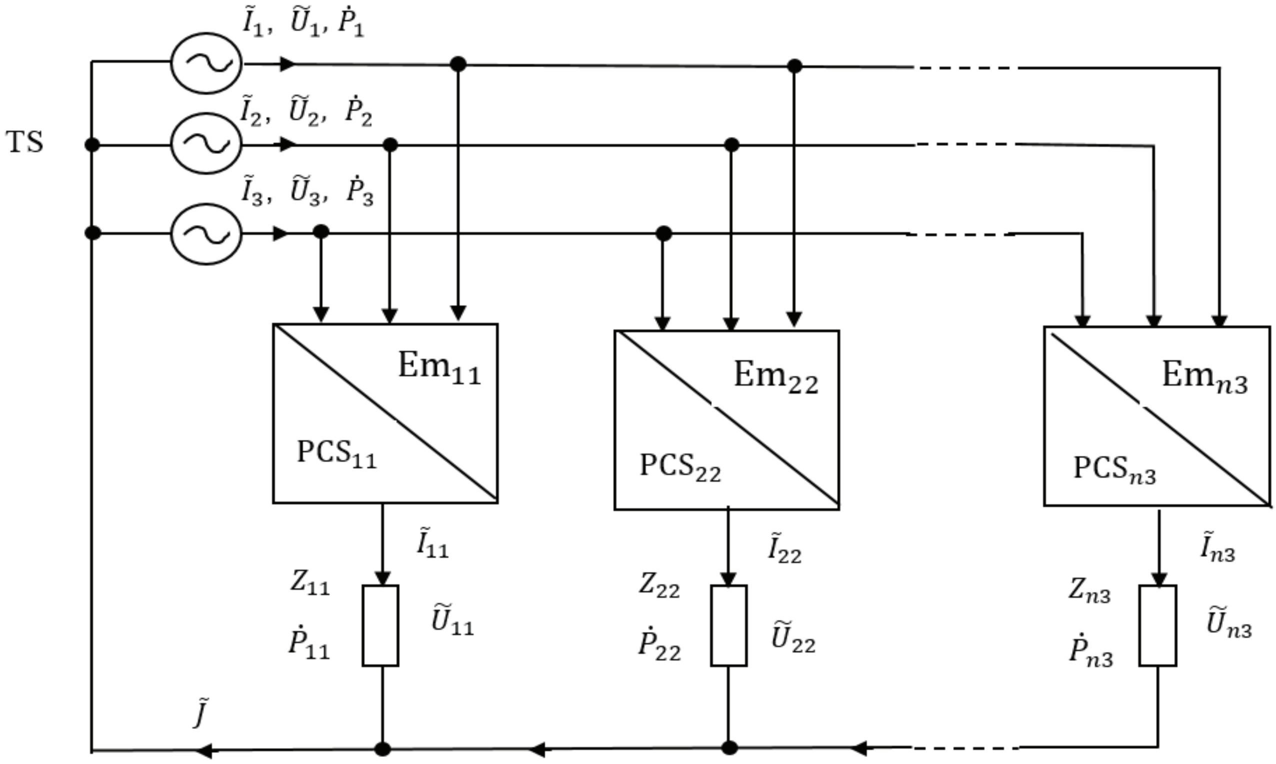

Fig. 1. Simplified diagram of the distribution network with Em_{vk} and PCS_{vk}

Technical losses of electricity in the transformer substation and the network are largely determined by the value of current J flowing at the head-end of the zero wire. Moreover, the lower the value of this current, the higher the level of the network balance and the lower the power loss there. Therefore, the quality and efficiency of the distribution network can be assessed by the following objective function [15]:

$$E = J. \tag{1}$$

Minimizing the efficiency index of system E is equivalent to optimizing the operating condition of an unbalanced distribution network, which provides a minimum unbalance in the values of the total power consumed by each phase of the network. To this end, we propose creating an appropriate information control system (ICS) as part of the modern (conventional) AMCS. The development of the ICS is to be based on the principles of building automatic systems [18] and digital technologies, the functional structure of which is shown in Fig. 2. In this case, the group of loads $\{Z_{\nu k}\}$ of network consumers to which the electricity meters $\{Em_{\nu k}\}$ are connected, together with the

ICS actuating elements, is a control object. The key functional block of the system is a digital controller (DC) based on a microprocessor controller [19, 20]. The DC block generates control actions u^* to be performed on the facility based on a dedicated algorithm (control rule). The DC operation program is built by the automatic system initial state identifier (ISI) as setting action ρ^*. In this case, the control signal u^* is a digital code of the command, which is formed as vector $F = [F_1, F_2, \beta]$, where F_1, F_2 are numbers (names) of a pair of phases in which it is necessary to switch network consumers with a more loaded phase (F_1) to a less loaded one (F_2); β is a vector composed of addresses (numbers) of users of phase F_1 to be switched. This control signal u^* is transmitted via the communication channel (CC) to the system actuating elements, which are used as phase current switches (PCS) designed to perform the required switching of the network users' loads from one phase to another [15]. Conventional AMCSs employ various data transmission technologies (PLC, GSM, and others) as the CC.

The task is to synthesize an algorithm for the operation of a digital controller that optimizes the functioning of an unbalanced distribution network.

III. The control problem

The above control problem-solving process includes the following main steps:

1. Define the input data of the control problem.
2. Conduct a case study of the facility.
3. Construct criterion functions.
4. Build an algorithm for minimizing criterion functions.
5. Generate control actions to be performed on the facility.

A. Define the input data of the problem

Based on the data obtained from the main three-phase meter and consumer meters, the complex powers $\dot{P}_k$ and $\dot{P}_{\nu k}$, respectively, at the network input and consumer loads, are represented as [21]:

$$\dot{P}_k = p_k + jq_k, \quad k = \overline{1,3},$$

$$\dot{P}_{\nu k} = p_{\nu k} + jq_{\nu k}, \ \nu = \overline{1,n}, \ k = \overline{1,3}, \ j = \sqrt{-1},$$

Where j is an imaginary number. In this case, absolute values of these complex quantities are determined by the expressions:

$$P_k = \sqrt{p_k^2 + q_k^2}, \ k = \overline{1,3}, \tag{2}$$

$$P_{\nu k} = \sqrt{p_{\nu k}^2 + q_{\nu k}^2}, \ \nu = \overline{1,n}, \ k = \overline{1,3}. \tag{3}$$

It is worth noting that to solve the above-stated control problem, it is sufficient to poll only a small group of single-phase consumer electricity meters, except for meters installed at two-phase consumers. Further, we denote by n_1, n_2, and n_3 the total number of simplified consumer meters connected to phases A, B, and C, respectively. For brevity of notation and convenience of further transformations, the data on absolute values of complex powers of network consumers, determined as per

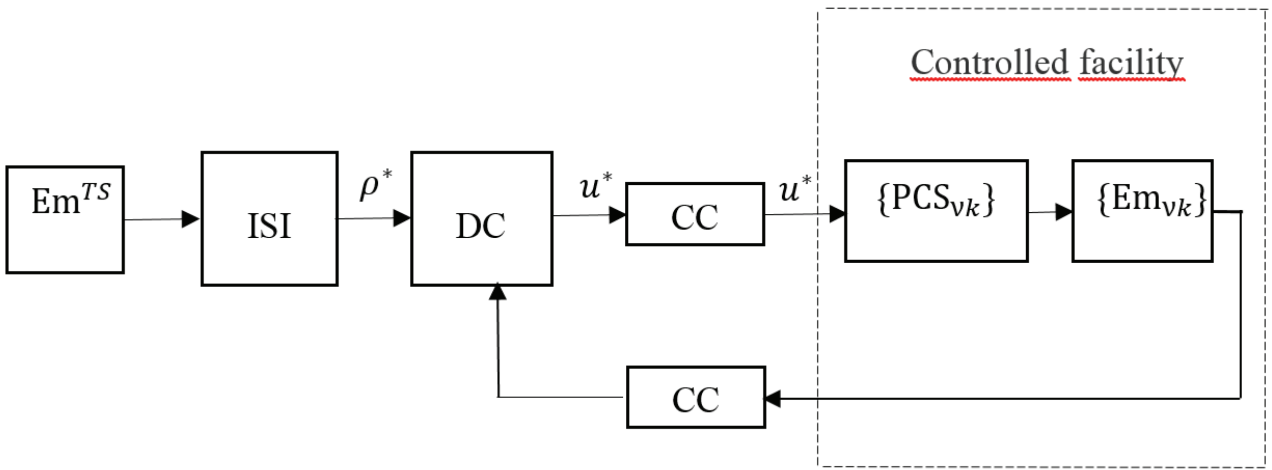

Fig. 2. ICS functional structure.

formulas (3), are provisionally presented in the form of the following vectors:

$$P^A = \left[P_1^A, P_2^A, \ldots, P_{n_1}^A \right],$$

$$P^B = \left[P_1^B, P_2^B, \ldots, P_{n_2}^B \right],$$

$$P^C = \left[P_1^C, P_2^C, \ldots, P_{n_3}^C \right],$$

and the coordinates of their elements are set by vectors:

$$\beta^A = \left[\beta_1^A, \beta_2^A, \ldots, \beta_{n_1}^A \right],$$

$$\beta^B = \left[\beta_1^B, \beta_2^B, \ldots, \beta_{n_2}^B \right],$$

$$\beta^C = \left[\beta_1^C, \beta_2^C, \ldots, \beta_{n_3}^C \right],$$

where superscripts A, B, and C indicate that the introduced vectors and their elements refer to the corresponding phases of the three-phase network. When forming vectors P^A, P^B, P^C, their components can be positioned arbitrarily. In this case, the set of components of indicated vectors make up the sets Λ_A, Λ_B, Λ_C, respectively:

$$\Lambda_A = \left\{ P_v^A \right\}_{1\times n_1}, \ \Lambda_B = \left\{ P_v^B \right\}_{1\times n_2}, \ \Lambda_C = \left\{ P_v^C \right\}_{1\times n_3}.$$

B. Conduct the case study of the facility

Such a study is performed to determine the structure of phase switching, i.e., to identify names of phases (F_1, F_2), in which corresponding loads of network consumers are to be switched. To this end, the average value P_0 of the phase power absolute values is provisionally calculated based on the formulas (2):

$$P_0 = (P_1 + P_2 + P_3)/3. \tag{4}$$

Similarly, one can determine the average value of effective phase currents I_1, I_2, and I_3 at the network input:

$$I_0 = (I_1 + I_2 + I_3)/3.$$

To assess the level of unbalance (deviations) of phase powers and currents from their average values, we introduce the following differences (residuals) into consideration:

$$e_k = P_k - P_0, \quad k = \overline{1,3},$$
$$\varepsilon_k = I_k - I_0, \quad k = \overline{1,3}. \tag{5}$$

Note that the values e_1, e_2, and e_3, as determined by formulas (5), are essentially control errors (residuals) that should tend to zero during control. In this case, current absolute values of phase powers at the input of the distribution network are determined by the formulas

$$P_k = P_0 + e_k, \ \ k = \overline{1,3}.$$

Hence one can see that at $e_k \to 0$ phase powers are $P_k \to P_0$, $k = \overline{1,3}$. Thus, the problem of optimizing the operating condition of the distribution network in each interval $[t_\xi, t_{\xi+1}]$ is reduced to minimizing control errors e_1, e_2, and e_3. In this case, control actions u^*, when performed on the facility, also lead to desired changes in effective phase currents I_1, I_2, and I_3 at the network inputs. Indeed, by definition, complex powers P_k at inputs of corresponding phases are determined by the formulas [21]:

$$\dot{P}_k = \dot{U}_k \dot{I}_k^* = I_k^2 z_k, \ \ k = \overline{1,3},$$

where $\dot{U}_k$, $\dot{I}_k$ are complex voltage and current at the input of the k-th phase; $\dot{I}_k^*$ is a complex conjugate value corresponding to current $\dot{I}_k$; z_k is complex resistance of the k-th phase. Therefore, the following expressions can be written for absolute values:

$$P_k = I_k^2 Z_k, \ \ k = \overline{1,3},$$

where Z_k is the absolute value of complex impedance z_k. Therefore, for effective phase currents I_k, the following formulas are valid:

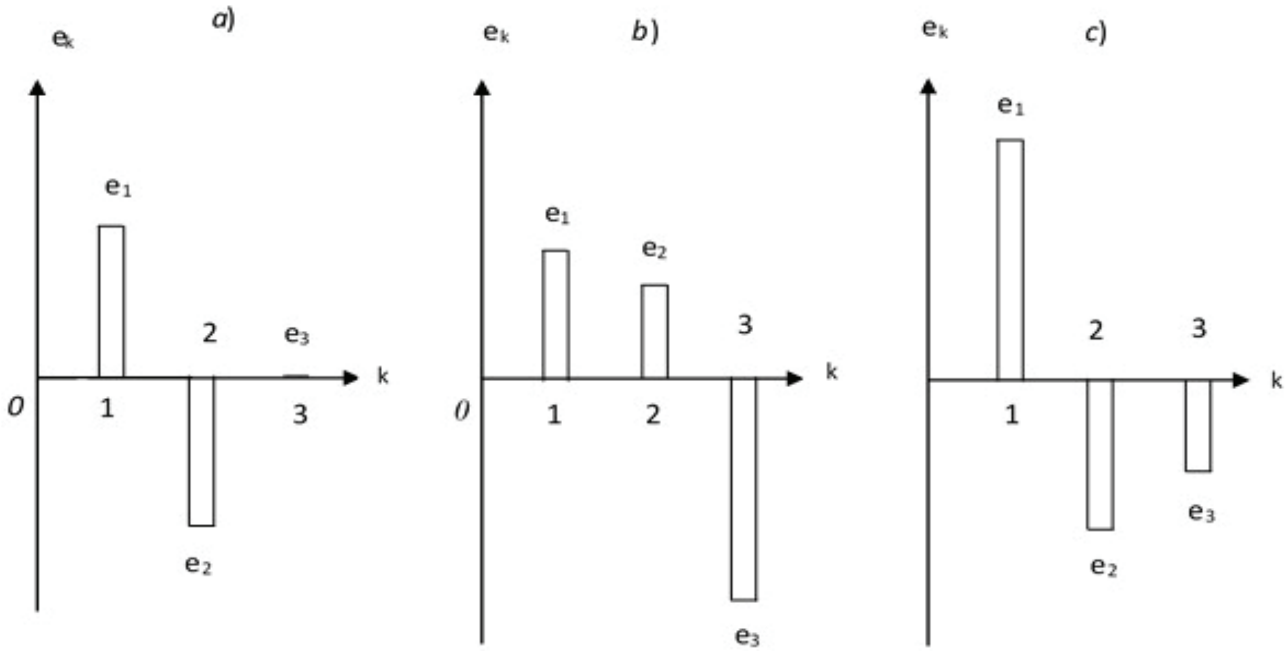

Fig. 3. Illustration of possible variants of control errors e_k.

$$I_k = \sqrt{P_k / Z_k}\ ,\quad k = \overline{1,3}\ .$$

It is worth noting here that the connection of a new load to the selected phase leads to an increase in the magnitude of the absolute value of power P_k and a decrease in its impedance Z_k. Therefore, in this case, the ratio P_k/Z_k increases, and when the load is disconnected, the value of P_k/Z_k decreases. Thus, in the process of control, an increase or decrease in the absolute values of power P_1, P_2, and P_3 leads to the same changes in the dynamics of operating phase currents I_1, I_2, and I_3.

In this case, corresponding absolute values of residuals for phase currents $|\varepsilon_1|$, $|\varepsilon_2|$, and $|\varepsilon_3|$ decrease so that the minimum of their unbalance is ensured. As a result, along with the equalization (balancing) of phases in terms of power, control of electricity flows in the distribution network also makes phase currents get balanced, which leads to the minimization of effective current J flowing in the head-end of the zero wire of the three-phase network.

Based on the results of calculating the residuals e_k, $k = \overline{1,3}$, the following cases can be distinguished:

Case 1. One of the components of the control error vector has a positive value $e = [e_1, e_2, e_3]$, one of them is negative, and one of them is equal to zero. For example, $e_1 > 0$, $e_2 < 0$, $e_3 = 0$, which is shown in Fig. 3a. In this case, phase A is overloaded, therefore, it is necessary to switch its consumers to phase B, which we denote further by $A \to B$ (F_1 = A, F_2 = B). In this case, phase C should retain the previous state since $e_3 = 0$.

Case 2. Two components of the residual vector e are positive, and the third one has a negative value. For example, $e_1 > 0$, $e_2 > 0$, $e_3 < 0$ (Fig. 3b). In this case, phases A and B are overloaded. It is, therefore, necessary to switch $A \to C$ and $B \to C$.

Case 3. One of the elements of vector e is positive, and the rest are negative. For example, $e_1 > 0$, $e_2 < 0$, $e_3 < 0$ (Fig. 3c). In this case, it is necessary to switch $A \to B$ and $A \to C$.

Thus, to identify the required switchings of the distribution network phases, it is necessary to perform a case study of the signs of values of e_k, $k = \overline{1,3}$. In this case, it is necessary to switch some consumers from phases with positive values of errors e_k to those with negative signs of control errors.

As a result, the case study of the facility provides for the following operations:

1. Poll the head-end three-phase electricity meter (Em^{TS}) and a given set of meters installed at network consumers connected to phases A, B, C, and define input data of the control problem.
2. Form vector $P = [P_1, P_2, P_3]$, consisting of the absolute values of complex powers consumed by phases A, B, and C, according to formulas (2).
3. Calculate average value P_0 of the phase power absolute values, as determined by formula (4).
4. Determine values and signs of the components of the vector of control errors $e = [e_1, e_2, e_3]$ as per formulas (5).
5. Identify names of phases (F_1, F_2), in which load switching operations are necessary, based on the analysis of signs of control error vector components $e = [e_1, e_2, e_3]$.

C. Construct the criterion function

It is easy to show that the initial state of the facility as it manifests itself by the components of the control error vector $e = [e_1, e_2, e_3]$ satisfies the following condition:

$$e_1 + e_2 + e_3 = 0. \tag{6}$$

Next, without loss of generality, consider Case 1 at the facility. In the case under consideration, the synthesized controller must output the initial mismatch $\rho^* = \rho_1^*$ through the control error, which is formed by the ISI block. Its value can be determined from condition (6). Since following the considered Case the residual $e_3 = 0$, condition (6) will have the form

$$e_1 = |e_2|.$$

Therefore, we arrive at $\rho_1^* = |e2|$. Next, we form subset λ_1 consisting of a set of elements of the set Λ_A, i.e., $\lambda_1 \in \Lambda_A$. In particular, λ_1 can consist of only one element. Let R_1 denote subset of indices (numbers) of vector components β^A: $R_1 = \{1, 2, \ldots, n_1\}$.

Now let us introduce the following function:

$$F_1(\lambda_1) = \left|S_1(\lambda_1) - \rho_1^*\right|, \tag{7}$$

where $S_1(\lambda_1)$ is a discrete function determined by the sum of elements of subset λ_1:

$$S_1(\lambda_1) = \sum_{l \in R_1} P_l^A .$$

The function $F_1(\lambda_1)$ defined by formula (7) can be used to indirectly estimate the value of the objective function E defined by expression (1). The analysis shows that when $F_1(\lambda_1) \to 0$, the control errors e_1 and e_2 also tend to zero when switching consumers with more loads connected to the first phase (phase A).

D. The algorithm for minimizing criterion functions

Now it can be seen that in the case under consideration, coordinates of loads of phase A users can be identified by solving the following extremal problem:

$$\min_{\lambda_1 \in \Lambda_A} F_1(\lambda_1) = F_1(\lambda_1^*), \tag{8}$$

where λ_1^* is the optimal set of absolute values of complex power consumed by phase A loads (k =1) to be switched to phase B. The set λ_1^* found this way contains complete information about the coordinates of consumer loads to be switched.

The minimization problem (8) is discrete and can be solved by enumerating options, which leads to time-consuming computational operations and inadequate efficiency of the procedure for generating control actions to be performed on the facility. The analysis shows that a simpler and more efficient scheme for solving the extremal problem (8) can be constructed by transforming the input data of the problem in a certain way and constructing criterion functions so that in the process of solving it, a purposeful movement towards the optimum is provided by analogy with the gradient method [22]. For this purpose, we propose a computational procedure. First, we preliminarily transform input data of the problem, represented by power vectors P^A, P^B, and P^C. Such a transformation involves sorting the latter to arrange their components in ascending order. In this case, new vectors $\hat{P}^A$, $\hat{P}^B$, and $\hat{P}^C$ with the same dimensions as the original ones are formed:

$$\hat{P}^A = \left[\hat{P}_1^A, \hat{P}_2^A, \ldots, \hat{P}_{n_1}^A \right],$$

$$\hat{P}^B = \left[\hat{P}_1^B, \hat{P}_2^B, \ldots, \hat{P}_{n_2}^B \right],$$

$$\hat{P}^C = \left[\hat{P}_1^C, \hat{P}_2^C, \ldots, \hat{P}_{n_3}^C \right],$$

where

$$\hat{P}_{\nu-1}^A \le \hat{P}_\nu^A,\ \hat{P}_{\xi-1}^B \le \hat{P}_\xi^B,\ \hat{P}_{\eta-1}^C \le \hat{P}_\eta^C,$$

$$\nu = \overline{2, n_1},\ \xi = \overline{2, n_2},\ \eta = \overline{2, n_3}.$$

In this case, new coordinates of the components of the indicated vectors are formed:

$$\hat{\beta}^A = \left[\hat{\beta}_1^A, \hat{\beta}_1^A, \ldots, \hat{\beta}_{n_1}^A \right],$$

$$\hat{\beta}^B = \left[\hat{\beta}_1^B, \hat{\beta}_2^B, \ldots, \hat{\beta}_{n_2}^B \right],$$

$$\hat{\beta}^C = \left[\hat{\beta}_1^C, \hat{\beta}_2^C, \ldots, \hat{\beta}_{n_2}^C \right].$$

A simple analysis shows that to define functions $F_1(\lambda_1)$, depending on a situation at the facility, it is more expedient to use components of new vectors $\hat{P}^A$, $\hat{P}^B$, and $\hat{P}^C$. Now let us consider Case 1 of the facility, residuals are $e_1 > 0$, $e_2 < 0$, and error is $e_3 = 0$. In this case, the criterion function $F_1(\lambda_1)$ must be specified in the form

$$F_1(\lambda_1) = F_1(r) = \sum_{l=1}^{r} \hat{P}_l^A, \tag{9}$$

where r is some integer ($r \ge 1$).

As a result, problem (8) will be written as

$$\min_{r \in R_1} F_1(r) = F_1(r^*). \tag{10}$$

Thus, the original problem is reduced to determining integer $r = r^*$ at which the optimum criterion function $F_1(\lambda_1)$ is achieved.

By solving (10), we identify vector β^* that consists of addresses of loads of phase A users to be switched to phase B. Vector β^* found in this way is a truncated part of original vector $\hat{\beta}^A = [\hat{\beta}_1, \hat{\beta}_2, \ldots, \hat{\beta}_{n_1}]$, that is, $\beta^* = [\hat{\beta}_1, \hat{\beta}_2, \ldots, \hat{\beta}_{r^*}]$. In this case, the desired control vector u^* has the following form:

$$u^* = [A,\ B,\ \beta^*] = [1, 2,\ \hat{\beta}_1,\ \hat{\beta}_2, \ldots, \hat{\beta}_{r^*}].$$

The above algorithm for solving the control problem can also be used for cases where the facility operation corresponds to Case 2 and Case 3. Consider the features of constructing algorithms of the functioning of a digital controller for these cases.

Suppose that Case 2 is observed in the controlled facility. Without loss of generality, we assume that the control errors are $e_1 > 0$, $e_2 > 0$, and $e_3 < 0$. In this case, condition (6) will be written in the form

$$e_1 + e_2 = |e_3|.$$

In this case, it is necessary to carry out two switchings $A \to C$ and $B \to C$. Therefore, based on the data received from the consumer electricity meters, we will form two vectors of the input data:

$$P^A = \left[P_1^A, P_2^A, \ldots, P_{m_1}^A \right],$$

$$P^B = \left[P_1^B, P_2^B, \ldots, P_{m_2}^B \right],$$

and two vectors of their coordinates:

$$\beta^A = \left[\beta_1^A, \beta_2^A, \ldots, \beta_{m_1}^A \right],$$

$$\beta^B = \left[\beta_1^B, \beta_2^B, \ldots, \beta_{m_2}^B \right],$$

where m_1, m_2 are dimensions of corresponding vectors.

Next, components of vectors P^A and P^B are sorted similarly to the previous case, i.e., new vectors $\hat{P}^A$ and $\hat{P}^A$ are formed with their components arranged in ascending order:

$$\hat{P}^A = \left[\hat{P}_1^A, \hat{P}_2^A, \ldots, \hat{P}_{m_1}^A \right],$$

$$\hat{P}^A = \left[\hat{P}_1^A, \hat{P}_2^A, \ldots, \hat{P}_{m_1}^A \right],$$

Now, as previously, subsets R_2 and R_3 are introduced for the indices of vectors $\hat{\beta}^A$ and $\hat{\beta}^B$, respectively, i.e., $R_2 = \{1, 2, \ldots, m_1\}$ and $R_3 = \{1, 2, \ldots, m_2\}$.

Following condition (6), the levels of mismatches ρ_2^* and ρ_3^* for the absolute values of corresponding complex powers of switched phases A and B are set as follows:

$$\rho_2^* = e_1,\ \ \rho_3^* = e_2.$$

Now, to find the required coordinates of network consumer loads, it is necessary to carry out two types of switchings, $A \to C$ and $B \to C$. In this case, the following two criterion functions are constructed:

$$F_2(\lambda_2) = \left| S_2(\lambda_2) - \rho_2^* \right|,$$

$$F_3(\lambda_3) = \left| S_3(\lambda_3) - \rho_3^* \right|,$$

Where λ_2, λ_3 are subsets composed of components of vectors $\hat{P}^A$ and $\hat{P}^B$, respectively, i.e., $\lambda_2 \in \Lambda_A$, $\lambda_3 \in \Lambda_B$. In this case, functions $S_2(\lambda_2)$ and $S_3(\lambda_3)$ are determined using the components of vectors $\hat{P}^A$ and $\hat{P}^B$ similarly to the previous case (Case 1) according to (9):

$$S_2(\lambda_2) = S_2(\eta) = \sum_{\ell=1}^{\eta} \hat{P}_\ell^A,$$

$$S_3(\lambda_3) = S_3(\theta) = \sum_{\gamma=1}^{\theta} \hat{P}_\gamma^B.$$

Further, to find the desired coordinates of the loads connected to phases A and B, two extremal problems are solved:

$$\min_{\lambda \in R_2} F_2(\eta) = F_2(\eta^*), \tag{11}$$

$$\min_{\theta \in R_3} F_3(\theta) = F_3(\theta^*), \tag{12}$$

where η^* and θ^* are the optimal quantities of absolute values of complex powers consumed by loads of consumers of phases *A* and *B*, respectively.

Extremal problems (11) and (12) are solved using the above algorithm for minimizing the criterion function F1(λ1). Since in the considered case it is necessary to carry out two types of switchings A → C and B → C, then solving the last extremal problems, we obtain vector u* = [u1, u2], where u_1 = [A, C, β_1^*], u_2 = [B, C, β_2^*], $\beta_1^* = [\hat\beta_1^A, \hat\beta_2^A, \ldots, \hat\beta_{\eta^*}^A]$, $\beta_2^* = [\hat\beta_1^B, \hat\beta_2^B, \ldots, \hat\beta_{\theta^*}^B]$.

When Case 3 is observed at the facility and, for example, errors are $e_1 > 0$, $e_2 < 0$, $e_3 < 0$, condition (6) takes the form

$$e_1 = |e_2| + |e_3|.$$

In this case, it is necessary to carry out switchings $A \to B$ and $A \to C$. Therefore, two vectors are formed from the set Λ_A:

$$P^A = \left[P_1^A, P_1^A, \ldots, P_{m_1}^A\right],$$

$$\tilde P^A = \left[\tilde P_1^A, \tilde P_1^A, \ldots, \tilde P_{m_2}^A\right],$$

as well as vectors β^A and $\tilde\beta^A$, respectively, for their coordinates. Moreover, vectors P^A and $\tilde P^A$ must have different components. Respectively, the components of these vectors form sets that do not intersect in this case. Next, we form the subsets $\lambda_4 \in \Lambda_A$ and $\lambda_5 \in \tilde\Lambda_A$. These input data are used in the above computational scheme to determine the desired control vector u^*. Firstly, by sorting components of vectors P^A and P^A, new vectors $\hat P^A$ and $\tilde P^A$ are formed with their components arranged in ascending order. Then, criterion functions $F_4(\lambda_4)$ and $F_5(\lambda_5)$ are determined:

$$F_4(\lambda_4) = \left|S_4(\lambda_4) - \rho_4^*\right|,$$

$$F_5(\lambda_5) = \left|S_5(\lambda_5) - \rho_5^*\right|,$$

where $\rho_4^* = |e_2|$ and $\rho_5^* = |e_3|$, and the functions $S_4(\lambda_4)$ and $S_5(\lambda_5)$ are defined similarly to the previous case. As in previous cases, the desired control vector u^* is determined based on minimizing criterion functions $F_4(\lambda_4)$ and $F_5(\lambda_5)$. In this case, the algorithm for solving the extremal problem (10) is used.

To improve the ICS reliability and extend the service life of the phase current switch (PCS), it is advisable to limit the number of switchings of consumer electricity meters. To this end, a current sensor installed at the transformer substation can be used, the output of which is fed to a digital controller (DC). Based on the value of current *J* of zero wire, DC checks the balance (quasi-optimality) condition of the system in each control interval. This condition, in particular, can be specified by the following inequality:

$$J \le \Delta, \tag{13}$$

where Δ is the maximum permissible value of current *J*, at which permissible level of the distribution network balance is ensured. To limit the number of switchings of consumer meters, control actions are generated and implemented only when condition (13) is not met.

The ICS constructed in this way with a digital controller can be considered as a system of a variable structure [23] since this will ensure the adaptation of the three-phase distribution network to the conditions that arise during uncontrolled random changes in its loads by automatic self-adjustment of its structure in real-time.

Based on the results obtained above, one can formulate a generalized algorithm of the ICS operation, which includes the following basic operations:

1. Poll the main three-phase electricity meter (Em^{TS}) and a given set of single-phase consumer meters connected to phases *A, B*, and *C*, except for meters installed at two-phase consumers.
2. Measure effective current J of zero wire and verify condition (13). If it is not met, go to step 3. Otherwise, the DC block does not generate control commands for the facility.
3. Formulate the input data of the control problem determined by vectors P, P^A, P^B, P^C, β^A, β^B, β^C.
4. Estimate components of control error vector $e = [e_1, e_2, e_3]$ by formulas (5).
5. Conduct a case study of the facility based on the signs of components of the control error vector $e = [e_1, e_2, e_3]$ and identify an interphase switching structure determined by vector $F = [F_1, F_2]$.
6. Determine the initial mismatch ρ* by the ICS unit and construct corresponding criterion functions {Fi (λ)} depending on the identified situation at the facility. For example, for Case 1 at the facility $\rho^* = \rho_1^* = |e_2|$, and $F_1(\lambda_1)$ is constructed as a criterion function.
7. Minimize selected criterion functions $\{F_i(\lambda)\}$. In this case, the DC block solves the extremal problems (10) or (11), (12), depending on the situation at the facility.
8. Generate digital control commands u^* and transfer them to corresponding phase current switches to implement the required switching of the selected loads (meters) of the distribution network users.

IV. Conclusion

Most three-phase distribution networks operate under unbalanced currents and voltages due to the unbalance of loads and their uneven distribution over phases. The unbalance factor causes an increase in active power losses in networks and transformer substations, which significantly diminishes the technical and economic performance of distribution companies.

At the same time, modern AMCS systems do not solve the problem of electricity flow control in unbalanced distribution networks as they focus on optimization of their operating conditions. We have proposed a novel approach to the construction of an information control system (ICS) aimed at solving this problem as part of a conventional AMCS system. The main idea, in this case, is the distribution of electricity flows between the phases of the network by switching its consumers from a more loaded phase to a less loaded one. To assess the quality of control processes, we have introduced criterion functions that characterize technical losses of electricity in the transformer substation and distribution network. We have proposed computational schemes for constructing them in terms of the situation at the facility. We have developed algorithms of operation of ICS of digital controller and minimization of criterion functions, which ensure minimization of unbalance of phase powers and currents at the network input, and that of technical electricity losses in network and supply transformer substation. The obtained findings are aimed at creating more efficient information control systems by improving conventional AMCS systems that belong to the category of information and measurement systems.

References

[1] Yakushkov K.V. "Automated system of the fiscal electricity metering for the retail market," Informatizatsiya i sistemy upravleniya v promyshlennosti, 2009, no. 3 (23), pp. 9-13 (in Russian).

[2] El-Hawary, M.E. "The Smart Grid—State-of-the-art and Future Trends," Electr. Power Compon. Syst. 2014, 42, pp. 239-250.

[3] Kosoukhob F.D., Vasilev N.V., Filipov A.O. "Reducing losses from current unbalance and improving electric-energy quality in 0.38-kV networks with municipal loads", Russian electrical engineering, Allerton Press, Inc. (New York), vol. 85, no. 6, 2014, pp. 350-353.

[4] Omorov T.T. "AMCS-based assessment of the current and voltage unbalance effect on power losses in the distribution grid," Elektrichestvo, 2017, no. 9, pp. 17-23 (in Russian).

[5] Czarnecki L.S., Bhattarai P.D. "Currents' physical components (CPC) in three-phase systems with asymmetrical voltage," Przegląd Elektrotechniczny, 2015, no.6, pp. 40-47. DOI: 10.15199/48.2015.06.06.

[6] Ponomarenko O. I., Holodinov I.H. "Effect of unbalanced conditions on power losses in power grids of distributed power supply systems," Energetik, 2015, no.12, pp. 6-8 (in Russian).

[7] Mahmoud, K.; Yorino, N.; Ahmed, A. "Optimal Distributed Generation Allocation in Distribution Systems for Loss Minimization," IEEE Trans. Power Syst. 2016, 31, pp. 960–969.

[8] Harutyunyan A.G. "On the calculation of additional power losses in three-phase four-wire grids," Elektrichestvo, 2015, no.10, pp. 55-58 (in Russian).

[9] Averbukh M.A., Zhilin E.V. On the loss of electricity in power supply systems for individual housing construction. Energetik. 2016. no. 6. pp. 54-56 (in Russian).

[10] Samokish V.V. Patent No. 2548656 (Russian Federation). "Method of balancing phase currents of three-phase four-wire line and device for its implementation," Bull. no.11. 20.04.2015 (in Russian).

[11] G.A.Bolshanin. "Patent No. 2249286 (Russian Federation). Method for computer-aided online measurement of current and voltage unbalance level, Bull. no.9. 28.03.2005. (in Russian)

[12] I.V.Naumov, D.A.Ivanov, S.V.Podjachikh. Patent No. 2490768 (Russian Federation). Balancer for three-phase networks with neutral wire. Bull. no. 23. 21.08.2013 (in Russian).

[13] Kiselyov M. G., Lepanov M.G. "Balancing of currents in electrical grids by a power electronic controller of non-active power." Elektrotekhnika, 2018, no.11, pp. 63-70 (in Russian).

[14] Omorov T.T. "Balancing of a power distribution network by digital control," Mekhatronika, Avtomatizatsiya, Upravlenie, 2018, vol. 19, no.3, pp. 194-200 (In Russian).

[15] Omorov T.T. "Synthesis of a digital controller for balancing the power distribution network," Instruments and Systems: Monitoring, Control, and Diagnostics, 2019, no. 11, pp.51-56 (in Russian).

[16] https://mir-omsk.ru/products/oborudovanie-dlya-tsifrovykh-setey/umnye-schetchiki-elektroenergii/ .

[17] Tanveer A. "Non-technical loss analysis and prevention using smart meters," Renewable and Sustainable Energy Reviews. 2017. Vol. 72. pp. 573-589.

[18] "Methods of the classical and modern theory of automatic control: in 5 volumes", Ed. by K.A. Pupkova, N. D. Egupova. M.: Publishing House of the Bauman Moscow State Technical University, 2004. (in Russian)

[19] Yiu, Joseph. The Definitive Guide to the Arm Cortex-M3 / Joseph Yiu; translated by A. V. Evstifeev. Moscow: Dodeka XXI, 2012. 552 p.

[20] Developing a New Generation of Smart Automation with ARM Cortex-M3 (https://www.radiolocman.com/review/article.html?di=134036).

[21] Demirchyan K.S., Nejman L.R, Korovkin N.V et al. Theoretical foundations of electrical engineering, vol.1. St.Petersburg: Piter, 2009, 512 p. (in Russian).

[22] Aoki M. Introduction to optimization methods. Moscow: Nauka, 1977, 334 p. (in Russian).

[23] Emeljanov S.I., Utkin V. I., Taran V. A. The theory of systems of a variable structure. Moscow: Nauka, 1970, 592 p. (in Russian).

Turatbek Omorov is D.Sc. in engineering, Head of the Laboratory "Adaptive and Intelligent Systems" of the National Academy of Sciences of the Kyrgyz Republic (NAS KR), Bishkek. He is a Corresponding Member of the NAS KR. He graduated from the Faculty of Automation and Electrical Engineering of Leningrad Electrotechnical Institute in 1975. T. Omorov received his Ph.D. degree in engineering from the Bauman Moscow State Technical University in 1981 and a D.Sc. degree in engineering from the Scientific and Production Association "Cybernetics" of the Academy of Sciences of the Republic of Uzbekistan in 1997. He worked as the Director of the Institute of Automation (2000-2008), and Vice-President of the National Academy of Sciences of the Kyrgyz Republic (2008-2013).
Key research areas are automatic control, informatization and optimization of control processes, and automation of power systems.

Takyrbashev Beishenaly is a Ph.D. in engineering, a Senior Researcher at the "Adaptive and Intelligent Systems" Laboratory at the NAS KR, Bishkek. He graduated from Frunze Polytechnic Institute in 1973 with a major in automation and remote control. He was the Head of the Power Systems Protection Service at JSC «Severelectro».
Key research areas are automatic control and automation of power systems.

Kubanychbek Zakiriaev is a senior lecturer at Issyk-Kul State University, Karakol, Kyrgyz Republic. He graduated from the Faculty of Automation and Computer Engineering of Tomsk Polytechnic University in 1992.
Key research areas are information technology and automation of power systems

Taalaibek Koibagarov is a Ph.D. student at NAS KR, Bishkek. He graduated from the Faculty of Energy of the Kyrgyz Technical University in 2002. He is the Head of the Metrological Service of JSC "Severelectro."
Key research areas are automatic control and automation of power systems.

Aspects of Atlas Mapping for Analysis of Energy Infrastructure in Different Regions

I.L. Trofimov*, L.N. Trofimov

Melentiev Energy Systems Institute of Siberian Branch of Russian Academy of Sciences, Irkutsk, Russiaa

***Abstract* — The paper addresses the visualization and systematization of cartographic material for analyzing energy infrastructure in various world regions. It discusses the technology (architecture) for building maps based on the concept of atlas mapping. An interface was developed for the construction of interactive maps and navigation in any section of the world atlas - from the level of world continents to a detailed map of any region within the country. We have constructed and stored contour maps of all countries of the world in the database of the computing geo-information system (CGIS). CGIS allows constructing hybrid maps, which contain vector and raster map layers with the energy infrastructure overlaid on them in the selected territory. An algorithm was constructed to search for energy objects and administrative entities in any country or region of the world. The atlases built by CGIS are used at Melentiev Energy Systems Institute (MESI) of the Siberian Branch of the Russian Academy of Sciences to plot the solutions obtained with the optimization model ORIRES (which reflects the optimal operation of the interconnected power systems in different scenarios) on a map of a selected area or region.**

***Index Terms*: Atlas mapping, geo-information system, computing system, data processing, hybrid map, tiles, map layer.**

* Corresponding author.
E-mail: t_john88@isem.irk.ru

http://dx.doi.org/10.38028/esr.2021.01.0006
Received March 29, 2021. Revised April 13, 2021.
Accepted April 22, 2021. Available online May 26, 2021.

I. Introduction

International experience in establishing Interstate Power Grids (ISPG) shows that electric power integration is cost-effective for the parties involved. The pre-design stage of the ISPG development requires its technical and economic analysis, justification, and comprehensive analysis of the energy infrastructure in the region. This is especially relevant because the project of Northeast Asia ISPG has begun to actively develop in recent years owing to the efforts made by the United Nations ESCAP (Energy and Social Commission of Asia Pacific region) and the GEIDCO (Global Energy Integration Organization) from China. A research team from MESI is also involved in this research. The study on the prospective ISPG expansion relies on the optimization model ORIRES.

The ORIRES model is used to identify the optimal installed capacities by generation type (thermal, hydro, wind, and solar), optimal transfer capabilities, and operating conditions of electric ties for each power system in the ISPG scheme for the target year. The optimal solution of the model is determined by the minimum value of the objective function (annualized costs) for the entire power system or interconnection. These costs consist of fuel, investment, operating, and maintenance costs for power plants; and investment, operating, and maintenance costs for transmission lines. Transmission losses are also factored in. Environmental policy tools, like CO_2 emission taxes, can also be incorporated into the objective function if needed. The model was developed by Lev Belyaev, Vladimir Savel'ev, Oleg Khamisov, Sergei Podkovalnikov and Lyudmila Chudinova. The ORIRES model is described in detail in the monograph "The effectiveness of interstate electric power interconnections," 2008 (in Russian) [1, 2].

The model is an essential part of the developed geo-information computing system (CGIS). CGIS allows us to enter, configure, and change all the model parameters; run the lp optimizer (for optimal solution finding); create and

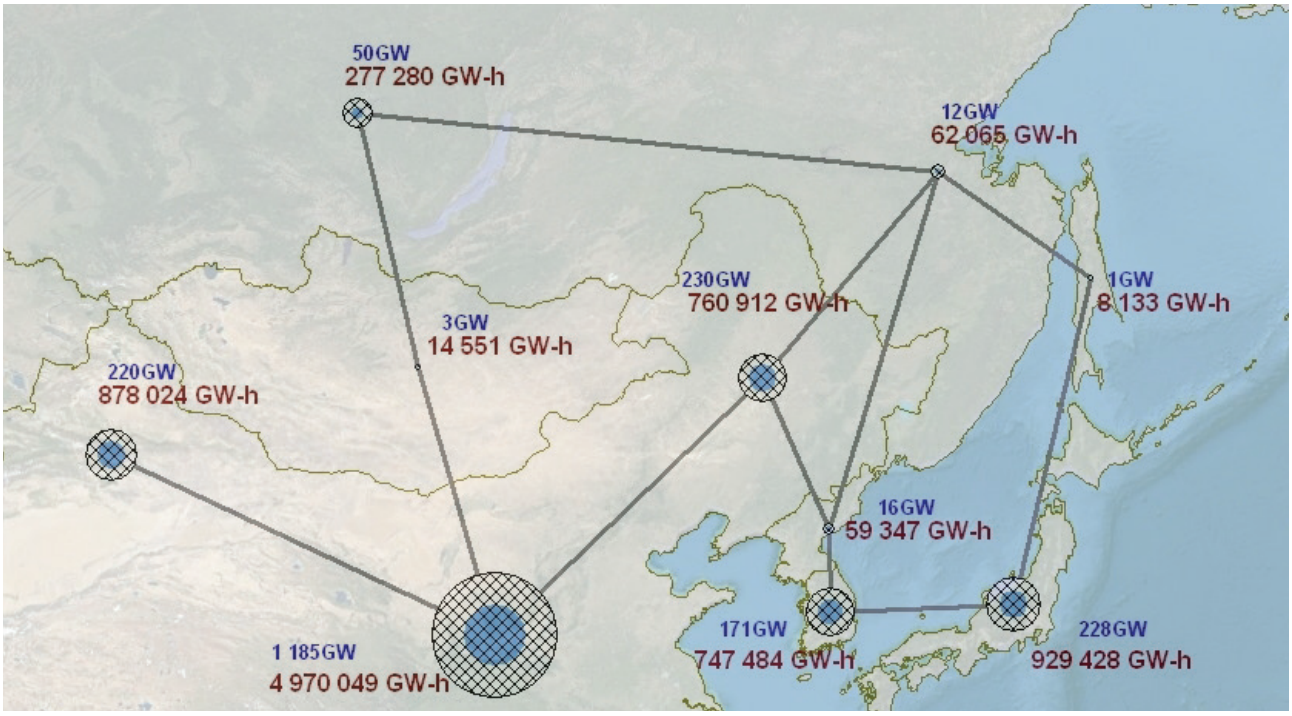

Fig. 1. Representation of a 10-node (aggregated energy power system) Northeast Asia interstate power grid.

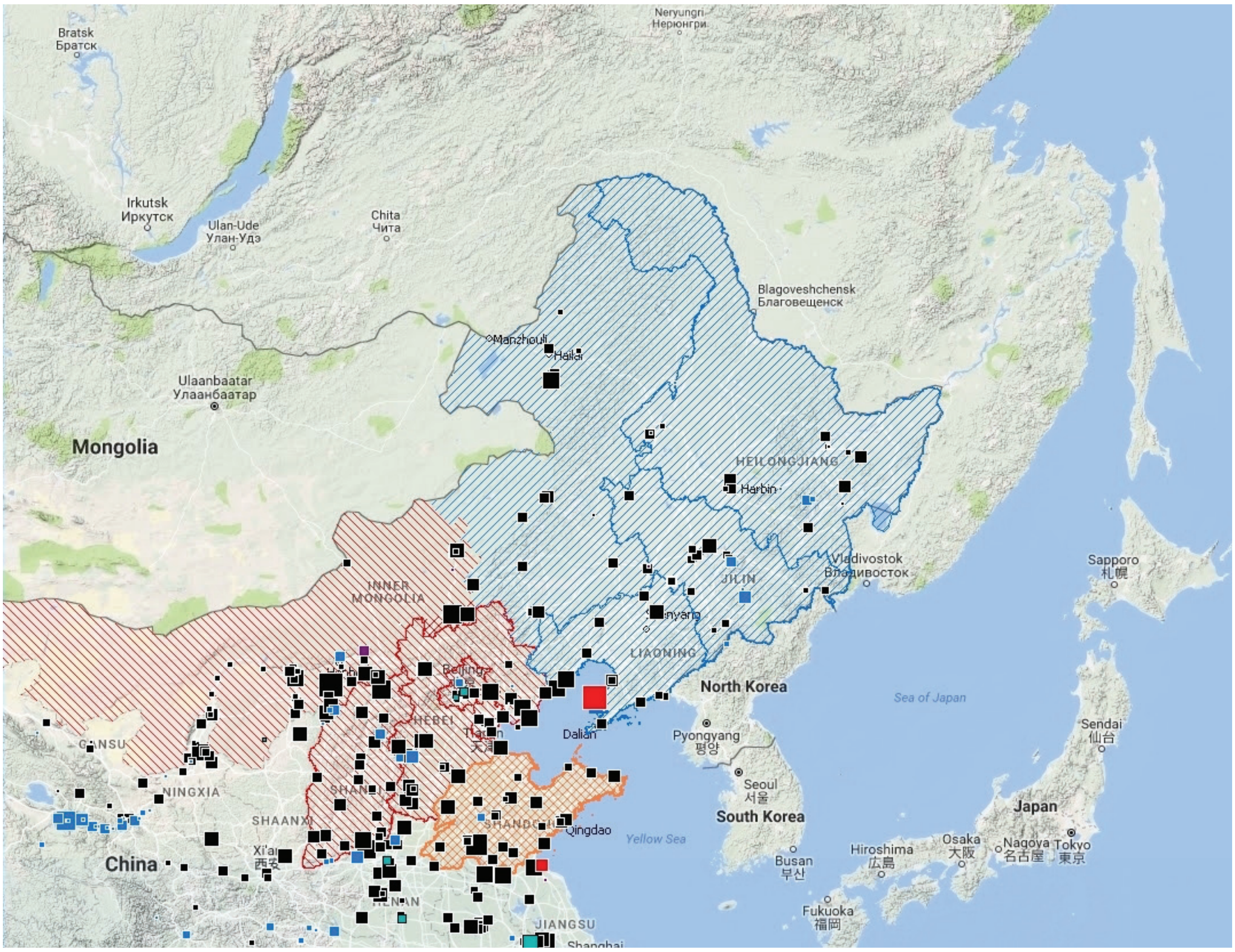

Fig. 2. Northeast China power plants geo-location from the database.

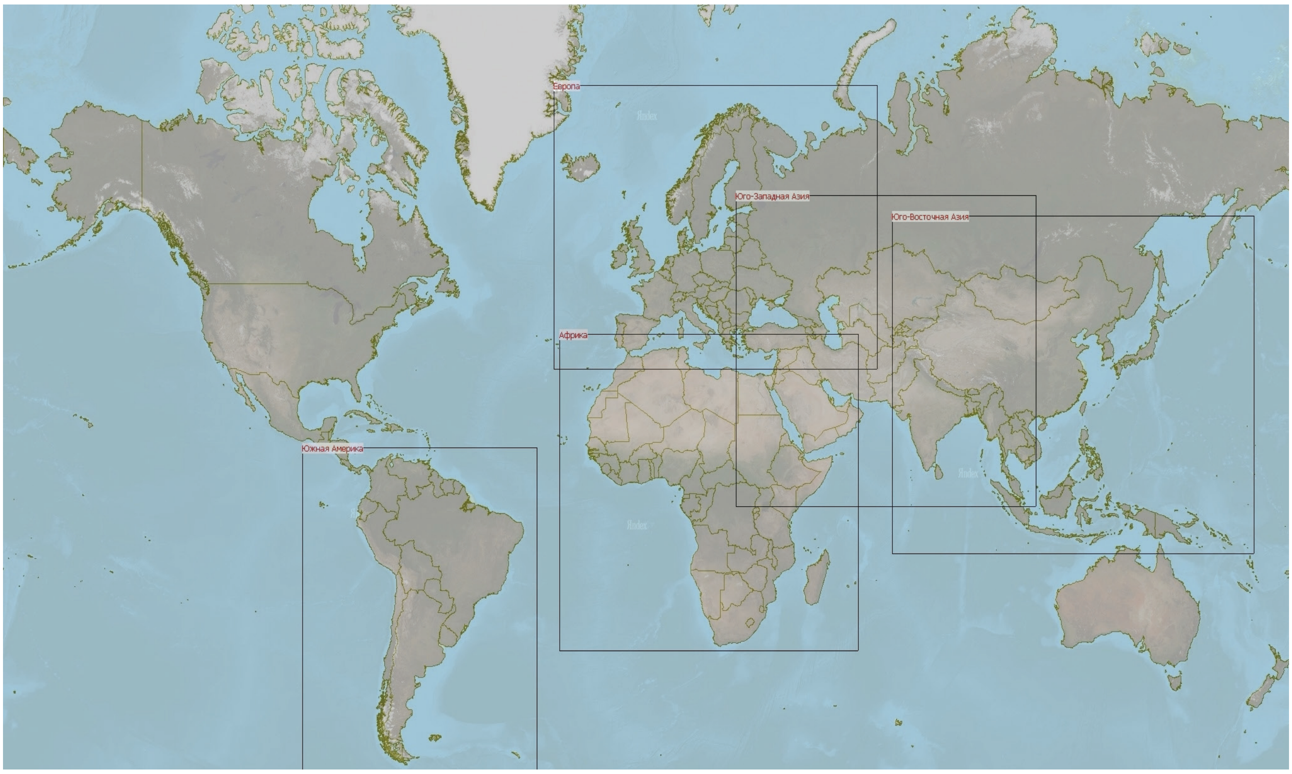

Fig. 3. Setting a rectangular area/region on a world map.

Fig. 4. List of the world's countries with provinces in the CGIS interface.

store results in the original energy database and display the obtained results in tabular, graphic, and cartographic forms [3–6].

This paper discusses a study on the visualization of processed data in a cartographic interface.

II. Software Overview

Many researchers in many countries investigate interstate power grid expansion. Different kinds of software were developed for power grids modeling. Nevertheless, most of them can only solve the problem of electricity redistribution and do not use any optimization models [7–11].

There is a need for more comprehensive research on ISPG expansion. Therefore, our study relies on an optimization model. We collect and process large arrays of data for the optimization model, which requires visual analysis of the obtained results.

Most GIS systems have no computing part and do not work with optimization models. We have developed both the data processing and computing geo-information system in one software product.

Multipurpose geo-information systems like ArcGIS or MapInfo solve a great number of problems associated with geospatial data processing [12, 13]. They have some similar functions:

- support of raster and vector data,
- use geocoding algorithms,
- work with geo-databases,
- support various geo-projections.

These systems, however, have disadvantages:

- high price (from 5000 $ per 1 license of ArcGIS),
- complex control elements,
- are not intended for energy data processing and representation.

Multipurpose software does not solve our research problems. We needed problem-oriented software with a convenient user interface to work with the optimization model and analyze the obtained results.

CGIS integrates both computing and informational components in one software product. CGIS consists of several functional parts (software modules): a graphic module for visual analysis of processed data, a geo-information and cartographic module, and a module for working with the ORIRES model.

The main features of CGIS for working with the ORIRES model are:

- Making changes to the mathematical equations written in linear programming (lp optimizer) language;
- Enabling/disabling model constraints;
- Operational tuning/editing of input parameters for the model;
- Including/deleting model nodes (and corresponding ties) in the diagram of electric power systems and interconnections;
- Creating the inherited scenarios (scenario tree), their storage in the database, and comparison;
- Controlling and analyzing input parameters of the model (meeting given constraints).

All data used in the CGIS are stored and processed in their energy/power database.

We propose an original CGIS for the representation and analysis of energy infrastructure in various regions of the world with an integrated computing part. The data overlaid on the map can be those on energy facilities (power plants) and electric power systems, as well as the data from calculations with the built-in optimization model. This feature distinguishes the proposed software from others.

Another feature of the developed software is that it allows visualization of the model results and the energy infrastructure of any region of the world (data on all energy/power facilities collected in the database) on a map. This provides the most complete information on the energy infrastructure in any region to conduct further research.

The processing and analysis of a large amount of complex and rapidly growing data require dedicated technologies for data management and storage. CGIS works with its object-oriented energy database developed by the authors. The database objects contain geographical information for visual representation and qualitative analysis, information on the relationships between objects and their regional affiliation, technical and economic parameters, and other information.

These data are downloaded to the database from various sources: world energy outlook, world power plant database, enipedia.org, and others. All data are stored in a special object format. Details on the object format of the database can be found in the paper “The Computing and Information System for Study of Scenarios for Interstate Power Grid Expansion” [6].

To analyze the results of solving the model in the cartographic module, the user can build a scheme of ISPG with set parameters and connections between the nodes (interstate electric ties) on the map. Fig. 1 shows the hybrid map with a 10-node scheme of the Northeast Asia interstate power grid for the 2040 target year.

In addition, the user can construct a map with energy/power plants in any part of the studied region, Fig. 2.

III. A Concept of Atlas Mapping

A dedicated interface was developed for the construction of interactive maps and navigation in any section of the world atlas, from the level of world continents to a detailed map of any region within the country, Fig. 3.

Over the year 2019, we constructed and stored contour maps of all countries of the world with administrative divisions (country regions), with their names in Russian and English, in the CGIS database. This interface allows building maps of any territory, including several countries or regions, on a given scale. One of our energy database

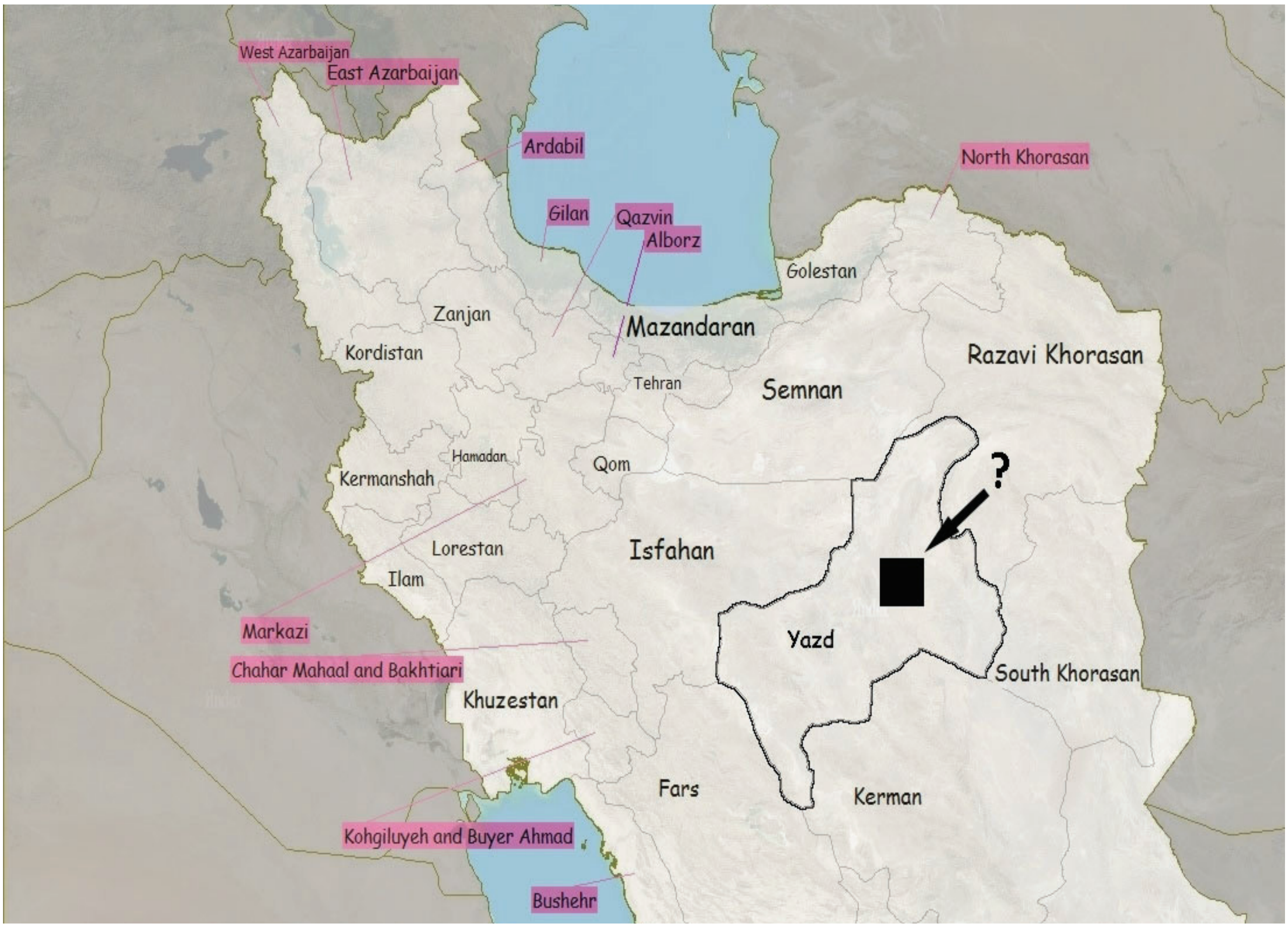

Fig. 5. Search for an object belonging to a specific closed polygon.

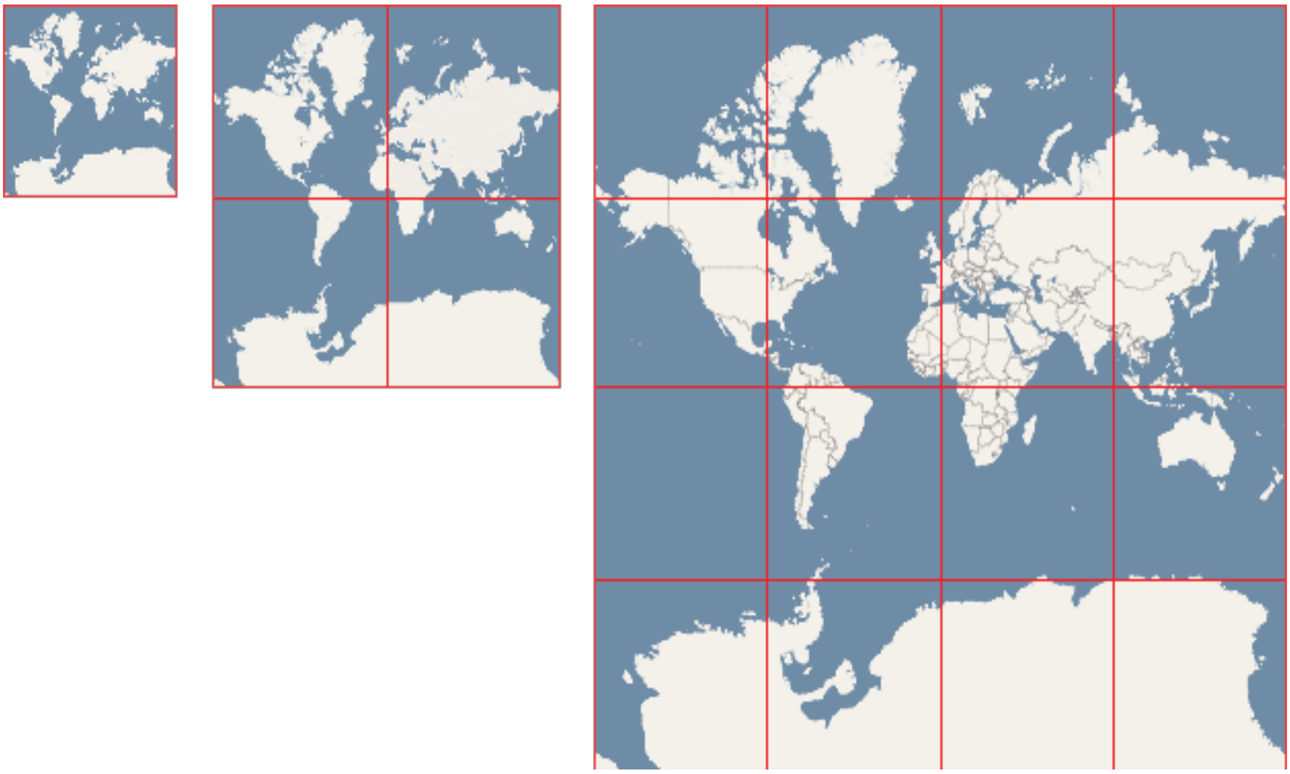

Fig. 6. Google and Yandex map tile zooming.

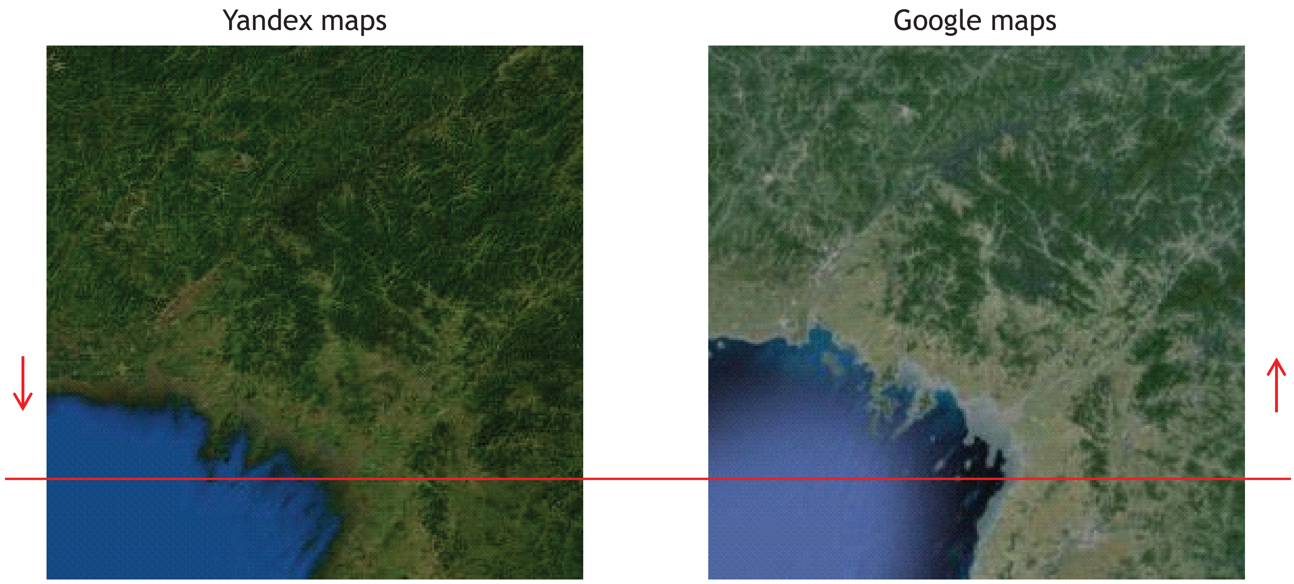

Fig. 7. Difference between the Google and Yandex map tiles of the selected region.

sources is the DIVA-GIS [14]. We have stored vector/contour maps of more than 200 countries with provinces, rivers, and cities, Fig. 4.

Owing to this work, one can navigate through the list of countries with already prepared maps in CGIS, like a world interactive atlas [15]. This database allows us to effectively create maps of any regions for research.

Any area/region on the world map can be marked with a rectangle in the CGIS interface and stored in a temporary folder in our database for further work. Then the combined raster and vector layers are created for the map of this region. Then we can overlay the layers of texts, energy data, and geospatial objects on this map.

We have developed algorithms for searching objects or groups of objects united by one attribute inside a closed polygon (Fig. 5), for example, if we need to find some objects belonging to a specific country or province (an object inside a closed polygon). The selection of a rectangular area on a world map significantly reduces the number of closed polygons.

IV. Technical Features and Problems

CGIS allows constructing hybrid maps that contain vector and raster layers of the map, with the energy infrastructure overlaid on it.

The CGIS database contains:

- Raster data, including space satellite snapshots (tiles) of the selected territory (geospatial data on countries and regions used as the background);
- Vector data, including the data in the SHP format, that contain geo-coordinates of power plants, country borders, and administrative divisions;
- Energy infrastructure data, including technical and economic data on power plants, electric ties, energy power systems (EPS), and others.

With 0 zoom level on Google and Yandex maps, the entire Earth is placed in one square tile (a side equals the equator length). For the other levels, the number of tiles is determined by N = H (height)·W (width), Fig. 6.

Due to a change in the policy for providing free Google maps, it was necessary to convert all maps to Yandex maps. The technologies of map constructing are based on the tiles downloaded from the Internet and "glued," i.e., selected territory snapshots made by space satellites with the pictures differing (offsetting) in their physical coordinates, Fig. 7.

The problem is that Google uses the Mercator spherical projection (EPSG: 3857 – WGS 84/Pseudo-Mercator), and Yandex employs the Mercator elliptical projection (EPSG: 3395 – WGS 84/World Mercator) [16].

We implemented algorithms for converting coordinates from one system to the other so that the vector layers exactly "fit" into the specified area. Additionally, the algorithms were implemented to interactively determine the geographical coordinates of any object on the map. Algorithms were designed to search for the database objects in any region.

V. Conclusion

The maps of about 200 countries with administrative divisions were constructed and stored in the CGIS database. Search geocoding algorithms were implemented for energy objects in any region of the world. Statistical data processing algorithms were developed (output of the total number of energy objects in a given territory, and others). Algorithms were designed for conversion from Google map to Yandex map to enable vector layers to exactly "fit" into the specified area.

The atlases built by CGIS are used at MESI to plot solutions obtained with the optimization model ORIRES (which reflects the optimal operation of the interconnected power systems in different scenarios) on a map of the selected territory or region.

Acknowledgment

The research was carried out under State Assignment Project (no. FWEU-2021-0001) of the Fundamental Research Program of the Russian Federation 2021-2025.

References

[1] Belyaev, L. Chudinova, O. Khamisov, G. Kovalev, L. Lebedeva, S. Podkovalnikov, and V. Savel'ev, "Studies of interstate electric ties in Northeast Asia," *International Journal of Global Energy Issues,* vol. 17, no. 3, pp. 228–249, 2002.

[2] Podkovalnikov, V. Savelev, O. Khamisov, L. Chudinova, "Justification of Effectiveness of International Power Interconnections with Separation of Effects between Participants," *Automation and remote control*, vol. 10, pp. 1756–1765, 2018. DOI: 10.1134/S0005117918100028

[3] Podkovalnikov, I. Trofimov, L. Trofimov, L. Chudinova, L. Belyaev, V. Savelev, "Computing and Information System for Research of Prospective Electric Power Grids Expansion," *Yugoslav Journal of Operations Research*, [S.l.], vol. 29, no. 4, pp. 465–481, 2019. DOI: 10.2298/YJOR1811.

[4] Podkovalnikov, I. Trofimov, and L. Trofimov, "Data processing and optimization system to study prospective interstate power interconnections," in *10th International Conference on Asian Energy Cooperation (AEC 2017), E3S Web Conf.*, vol. 27, pp. 32–40, DOI: 10.1051/e3sconf/20182701007.

[5] Energy Statistical Analytical Service. Available at: http://www.esas.com.ru/en, [accessed 26 July 2019].

[6] Podkovalnikov, I. Trofimov, L. Trofimov, and L. Chudinova, "The Computing and Information System for Study of Scenarios for Interstate Power Grid Expansion," in *IEEE 2019 16th International Conference on Electrical Engineering/Electronics, Computer, Telecommunications and Information Technology (ECTI-CON)*, Pattaya, Chonburi, Thailand, 2019, pp. 1–4. DOI: 10.1109/ECTI-CON47248.2019.8955179

[7] Omatsu, "Interim Report by Asia International Grid Connection Study Group," in *10th International Conference on Asian Energy Cooperation (AEC 2017), E3S Web Conf.*, vol. 27, pp. 9–18, 2018.

[8] Xuming, "Application and research of global grid database design based on geographic information," *Academic Journal of the Global Energy Interconnection Development and Cooperation Organization*, vol. 1, no. 1, pp. 87–95, 2018.

[9] The United Nations Economic and Social Commission for Asia and the Pacific (UN ESCAP). Available at: https://unescap.org/research [accessed: 25 March 2019].

[10] Asia Pacific Energy Portal, UN ESCAP. Available at: https://asiapacificenergy.org/, [accessed: 23 April 2019].

[11] Global Energy Interconnection Development and Cooperation Organization (GEIDCO). Available at: https://en.geidco.org/journal/ [accessed: 07 August 2019].

[12] ArcGIS. Mapping and Analyzing. Available at: https://www.arcgis.com/, [accessed: 22 January 2020].

[13] MapInfo. GIS Mapping. Available at: http://www.mapinfo.ru/, [accessed: 23 January 2020].

[14] DIVA-GIS. Available at: https://www.diva-gis.org/, [accessed: 13 April 2019].

[15] O. Zolotova, E. Skupinova, D. Bondarenko, V. Drobyshev, "GIS and Atlas mapping," *ArcReview Electronic Journal*, vol. 1, no. 44, 2008. (In Russian).

[16] World Geodetic System Projections. Available at: https://gisgeography.com/ellipsoid-oblate-spheroid-earth/, [accessed: 10 February 2020].

Ivan Trofimov is a junior researcher at the Melentiev Energy Systems Institute of the Siberian Branch of the Russian Academy of Sciences. His research interests are web & information technologies and their implementation in the energy field.

Leonid Trofimov is a lead programmer at the Melentiev Energy Systems Institute of the Siberian Branch of the Russian Academy of Sciences. His professional interests are software development, data visualization, geo-information systems, object data structure, and data processing.

Determination of an Effective Heating Radius in District Heating Systems in terms of Reliability

V.A. Stennikov, E.E. Mednikova, I.V. Postnikov*

Melentiev Energy Systems Institute of Siberian Branch of Russian Academy of Sciences, Irkutsk, Russia

Abstract — **The paper presents a method developed to determine an effective heating radius (EHR) in district heating systems (DHSs) in terms of reliable heat supply to consumers. The search for EHR for various heating mains from the considered district heating source in DHS involves identifying heat source operation zones in various city areas. At the same time, apart from the search for EHR, the nodal reliability indices are estimated for each consumer and then used (if necessary) to adjust the obtained EHR. The paper briefly discusses some of the practical research results.**

Index Terms: **district heating system, mathematical modeling, effective heating radius, specific costs of heat production and distribution, reliability analysis, nodal reliability indices, theory of hydraulic circuits.**

I. Introduction

The effectiveness of the enhancement and preservation of district heating advantages is provided by optimal planning of the DHS functioning and modernization, which implies the determination of DHS scale, the distance of heat-carrying agent transportation, and the fulfillment of the heat supply quality and reliability requirements in the context of increasing heat demand. The validity of the decisions made on these issues is determined by the heating radius or the heat network length from the heating source to the consumer. In this regard, finding an effective heating radius (EHR) is one of the essential objectives when constructing efficient heating systems. The determination of EHR is also instrumental in designing the efficient 4th generation DHS [1–3].

According to the adopted procedure for preparing and making decisions, this and some other tasks related to the construction of optimal DHS are considered in various stages of the heating system design with varying degrees of their detail (detailed planning of the city, heat supply scheme, etc.). The regulations for accomplishing these tasks are prescribed by dedicated normative and legislation acts that determine their order, sequence, composition, scope, terms, and other conditions [4–8].

The Federal Law "On Heat Supply" [4] is a fundamental regulatory document that establishes the legal framework for economic relations in heat production, transmission, and consumption in DHS. This document defines the basic concepts used in the development of heat supply schemes, including EHR. According to clause 30 of Article 2 of the Law "On Heat Supply", EHR is a maximum distance between the heat-consuming node and the nearest heat source in DHS, which, when exceeded, makes it cost-ineffective to connect the heat-consuming node to this system due to an increase in total costs in the system. Sections 2, 3, and 10 of the Resolution [5] declare the need to calculate the EHR to determine optimal coverage areas for existing, reconstructed and new heat source providing an expected heat load in new city areas.

The recommendations for the development of heat supply schemes are approved by the Order of the Ministry of Energy of the Russian Federation [7]. They define the EHR concept and note the need for its assessment. They also propose a simplified methodology for its calculation, which is aimed at obtaining integral EHR estimates (in contrast to nodal ones) without considering reliability. Thus, the determination of the optimal scale of DHS based on EHR, which is crucial in substantiating the efficiency of heat supply scheme, requires the development of a scientifically grounded methodology.

The analysis of the scientific and technical literature indicates that despite the absence of methods approved by normative documents, the EHR calculation issue has been given much attention since the time of the district heating establishment. The objective of determining the limiting radius of district heating was formulated for the first time in [9], and concepts of "economic" and "limiting" heating radius were pioneered in [10]. Most further studies focusing on the determination of EHR or optimal areas of heat source operation fall on the 1960s–the 1980s

* Corresponding V. A. Stennikov.
E-mail: postnikov@isem.irk.ru

http://dx.doi.org/10.38028/esr.2021.01.0007
Received March 16, 2021. Revised March 19, 2021.
Accepted March 26, 2021. Available online May 26, 2021.

[11–14] since this was the period that saw the most intensive growth in both the number and the scale of DHS. The findings obtained suggest that the optimal EHR and the area of heat source operation depend significantly on the structure and parameters of the considered system. Recently, the research has been resumed to determine the effective zones of district heating [15–17]. The proposed methods are instrumental for aggregate solutions for the DHS development strategy. At the same time, they aim to determine a single EHR value for the system under the assumption that heat loads are evenly distributed. This assumption, however, is very rarely consistent with actual systems and cannot be applied to most operating heating systems. Also, the considered methods used to assess EHR do not consider reliability requirements, which in practice can lead to frequent disconnections of consumers located in the EHR zone.

II. Methodology

The main idea of the proposed methodological approach to determining EHR is that for each district heat source, one should calculate EHR for each direction of the main transmission pipelines of the heat network connected to this source. At the same time, consumers in the EHR zone should be provided with the required (normative) level of heat supply reliability.

The method designed to determine EHR relies on the following assumptions and propositions:

1. The areas of prospective and existing housing development are determined following the general plan of the city and applications for technical connection of heat load;
2. The criterion that limits EHR for heat source, and beyond which the connection of new consumers leads to an increase in the specific costs for the considered DHS, is the cost of heat production and transportation;
3. The EHR boundary is calculated for each transmission pipeline from heat source, given the technical and economic parameters of the heat source and heat network, climatic conditions, and other properties and features of the studied system;
4. The EHR is limited by network nodes, at which the heat prime cost (nodal prime cost) exceeds the average cost for DHS;
5. The optimal distance of the heat carrier transport along each transmission pipeline of heat network from a heat source to the most distant consumer node is determined according to the calculated EHR value.

The proposed method for determining the EHR for DHS with regard to reliability requirements consists of the following main stages.

1. Build an information base for district heating zones, including territorial planning; consumer loads; locations; technical and economic indices of heat source; length, parameters of existing heat network sections and new ones.
2. Calculate the connected heat load for each district heat source:

$$Q_i = \sum_{j \in J(i)} Q_j + Q_{loss}, \, i \in I, \tag{1}$$

where i and j are the number of heat sources and the number of consumers, respectively; I is a set of heat sources; $J(i)$ is a subset of consumers connected to the i-th source (J is a total set of consumers); Q_j is heat

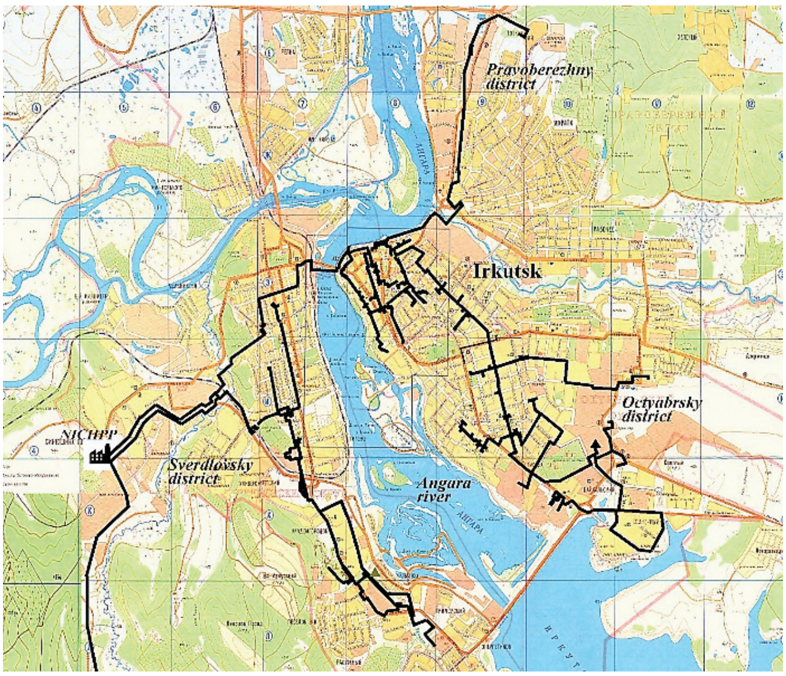

Fig. 1. DHS of Irkutsk on the city map.

load of the j-th consumer connected to the considered source, MW; Q_{loss} is heat losses in the system, MW.

Expression (1) is used to formulate the total heat balance in the considered DHS given all heat sources and consumers:

$$Q_i = \sum_{j\in J} Q_j + Q_{loss} \quad . \tag{2}$$

Each EHR solution obtained subsequently must satisfy this condition.

3. Determine the length of transmission pipeline for each heat source based on the calculated scheme of the system at issue and the main characteristics of the heat network sections (diameters, lengths, actual heat carrier flow rate).
4. Calculate thermal and hydraulic conditions in the heat network using the methods of the theory of hydraulic circuits (THS) [18], according to which the heat carrier flow distribution in the network is described by the following system of equations in matrix form:

$$\mathbf{Ax} = \mathbf{G}, \tag{3}$$

$$\bar{\mathrm{A}}^{\mathrm{T}}\mathbf{p} = \mathbf{h} - \mathbf{H}, \tag{4}$$

$$\mathbf{h} = \mathbf{SXx}, \tag{5}$$

where **A** is a matrix of connections of linearly independent nodes and sections of the network; **x** is a vector of heat flow rates in the network sections, t/h; **G** is a vector of flow rates at nodes, t/h; $\bar{\mathrm{A}}^{\mathrm{T}}$ is a transposed matrix of connections of nodes and branches in the scheme; **p** is a vector of pressures at nodes, mWC; **h**, **H** are vectors of losses and operating heads, mWC; **S** is a diagonal matrix of hydraulic resistances, mh^2/t^2; **X** is a diagonal matrix of absolute values of flows on network sections, t/h.

5. Test if there is an available capacity of the existing district heat source, given the maximum heat load of the i-th source – Q_i^{max}, MW.

   Based on the test results, the following conclusions are made:

   a) in the case of available capacity in the operation area of the considered source ($Q_i > Q_i^{max}$), additional capital investments are not required to connect consumers;
   b) in the case of no available capacity in the operation area of the considered source ($Q_i \le Q_i^{max}$), it is necessary to expand the source capacity and assess the corresponding investment.
6. Calculate annual specific costs for the heat production and transportation (prime cost) in DHS from the considered i-th heat source [14]:

$$Z_i = c_i^h + \alpha k_i + (f+\alpha)\frac{1}{Q_i}\sum_{n\in N(i)}(k_n d_n l_n) + \\ + c_e \tau_p \frac{1}{367\eta Q_i}\sum_{n\in N(i)}(\psi_n x_n l_n), \tag{6}$$

where n is the number of the heat network section; $N(i)$ is a subset of network sections that belong to the heat load area from the i-th heat source (N is a full set of network sections); c_i^h is a heat production prime cost at the i-th heat source, RUB/MWh; α is a discounting coefficient; k_i is the specific investment in capacity expansion of the i-th source, RUB/(MW); f is a share of deductions from capital costs for the heat network depreciation, repairs and maintenance; k_n is the specific investment in the construction of the n-th network section, RUB/m; d_n is diameter of the n-th network section, m; l_n is length of the n-th network section, m; c_e is electricity cost, RUB/kWh; τ_p is the number of operating hours of the pumping unit with the design load, h; η is the efficiency of the pumping unit; ψ_n is specific pressure drop in the n-th network section, mWC/m.

7. Calculate the specific costs for heat production and transportation (prime cost) for each node along each transmission pipeline from the i-th heat source:

$$Z_m = c_i^h + \alpha k_i + (f+\alpha)\frac{1}{Q_i^m}\sum_{n\in N(m)}(k_n d_n l_n) + \\ + c_e \tau_p \frac{1}{367\eta Q_i^m}\sum_{n\in N(m)}(\psi_n x_n l_n), \tag{7}$$

where m is the number of the network node ($m \in M$, where M is a set of nodes); $N(m)$ is a subset of network sections connecting nodes that belong to the transmission pipeline from the i-th heat source; Q_i^m is heat load at node m that belongs to the transmission pipeline from the i-th heat source, MW.

8. Assess a system-average level of specific annual costs for heat production and transportation:

$$\bar{Z} = \left(1/\sum_{i\in I} Q_i\right)\sum_{i\in I} Q_i Z_i \ . \tag{8}$$

9. Determine the EHR boundaries for each transmission pipeline, i.e., a subset of nodes, for which the heat production cost does not exceed its system-average level. A node's belonging to the EHR zone is formalized according to the condition:

$$m \notin M_{eff}\ , \text{ if } Z_m \ge \bar{Z}, \tag{9}$$

$$m \in M_{eff}\ , \text{ if } Z_m < \bar{Z} \tag{10}$$

where M_{eff} is a subset of network nodes located within the EHR zone.

10. Determine two main reliability indices (RI) [16], i.e., the availability factor (AF) and the failure-free operation probability (FOP). These indices can be calculated for each node m of the calculated scheme using the methodology for heating system reliability assessment presented in [19], according to the following formulas:

$$K_m = \sum_{s\in E} p_s[(\tau_0 - \tau_{sm})/\tau_0], \tag{11}$$

$$R_m = \exp\left(-p_0 \sum_{s\in E}\sum_{n\in N_s}\tau_{sm}\lambda_n\right), \tag{12}$$

where K_m and R_m are nodal AF and FOP, respwectively; s is the number of the system state; E is a set of system states; p_s is probability of state s; τ_0 is the calculated time, h; τ_{sm} is part of the calculated time, during which state s is a failure state for node m; p_0 is the probability of a fully

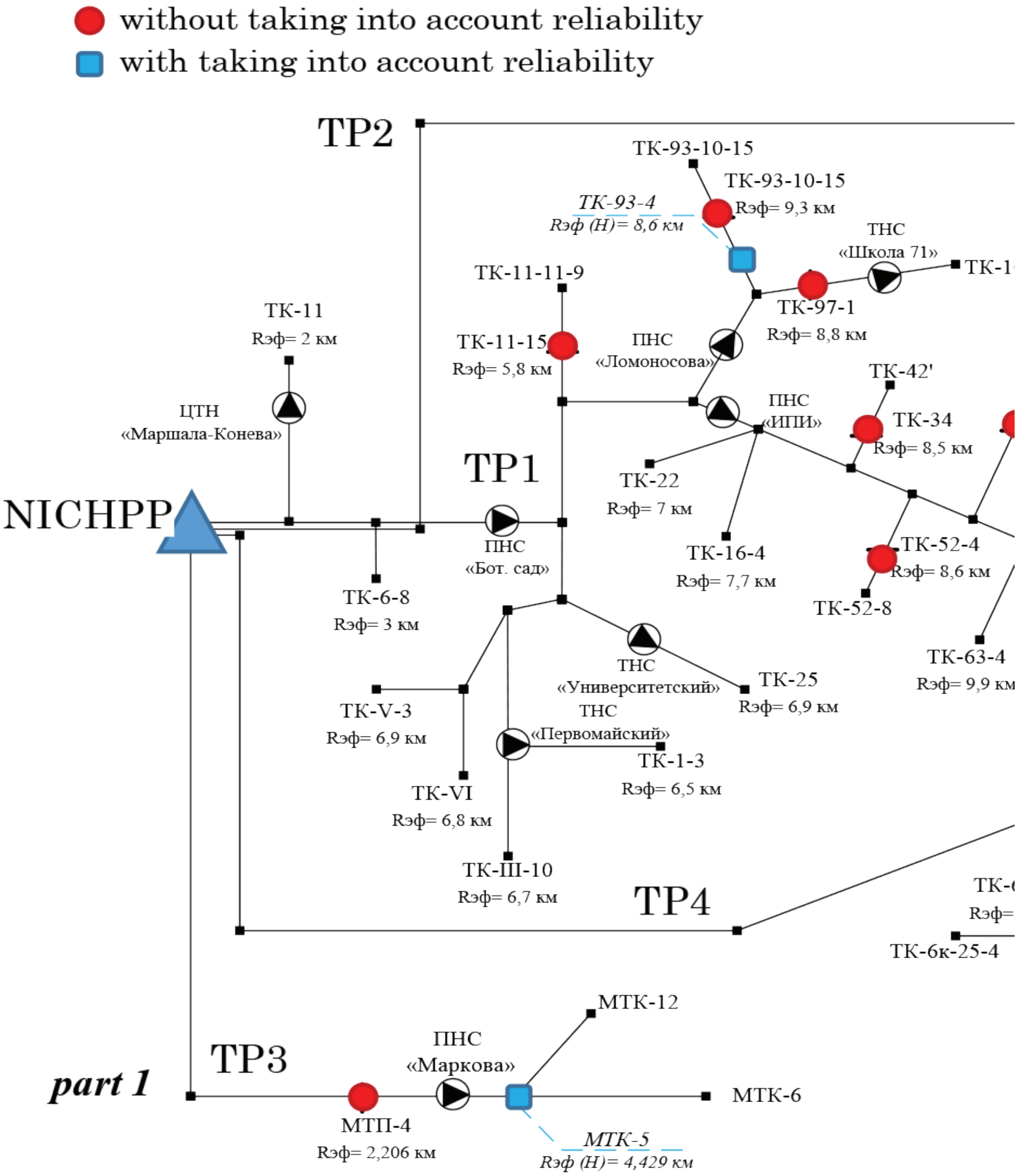

Fig. 2. Aggregate scheme of DHS with EHR solutions.

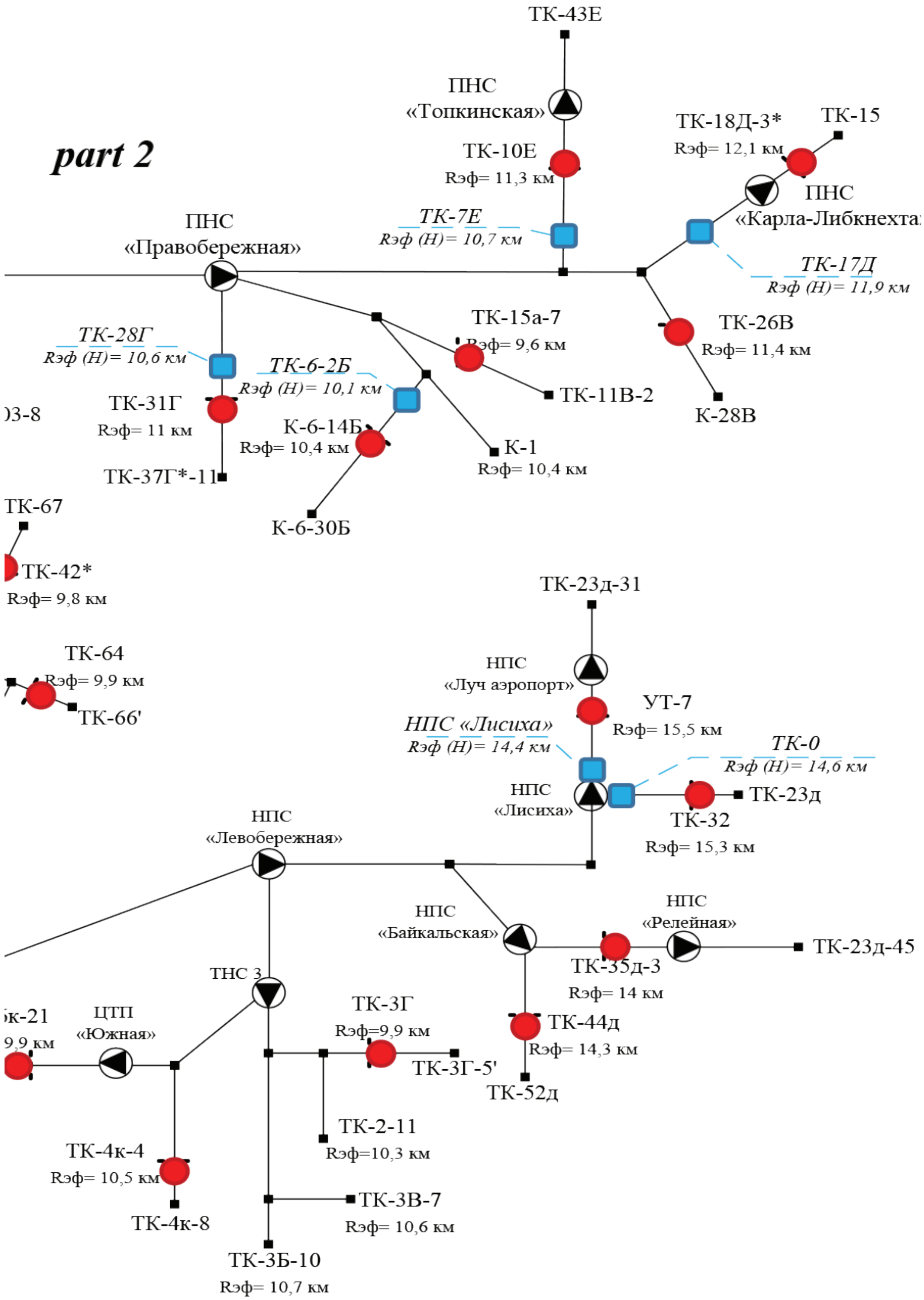

Fig. 2. Aggregate scheme of DHS with EHR solutions.

operational system state ($s = 0$); N_s is a subset of the system components (sections of the heating network), the failure of which corresponds to the transition to the state s; λ_n is a failure rate of component n, 1/h.

The probabilities of states p_s are determined by solving a system of equations that describe a stationary markov random process of the evolution of events in the system, i.e., failures and restorations of its components (network sections) [19, 20]:

$$\sum_{n\in N_s}(\lambda_n+\mu_n)=\sum_{z\in E_s}p_z\sum_{n\in N_z}(\lambda_n+\mu_n),\ s\in E \quad , \tag{13}$$

where z is the number of system state (introduced to formulate the defined system of equations); E_s is a subset of states from which a transition to state s is possible; p_z is the probability of state z of the system; N_z is a subset of components whose failure or recovery corresponds to a transition from state z to state s; μ_n is a recovery rate of component n, 1/h. Values τ_{sm} are determined using the Rossander equation [14, 21], which is also used to set the heat load at any time during the calculated period or the so-called heat load duration curve. The calculations employ the levels of heat supply in various system states, which are determined from the assessment of consequences of post-emergency thermal-hydraulic conditions in the heat network based on the system of equations (3)–(5). To this end, multivariate calculations of the flow distribution in the network are carried out for a failure condition of its various sections. In doing so, one takes into account the time reserve due to the heat storage effect. Methods and models for analyzing the DHS reliability, as well as their practical application, are discussed in detail in [19, 20, 22–25].

11. Verify EHR solutions for fulfillment of heat supply reliability requirements in terms of the standard values of the nodal reliability indices used. Thus, for each node belonging to the EHR zone, the following conditions must be met:

$$K_m \geq K_0,\ m\in M_{eff}, \tag{14}$$

$$R_m \geq R_0,\ m\in M_{eff}, \tag{15}$$

where K_0 and R_0 are standard values of AF and FOP, respectively. The methods for assessing the heating system reliability [19] usually rely on the AF to estimate the design level of heating, and FOP to estimate the reduced reliability level. In this case, the reliability criterion is the minimum permissible temperature of the internal air at the node under consideration, which is determined by the level of heat supply.

If conditions (14) and (15) are not met, the EHR zone is limited to the node, which is most distant from the heat source and at which the reliability requirements are satisfied, with the EHR zone reduced. If the EHR zone cannot be reduced (for example, if there are no other sources, to which consumers beyond the boundaries of this zone can be connected according to reliability conditions), then measures are developed to increase reliability, which involves designing redundant pipelines and assessing the necessary volume of re-laying the dilapidated and emergency heat network sections. After that, we return to point 3 of the method. At the same time, calculation of specific annual heat transportation costs should take into account additional capital investments in measures to improve reliability.

The obtained EHR solutions must be annually updated according to the growing heat loads. Normally, the connection of new consumers in the case of available heat source capacity and the throughput of pipelines leads to an increase in operating costs, which must be compensated for by the consumer that has an individual heat tariff set. The effectiveness of connecting a new consumer to the existing heat network within the EHR is assessed based on an additional criterion, the so-called local EHR, which allows estimating the economically feasible distance between the consumer and the point of connection to the system [26, 27].

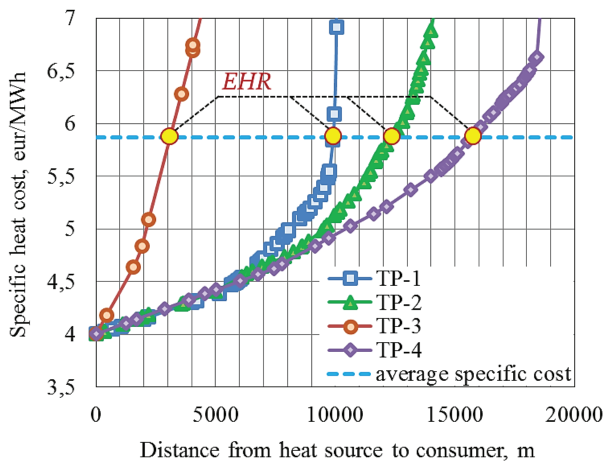

Fig. 3. Specific heat cost for the longest branches of the considered DHS transmission pipelines: the points of crossing the average level line (dashed line) correspond to EHR solutions

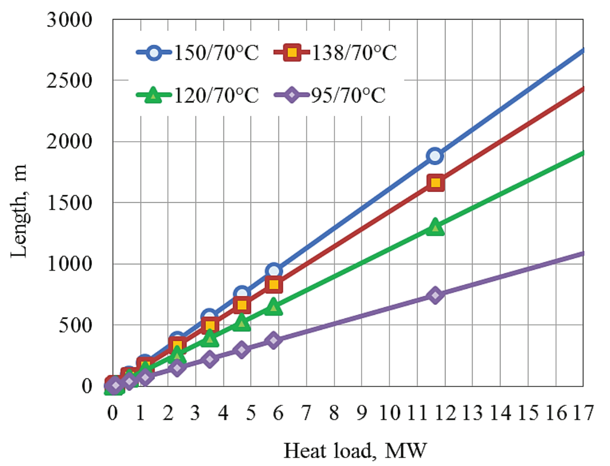

Fig. 4. The maximum length of a heat pipeline from the point of new consumer connection to transmission pipeline of DHS in question

III. Case Study

The presented methodology was used to calculate EHR for the DHS of the city of Irkutsk. The heat producer for the DHS is the Novo-Irkutskaya CHP (NICHP). Its installed heat capacity is 2010 MW and the installed electric capacity is 708 MW. The general scheme of the considered DHS is shown on the city map in Fig. 1. The supply-return temperature of heat supply is 150/70°C. Transmission and distribution pipelines of the heat network have a two-pipe design. There are heat network pipelines laid both above ground and underground (mainly in non-passable channels). The total heat network length from NICHP is 474 km, including about 113 km of transmission pipeline. The NICHP supplies heat partially or fully to three urban districts through three transmission pipelines (TP) – TP1, TP2, and TP4 (Fig. 2). TP3 is used to supply heat to consumers of a detached suburban village (Fig. 2).

The calculated scheme of the considered DHS with EHR solutions is shown in Fig. 2. It shows the EHR boundaries for four transmission pipelines from the NICHP. These boundaries were calculated both with and without reliability factored in, i.e., after adjusting the boundaries according to the nodal reliability requirements.

The required nodal reliability indices are set according to the standards presented in [19] and are 0.979 and 0.905 for AF and FOP respectively. The EHR values obtained disregarding reliability vary from 2 km to 15.5 km. The net heat cost for consumers located outside the allocated EHR zones exceeds the system-average value, and their connection seems to be economically unfeasible.

The analysis of the system reliability indicates that the requirements for the nodal reliability indices for some nodes within the EHR boundaries are not met. Therefore, the EHR boundaries are adjusted according to the specified requirements for the nodal reliability indices. Thus, to meet the reliability requirements, the maximum EHR value was decreased from 15.5 km to 14.6 km, and the length of heating mains in the EHR zone was reduced by 4.2 km and made up 67.7 km. From the reliability perspective, the EHR zone covers 284.3 km of pipelines out of the total 474.3 km, while about 40% of the heat network is located outside the EHR zone.

Figure 3 indicates the specific costs of heat supply for the most extended transmission pipeline of heat network in comparison with their system-average level. The relationship between the heat load and the material characteristic of the heat network has the main effect on the specific heat supply costs [26, 27]. The higher the specific material characteristic, the higher the specific costs, and vice versa.

Figure 4 shows the results of an assessment of the maximum allowable pipeline length from the point of new consumer connection to the existing heat network pipeline located in the EHR zone (assessment of the local EHR). The calculation was carried out for different consumer heat loads under various temperature conditions in the network. The Figure indicates, for example, that the connection of a new consumer is cost-effective if the pipeline is constructed assuming 1000 m for 6 MW at a temperature profile of 150°/70°C. A smaller difference between the temperatures in supply and return pipelines is characterized by an increase in capital and operating costs, which leads to a decrease in the maximum length of the network section for connecting new consumers. Heat supply to consumers outside the EHR zone, as a rule, requires the construction of a new heat source. At the same time, we can determine possible boundaries for expanding the EHR zone (i.e., the connection of new consumers outside the EHR zone) by using some additional indices that take into account various factors, such as uneven heat load distribution, the possibility of compensating for excess operating costs at the expense of the consumer, additional measures to ensure the heat supply reliability, and others.

IV. Conclusion

The paper proposes a method for determining optimal district heating zones based on the effective heating radius criterion, which is understood as a set of nodes of the system studied, at which heat production and transportation costs do not exceed its system-average value. The methodology provides the requirements for the heat supply reliability assessed using nodal reliability indices that allow pinpointing the most unreliable nodes in the heat network. The developed method is universal and can be applied to district heating systems of any structure and scale, given their characteristics.

Practical calculations show that the methodological approach to effective heating radius calculation for the network nodes for each heating main from the heat source provides the most informed and detailed effectiveness estimates of heating to consumers. At the same time, the substantiation of the connection of new consumers within the effective heating radius boundaries requires dedicated assessments using an additional criterion, i.e., the local effective heating radius. Some additional indices are also needed to determine possible boundaries for the effective heating radius zone expansion.

The proposed method for determining the effective heating radius in district heating systems can be recommended for designing urban heat supply schemes. The case study of effective heating radius estimation for Irkutsk district heating system has confirmed the effectiveness of the methodology and demonstrated the reliability of solutions obtained.

Acknowledgment

The research was carried out under State Assignment Project (no. FWEU-2021-0002) of the Fundamental Research Program of the Russian Federation 2021-2030.

References

[1] H. Lund, S. Werner, R. Wiltshire, et al, "4th Generation District Heating (4GDH): Integrating smart thermal grids into future sustainable energy systems," *Energy*, 2014, vol. 68, pp. 1–11.

[2] H. Lund, N. Duic, P. Østergaard, B. Mathiesen, "Smart energy systems and 4th generation district heating," *Energy*, 2016, vol. 110, pp. 1–4.

[3] H. Lund, P. Østergaard, M. Chang, et al, "The status of 4th generation district heating: Research and results," *Energy*, 2018, vol. 164, pp. 147–159.

[4] Federal Law of 27.07.2010 No. 190-FZ (as amended on 29.12.2014) "On Heat Supply".

[5] Decree of the Government of the Russian Federation of 22.02.2012 No. 154 (as amended on 07.10.2014) "On the requirements for heat supply schemes, the procedure for their development and approval".

[6] Decree of the Government of the Russian Federation dated 04.16.2012 No. 307 "On the procedure for connecting to heat supply systems and on amending some acts of the Government of the Russian Federation".

[7] Order of the Ministry of Energy of Russia No. 212 of 03.05.2019 "On approval of guidelines for the development of heat supply schemes".

[8] Decree of the Government of the Russian Federation of October 22, 2012 No. 1075 (as amended on January 24, 2017) "On pricing in the field of heat supply."

[9] L.K. Yakimov, "Limit radius of action of district heating," *Heat and Power*, 1931, vol. 9, pp. 8–10.

[10] V.V. Dmitriev, *The main issues of the district heating development in cities*. Leningrad: GONTI, 1933.

[11] V.Ya. Khasilev, "Issues of technical and economic calculation of heating networks," in *Design of urban heating networks*. Gosenergoizdat, 1957.

[12] E.P. Shubin, "Enlarged technical and economic indices for urban heat networks," in *Designing urban heat networks*. Gosenergoizdat, 1957.

[13] L.S. Khrilev, I.A. Smirnov, *Optimization of district heating and district heating systems*. Moscow: Energy, 1978.

[14] E.V. Sennova, V.G. Sidler, *Mathematical modeling and optimization of developing heat supply systems*. Novosibirsk: Science, 1987.

[15] V.G. Semenov, R.N. Razorenov, "Express analysis of the relationship between the heat transport efficiency and the remoteness of consumers," *Heat Supply News*, 2006, no. 6, pp. 36–38.

[16] V.N. Papushkin, "Heat supply radius. Well forgotten old swarm," *Heat Supply News*, 2010, no. 9, p. 44–49.

[17] N.D. Chichirova, I.G. Akhmetova, "Assessment of the effective radius of the district heating systems of the city of Kazan," *Academenergo Proceedings*, 2016, No. 1, pp. 89–95.

[18] A.P. Merenkov, V.Ya. Khasilev, *Theory of hydraulic circuits*. Moscow: Nauka, 1985.

[19] E.V. Sennova, A.V. Smirnov, A.A. Ionin, et al, *Reliability of heat supply systems*. Novosibirsk: Science, 2000.

[20] V.A. Stennikov, I.V. Postnikov, "Comprehensive analysis of the reliability of heat supply to consumers," *Izv. RAS. Energy*, 2011, No. 2, pp. 107–121.

[21] E.G. Sklovskaya et al, "Mathematical description of heat load duration curves for calculating technical and economic indices of heating systems," *Bulletin of Universities. Energy*, 1982, No. 1, pp. 75–77.

[22] V.A. Stennikov, I.V. Postnikov, "Methods for the integrated reliability analysis of heat supply," *Power Technology and Engineering*, 2014, vol. 47(6), pp. 446–453.

[23] V.A. Stennikov, I.V. Postnikov, "Methodological support for a comprehensive analysis of fuel and heat supply reliability," in «Sustaining power resources through energy optimization and engineering» (ed. by Vasant P. and Voropai N.I.). Hershey PA: Engineering Science Reference, IGI Global, 2016.

[24] I. Postnikov, V. Stennikov, E. Mednikova, A. Penkovskii, "Methodology for optimization of component reliability of heat supply systems," *Applied Energy*, 2018, vol. 227, pp. 365–374.

[25] I. Postnikov, V. Stennikov, "Modifications of probabilistic models of states evolution for reliability analysis of district heating systems," *Energy Reports*, 2020, vol. 6, pp. 293–298.

[26] V. Stennikov, E. Yakimets, "Optimal planning of heat supply systems in urban areas," *Energy*, 2016, vol. 110, pp. 157–165.

[27] V. Stennikov, E. Mednikova, I. Postnikov, A. Penkovskii, "Optimization of the effective heat supply radius for the district heating systems," *Environmental and Climate Technologies*, 2019, vol. 23(2), pp. 207–221.

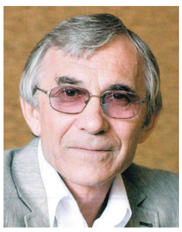

Valery Stennikov, Corresponding Member of RAS, Professor, Director of Melentiev Energy Systems Institute of Siberian Branch of the Russian Academy of Sciences (ESI SB RAS), Irkutsk, Russia. Valery Stennikov is author and co-author of more than 400 scientific publications. His research interests are systems research in the energy sector, theory of hydraulic circuits, mathematical modeling, optimization methods, heat supply systems, district heating systems, cogeneration, reliability, energy efficiency, energy saving, intelligent energy systems.

Ekaterina Mednikova, Researcher at the Laboratory of Heat Supply Systems of Melentiev Energy Systems Institute of Siberian Branch of the Russian Academy of Sciences (ESI SB RAS), Irkutsk, Russia. She is author and co-author of more than 40 scientific publications. Her research interests are energy systems, district heating, individual heating, territory zoning by type of heat supply, CHP, mathematical modeling, optimization, energy efficiency.

Ivan Postnikov, Ph.D., Senior Researcher in the Laboratory of Heat Supply Systems of Melentiev Energy Systems Institute of Siberian Branch of the Russian Academy of Sciences (ESI SB RAS), Irkutsk, Russia. Ivan Postnikov is author and co-author of more than 100 scientific publications. His research interests are energy systems, district heating systems, CHP, mathematical modeling, reliability, random processes, optimization, energy efficiency, intelligent energy systems, prosumer, renewable energy.